The kinetics of calcium carbonate, nucleation and growth

María del Pilar Ramírez-García

Submitted in accordance with the requirements for the degree of
Doctor of Philosophy

The University of Leeds

School of Earth and Environment

October 2018

Declaration

The candidate confirms that the work submitted is her own, except where work which has formed part of jointly-authored publications has been included. The contribution of the candidate and the other authors to this work has been explicitly indicated below. The candidate confirms that appropriate credit has been given within the thesis where reference has been made to the work of others.

The work in **Chapter 4** of the thesis reproduces a manuscript in preparation for submission to Geology.

Ramírez-García, M.P., Newton, R.J. and Benning, L.G., in prep. Temperature does not affect $CaCO_3$ polymorph distribution in the Phanerozoic "aragonite" and "calcite" seas.

MPRG performed all the experimental work, data collection and analyses, and concept development. ICP-MS analyses were carried out by S. Reid at the University of Leeds. EPMA analyses were carried out with the support of technical staff at the GeoForschungsZentrum Postdam. Data interpretation, writing and production of figures was done by MPRG with contributions from all co-authors.

The work in **Chapter 5** of the thesis reproduces a manuscript in preparation for submission to Geology.

Ramírez-García, M.P., Newton, R.J. and Benning, L.G., in prep. The role of pCO_2 on switching between calcite and aragonite seas.

MPRG performed all the experimental work, data collection and analyses, and concept development. ICP-MS analyses were carried out by S. Reid at the University of Leeds. EPMA analyses were carried out with the support of technical staff at the GeoForschungsZentrum Postdam. Data interpretation, writing and production of figures was done by MPRG with contributions from all co-authors.

The work in **Chapter 6** of the thesis reproduces a manuscript in preparation for submission to Geochimica Cosmochimica Acta.

Ramírez-García, M.P., Newton, R.J. and Benning, L.G., in prep. Influence of magnesium, sulfate and temperature on calcium carbonate morphogenesis.

MPRG performed all the experimental work, data collection and analyses, and concept development. ICP-MS analyses were carried out by S. Reid at the University of Leeds. The analyses of the precipitates were done by MPRG with support of technical staff at the University of Leeds. EPMA analyses were carried out with the support of technical staff at the GeoForschungsZentrum Postdam. Data interpretation, writing and production of figures was done by MPRG with contributions from all co-authors.

For the work presented in **Chapter 7** *"The incorporation of Mg and SO_4 into calcium carbonate and their possible role in regulating past ocean composition":*

MPRG performed all the laboratory synthesis of precipitates. ICP-MS analyses were carried out by S. Reid at the University of Leeds. The analyses of the precipitates were done by MPRG with support of technical staff at the University of Leeds. EPMA analyses were carried out with the support of technical staff at the GeoForschungsZentrum Postdam. STXM experiments were completed by MPRG, LGB, RJN and McCutcheon, Jenine and technical staff at Canadian Light Source (CLS) and Diamond Light Source. Data processing was done by MPRG and technical staff at Diamond Light Source.

Acknowledgements

I would like to thank Liane G. Benning and Robert J. Newton for always being immensely supportive and encouraging, for giving me endless opportunities to gain new experiences and enlarge my knowledge. They complement each other and form a balanced and easy-going team to work with.

I would like to thank the whole Cohen geochemistry group, especially to Andrea, Adriana, Daniela and Taher for keeping me smiling. Special thanks to all the technicians (including those from GeoForschungsZentrum Postdam) for their help and awesome work in the labs.

I am sincerely grateful to the Marie Skłodowska-Curie actions for sponsoring my PhD as part of the CO2-REACT Initial Training Research network and all the fancy network meetings I was allowed to go to.

And finally, I must express my very profound gratitude to my family, who has always supported me, no matter what I decided to do, and special thanks to my husband Marce, without your unfailing support throughout these years, this thesis would simply not exist.

Abstract

During the Phanerozoic, ocean chemistry has oscillated to favour the dominant non-biogenic polymorph of calcium carbonate ($CaCO_3$) to be either calcite or aragonite. The main driving force controlling these aragonite-calcite seas conditions is the Mg:Ca ratio of seawater. However, other parameters such us SO_4, temperature and partial pressure of carbon dioxide (pCO_2) are also known to influence $CaCO_3$ polymorph formation but are often overlooked in the context of aragonite-calcite seas. The main aim of this research project was to evaluate and quantify the key effects as well as the relative effects of changes in Mg:Ca ratio, SO_4 concentration, temperature and pCO_2 have on the formation, transformation and structure of $CaCO_3$ phases, in order to provide a better synergistic approach than those taken by previous studies.

We confirm seawater Mg:Ca ratio and SO_4 concentration as dominant drivers since small differences in their values can be invoked as controlling the variation in abiotic $CaCO_3$ polymorphs. We propose lower Mg:Ca and SO_4 thresholds on seawater chemistry for calcite predominance seas (Mg:Ca$\leq$ 0.65, SO4$\leq$ 10 mM) than those suggested by the geological records (Mg:Ca$\approx$ 2).

Our work demonstrates that there is not a significant response of abiotic marine $CaCO_3$ mineralogy to changing temperature. Our experimental data also reveal that neither changes in pCO_2 in the range 400 to 3000 ppm, or their respective changes in seawater pH (8.2, to 7.6) lead to major variations in the stability fields for aragonite and calcite precipitation. Hence, the view of Phanerozoic aragonite-calcite seas should not be temperature and atmospheric pCO_2 or seawater pH corrected.

We validate abiogenic calcite Mg:Ca as a reliable and quantitative proxy for past global seawater temperature change if its dependence on both the temperature and the Mg:Ca ratio of the seawater is considered.

We propose SO_4 content in abiogenic calcite as a reliable and quantitative proxy for past seawater pH and atmospheric pCO_2, but our results indicated that it is not possible to provide a single SO_4–pH calibration and the use of seawater SO_4-specific equations is needed.

It can also be concluded that switches between aragonite and calcite seas calculated from the stability fields from our experimental results would only match the proxy

data for seawater chemistry in the geological record if the lowest suggested seawater SO_4 concentrations are considered ($[SO_4] \leq 10$ mM).

Furthermore, this study shows that Mg, SO_4 and temperature significantly influence calcium carbonate morphology and addresses temperature turning out to be an important parameter for the control of particle size.

Table of Contents

List of Tables

List of Figures

List of Acronyms and Abbreviations

IC	Ion Chromatography
ICP-MS	Inductively Coupled Plasma Mass Spectrometry
ICP-OES	Inductively Coupled Plasma Optical Emission Spectroscopy
FIB	Focused ion beam
MilliQ	Ultrapure water (~18.2 MΩ cm)
XRD	X-ray Diffraction
XRF	X-Ray Fluorescence
EMPA	Electron Probe Micro-Analysis
STXM	Scattering Transmission X-ray Microscopy
NEXAFS	Near Edge X-ray Absorption Fine Structrure
XANES	X-ray Absorption Near Edge Structure
EDS	Energy Dispersive Spectroscopy
EELS	Electron Energy Loss Spectroscopy
SEM	Scanning Electron Microscopy
TEM	Transmission Electron Microscopy
AAC	Amorphous Calcium Carbonate
pCO_2	Partial pressure of carbon dioxide

Chapter 1
Introduction

1.1. Background

During the last 541 million years (the era called Phanerozoic), oscillations in calcium carbonate mineralogy in the oceans have led to alternating periods of carbonate mineral polymorph precipitation that are called “aragonite seas” and “calcite seas” (Figure 1.1) (Holt et al., 2014; Horita et al., 2002; Lowenstein et al., 2003; Sandberg, 1983b). Studies about the textures and composition of ancient ooids and carbonate cements, as well as data from evaporite fluid inclusions and fossil echinoderms have helped quantify a trend in seawater composition that is seemingly reflected in variations in aragonite and calcite dominant $CaCO_3$ polymorphs. These variations have changed the mineralogy, formation mechanism and precipitation kinetics of marine inorganic and biogenic calcium carbonate minerals (Burton, 1993; Burton, 1991; Morse et al., 1997b). To understand these processes is crucial because calcium carbonate minerals are the most widely used paleoproxies mineral phases that are applied when reconstructing past ocean conditions. This is because they are known to record the chemical and physical condition of the seawater environment they have formed in.

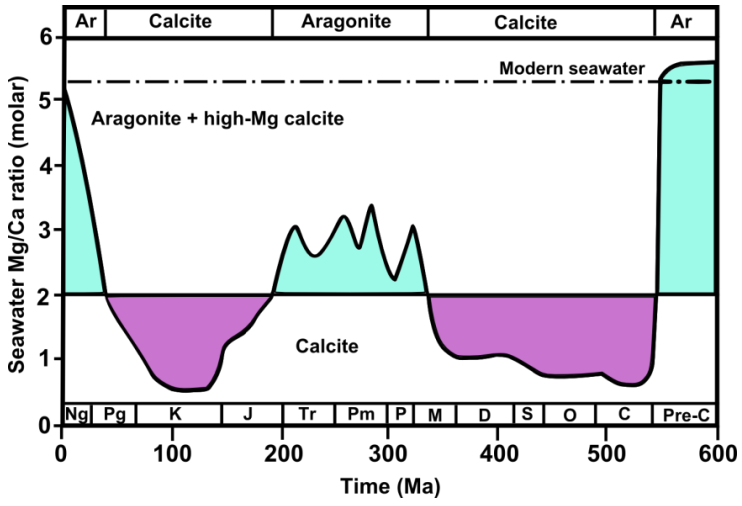

Figure 1. 1: Secular variation in the Mg:Ca ratio of seawater during Phanerozoic. Figure modified after Holt et al., 2014**.**

Based on data pertaining to calcium carbonate minerals in Phanerozoic rocks and specifically the magnesium to calcium ratio in these carbonates, it was concluded that Mg:Ca, the presence of other ions in solution as SO_4 and temperature are likely the main control on carbonate mineralogy and thus, on the oscillations between calcite and aragonite seas (Bots et al., 2011; Burton and Walter, 1987; Morse et al., 1997b). Magnesium exerts a significant influence on calcium carbonate precipitation and can inhibit calcite precipitation either, by being incorporated within the calcite lattice thus decreasing its thermodynamic stability and increasing its solubility (Branson et al., 2013b; Busenberg and Niel Plummer, 1989), or by being absorbed onto the surface of growing pre-formed calcite crystals (Burton, 1993; Walter, 1983). Interestingly so far all evidence indicated no significant kinetic obstacle to aragonite growth in the presence of Mg ions as they are known to not be incorporated into the aragonite structure (Berner, 1975; Mucci and Morse, 1983).

Until recently, only few studies have addressed the isotope fractionation of divalent metal impurities, including magnesium, within carbonate minerals. This was primarily due to instrumental limitations and the high reproducibility required for reliable measurements (Chang et al., 2004; Young and Galy, 2004). The application of the Ca and Mg isotope systems as paleo- environmental proxies (e.g., (Chang et al., 2004; Fantle and DePaolo, 2007; Galy et al., 2002)) normally relies on the assumption that natural carbonates were in isotopic equilibrium with their co-existing fluid during formation and did not subsequently re-equilibrate in response to changing environmental conditions. A thorough understanding of the processes affecting Mg isotope fractionation in abiogenic precipitation experiments will help separate the influence of temperature, growth rate and vital effects on $\Delta^{26}Mg_{carb\text{-}sol}$ in biogenic carbonates. As it was shown in recent studies (Li et al., 2012; Wang et al., 2013), higher growth temperatures may favour somewhat smaller Mg isotope fractionations, considering that measurements can now be done with a sensitivity of $\approx$0.01‰ $°C^{-1}$. Faster precipitation rates favour smaller Mg isotope fractionations, possibly because of enhanced incorporation of fluid inclusions and/or due to the fact that the Mg ion is much more hydrated compared to the Ca ion (Immenhauser et al., 2010; Li et al., 2012; Mavromatis et al., 2013; Wang et al., 2013). Higher magnesium concentrations, higher Mg:Ca ratios and higher pH values may all favour a temperature dependent fractionation effect and these in turn may minimize

the dependence of $\Delta^{26}Mg_{carb\text{-}sol}$ on the precipitation rate. This may be related to the formation of amorphous calcium carbonate (ACC) precursors or vaterite intermediate prior to the growth of calcite or aragonite (Bots et al., 2011; Rodriguez-Blanco et al., 2012), and this may affect the mode of $CaCO_3$ polymorph growth, attachment/detachment kinetics and/or aqueous Mg speciation (Saenger and Wang, 2014).

Sulphate has also been proposed as a major influence on calcium carbonate mineralogy (Burton, 1993; Busenberg and Niel Plummer, 1985, 1989). Experimental studies have shown that at elevated sulphate concentrations in solution aragonite becomes more stable, since SO_4 decreases calcite stability and precipitation rate compared to aragonite (Walter, 1986). A quantification of the effects of SO_4 and Mg:Ca ratio on $CaCO_3$ mineralogy was carried out by (Bots et al., 2011). Their results indicated that at 21°C an increase in dissolved SO_4 decreases the Mg:Ca ratio at which calcite becomes less stable and aragonite becomes the dominant calcium carbonate polymorph. They proposed new thresholds for these two parameters for 21°C and suggested that these parameters may have to be re-evaluated with respect to the proposed "aragonite" and "calcite" seas of the Phanerozoic.

Calcium carbonate mineralogy can also be influenced by temperature (e.g. (Burton and Walter, 1987; Morse, 1990; Morse et al., 1997a)). Temperature enhances the incorporation of magnesium into the calcite lattice, while the precipitation rates of aragonite relative to those of calcite increase strongly with increasing temperature (Burton and Walter, 1987) (Figure 1.2). A recent quantification of the proportion of $CaCO_3$ polymorphs as a function of Mg:Ca ratio and temperature has been carried out (Balthasar and Cusack, 2015). This work shows that abiotic calcite precipitation was inhibited during aragonite sea intervals at temperatures above 20°C, whereas calcite sea intervals were characterized by the co-precipitation of aragonite and calcite in environments above 20°C. These studies have shown that indeed in part the increase of aragonite over calcite skeletal composition in calcifying organisms during the Phanerozoic may be explained. However, open questions as to the role of the ubiquitously present vaterite at low magnesium and high sulphate contents is still puzzling and the effect of this intermediate (and possibly even amorphous calcium carbonate) are still unclear.

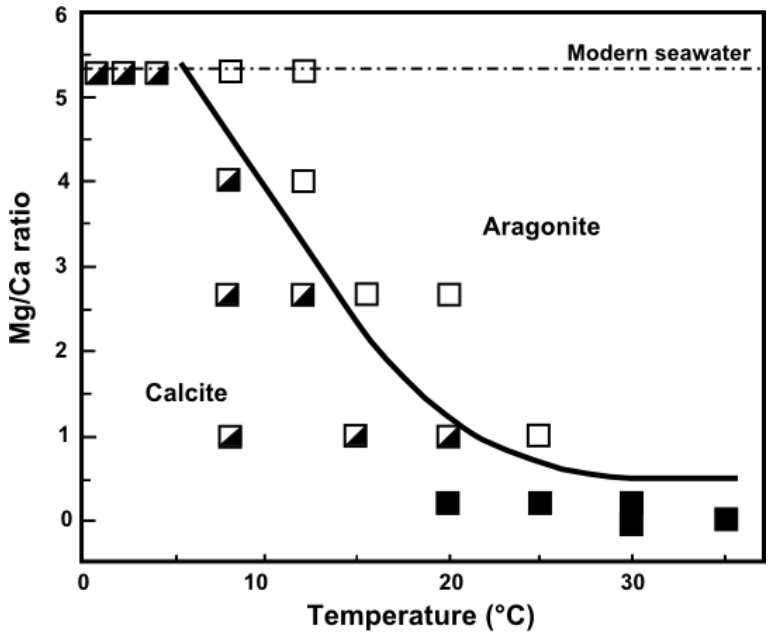

Figure 1. 2: *Influence of temperature and Mg:Ca on the calcium carbonate mineralogy (Morse et al. 1997). White squares are aragonite, black squares are calcite, and split squares are situations in which calcite initially precipitates but then aragonite grows on calcite*

Changes in atmospheric CO_2 levels during the Phanerozoic have also been hypothesized to contribute to changes in calcium carbonate mineralogy (Berner, 2004). It is been proposed that the observed mineralogical shifts were driven by tectonically induced shifts in atmospheric pCO_2 (Mackenzie and Pigott, 1981). It has also been argued that fluctuations in sea level, atmospheric pCO_2 and concomitant fluctuations in the saturation state of seawater with respect to calcium carbonate, were largely responsible for the observed secular shifts in the primary mineralogy of ooids and marine cements throughout Phanerozoic time (Wilkinson and Given, 1986). However, atmospheric pCO_2 would only be expected to cause a shift to calcite seas if pCO_2 caused seawater to be simultaneously oversaturated with respect to calcite and undersaturated with respect to aragonite. Furthermore, the effect of atmospheric pCO_2 on carbonate oceanic state will vary strongly with both latitude and depth. This is because temperature and pressure influences the solubility of CO_2 in seawater and thus, the effect of atmospheric pCO_2 on calcite vs. aragonite stability (Ries et al., 2009). Modern upwelling waters are also known to have much higher levels of dissolved inorganic carbon and reduced pH than surface waters (Feely et al., 2008), which would further moderate the effect of atmospheric pCO_2

on carbonate oceanic state. Additionally, ocean acidification may also have severe consequences for marine ecosystems; however, assessing its future impact is difficult because experiments and field observations are limited by their reduced ecologic complexity and sample period respectively (Hönisch et al., 2012).

As discussed above many experimental studies have identified various effects that changes in solution chemistry (e.g., pH, pCO_2 and composition) or physical parameters such as temperature have on the formation, transformation and structure of calcium carbonate phases. However, the lack of a synergistic and deterministic approach in currently used experimental approaches and thus also models about the role such parameters have in controlling carbonate mineralogy is a big gap in our knowledge and hinders our predictive capabilities. Thus the relative influence and effects of each of these parameters must be determined in order to assess the total influence of solution chemistry and temperature on calcium carbonate precipitation.

1.2. Aims and objectives

The main aim of this research project was to determine the key effects of various chemical and physical parameters such as Mg:Ca ratio, SO_4 concentration, temperature and pCO_2 on calcium carbonate formation pathways in order to provide a better synergistic approach than that taken by previous studies. To achieve this, a combination of laboratory and synchrotron experiments were performed both *in-situ* and *ex-situ*, with the goal to elucidate the kinetics, mechanisms and energetics of carbonate formation.

The research objectives can be divided into four main areas:

1. To quantify the effects of changing solution chemistry (i.e., magnesium and sulphate) and temperature on calcium carbonate polymorph distribution and morphology by performing laboratory-based $CaCO_3$ synthesis based on a constant addition experimental approach (Chapters 4 and 6).

This study provide a quantification of the effects of Mg:Ca ratio, SO_4 and temperature on the $CaCO_3$ mineralogy as well as analyse the interactive effects of these studied parameters. These results also allow us to evaluate whether temperature should or should not be included in the existing models relating seawater chemistry to $CaCO_3$ mineralogy throughout the Phanerozoic.

2. To determine the influence of variations in atmospheric pCO_2 on calcium carbonate mineralogy in order to better understand the occurrence of ocean acidification events in the past, and discuss the possible future marine ecosystem changes (Chapter 5). The main aims of this set of experiments at different atmospheric pCO_2 conditions are:

a) Determine the influence of pCO_2 on calcium carbonate polymorph distribution and morphology.

b) Evaluate if pCO_2 could be considered as a primary parameter responsible for changing seawater saturation with respect to carbonate minerals.

c) Get a better understand of events exhibiting evidence for elevated atmospheric CO_2, global warming and ocean acidification over the past ≈300 million years of Earth´s history, as well as to figure out if past events parallel future projections in terms of disrupting the balance of ocean carbonate chemistry.

3. To perform a molecular level study of the role and/or effects that SO_4 and Mg incorporation into $CaCO_3$ phases have on polymorphs selection. Both Mg and SO_4 are considered excellent palaeoenvironmental proxies (recorders of ancient environmental conditions) (Bots et al., 2011; Finch and Allison, 2008); however, the mechanism that drives and controls how the incorporations of these ions actually affects polymorphs selection is still unknown. This is because even minute changes in the chemical composition or temperature of the seawater in which $CaCO_3$ precipitate can dramatically change the Mg or SO_4 incorporation and polymorph selection. Thus, the aim of this study is therefore to address this gap in our knowledge via spatially resolved scanning transmission X-Ray microscopy (STXM) analyses of $CaCO_3$ polymorphs synthesized at various Mg and SO_4 seawater compositions, temperature and partial pressure of carbon dioxide (pCO_2) that are representative of the chemical conditions in ancient and modern oceans (Chapter 7).

1.3. Thesis outline

This thesis consists of eight chapters:

Chapter 1: contains the rational of the project, the research aims and objectives and the thesis outline.

Chapter 2: provides an overview of the literature on the effects of solution chemistry, temperature and partial pressure of carbon dioxide on calcium carbonate formation, transformation and mineralogy; and summarizes the known occurrence of calcium carbonate minerals throughout the geological history.

Chapter 3: contains a compilation of all the experimental and analytical methods used. Some of the laboratory techniques and instrument protocols were carried out according to the standard operational procedures available in the Cohen Geochemistry Labs (University of Leeds).

Chapter 4: "Temperature does not affect $CaCO_3$ polymorph distribution in the Phanerozoic "aragonite" and "calcite" seas" (in preparation for Geology).

This chapter contains an experimental study of the effect of temperature, seawater Mg:Ca ratio and SO_4 concentration on abiotic $CaCO_3$ precipitation and provides a new predictive framework for interpreting observations of primary $CaCO_3$ mineralogy in Phanerozoic rocks.

Chapter 5: "The role of pCO_2 on switching between calcite and aragonite seas" (in preparation for Geology).

This chapter contains a study of the influence of variations in atmospheric pCO_2 on calcium carbonate mineralogy in order to better understand the occurrence of ocean acidification events in the past, and discuss the possible future marine ecosystem changes.

Chapter 6: "Influence of magnesium, sulfate and temperature on calcium carbonate morphogenesis".

This chapter contains a study of the influence of inorganic additives such as Mg and SO_4 and temperature on $CaCO_3$ morphology, particle size and polymorphs distribution was evaluated by quantitative and qualitative analyses (XRD, EPMA and SEM).

Chapter 7: "The incorporation of Mg and SO_4 into calcium carbonate and their possible role in regulating past ocean composition". This chapter contains a work which is still ongoing and presents the preliminary results of a spatially and spectrally resolved data set on the mechanisms of Mg and S incorporation into various $CaCO_3$ polymorphs (calcite, aragonite and vaterite) to evaluate the role of Mg and SO_4 as good (or bad) paleo proxies in marine $CaCO_3$ for the "aragonite" and "calcite" seas hypothesis.

Chapter 8: contains a summary of the work presented in the thesis, conclusions and suggestions for future work.

References

Balthasar, U., and Cusack, M., 2015, Aragonite-calcite seas—Quantifying the gray area: Geology, v. 43, no. 2, p. 99-102.

Berner, R. A., 1975, The role of magnesium in the crystal growth of calcite and aragonite from sea water: Geochimica et Cosmochimica Acta, v. 39, no. 4, p. 489-504.

Berner, R. A., 2004, A model for calcium, magnesium and sulfate in seawater over Phanerozoic time: American Journal of Science, v. 304, no. 5, p. 438-453.

Bots, P., Benning, L., Rickaby, R., and Shaw, S., 2011, The role of SO4 in the switch from calcite to aragonite seas: Geology, v. 39, no. 4, p. 331-334.

Branson, O., Redfern, S. A. T., Tyliszczak, T., Sadekov, A., Langer, G., Kimoto, K., and Elderfield, H., 2013, The coordination of Mg in foraminiferal calcite: Earth and Planetary Science Letters, v. 383, p. 134-141.

Burton, E. A., 1993, Controls on marine carbonate cement mineralogy: review and reassessment: Chemical Geology, v. 105, no. 1, p. 163-179.

Burton, E. A., and Walter, L. M., 1987, Relative precipitation rates of aragonite and Mg calcite from seawater: Temperature or carbonate ion control?: Geology, v. 15, no. 2, p. 111-114.

-, 1991, The effects of PCO2 and temperature on magnesium incorporation in calcite in seawater and MgCl2-CaCl2 solutions: Geochimica et Cosmochimica Acta, v. 55, no. 3, p. 777-785.

Busenberg, E., and Niel Plummer, L., 1985, Kinetic and thermodynamic factors controlling the distribution of SO32− and Na+ in calcites and selected aragonites: Geochimica et Cosmochimica Acta, v. 49, no. 3, p. 713-725.

-, 1989, Thermodynamics of magnesian calcite solid-solutions at 25°C and 1 atm total pressure: Geochimica et Cosmochimica Acta, v. 53, no. 6, p. 1189-1208.

Chang, V. T. C., Williams, R. J. P., Makishima, A., Belshawl, N. S., and O'Nions, R. K., 2004, Mg and Ca isotope fractionation during CaCO3

biomineralisation: Biochemical and Biophysical Research Communications, v. 323, no. 1, p. 79-85.

Fantle, M. S., and DePaolo, D. J., 2007, Ca isotopes in carbonate sediment and pore fluid from ODP Site 807A: The Ca2+(aq)–calcite equilibrium fractionation factor and calcite recrystallization rates in Pleistocene sediments: Geochimica et Cosmochimica Acta, v. 71, no. 10, p. 2524-2546.

Feely, R. A., Sabine, C. L., Hernandez-Ayon, J. M., Ianson, D., and Hales, B., 2008, Evidence for Upwelling of Corrosive "Acidified" Water onto the Continental Shelf: Science, v. 320, no. 5882, p. 1490-1492.

Finch, A. A., and Allison, N., 2008, Mg structural state in coral aragonite and implications for the paleoenvironmental proxy: Geophysical Research Letters, v. 35, no. 8.

Galy, A., Bar-Matthews, M., Halicz, L., and O'Nions, R. K., 2002, Mg isotopic composition of carbonate: insight from speleothem formation: Earth and Planetary Science Letters, v. 201, no. 1, p. 105-115.

Holt, N. M., García-Veigas, J., Lowenstein, T. K., Giles, P. S., and Williams-Stroud, S., 2014, The major-ion composition of Carboniferous seawater: Geochimica et Cosmochimica Acta, v. 134, p. 317-334.

Hönisch, B., Ridgwell, A., Schmidt, D. N., Thomas, E., Gibbs, S. J., Sluijs, A., Zeebe, R., Kump, L., Martindale, R. C., Greene, S. E., Kiessling, W., Ries, J., Zachos, J. C., Royer, D. L., Barker, S., Marchitto, T. M., Moyer, R., Pelejero, C., Ziveri, P., Foster, G. L., and Williams, B., 2012, The Geological Record of Ocean Acidification: Science, v. 335, no. 6072, p. 1058-1063.

Horita, J., Zimmermann, H., and Holland, H. D., 2002, Chemical evolution of seawater during the Phanerozoic: Implications from the record of marine evaporites: Geochimica et Cosmochimica Acta, v. 66, no. 21, p. 3733-3756.

Immenhauser, A., Buhl, D., Richter, D., Niedermayr, A., Riechelmann, D., Dietzel, M., and Schulte, U., 2010, Magnesium-isotope fractionation during low-Mg calcite precipitation in a limestone cave–Field study and experiments: Geochimica et Cosmochimica Acta, v. 74, no. 15, p. 4346-4364.

Li, W., Chakraborty, S., Beard, B. L., Romanek, C. S., and Johnson, C. M., 2012, Magnesium isotope fractionation during precipitation of inorganic calcite under laboratory conditions: Earth and Planetary Science Letters, v. 333-334, p. 304-316.

Lowenstein, T. K., Hardie, L. A., Timofeeff, M. N., and Demicco, R. V., 2003, Secular variation in seawater chemistry and the origin of calcium chloride basinal brines: Geology, v. 31, no. 10, p. 857-860.

Mackenzie, F. T., and Pigott, J. D., 1981, Tectonic controls of Phanerozoic sedimentary rock cycling: Journal of the Geological Society, v. 138, no. 2, p. 183-196.

Mavromatis, V., Gautier, Q., Bosc, O., and Schott, J., 2013, Kinetics of Mg partition and Mg stable isotope fractionation during its incorporation in calcite: Geochimica et Cosmochimica Acta, v. 114, p. 188-203.

Morse, J. W., & Mackenzie, F. T., 1990, Geochemistry of sedimentary carbonates: Elsevier, v. 48.

Morse, J. W., Wang, Q., and Tsio, M. Y., 1997a, Influences of temperature and Mg: Ca ratio on CaCO3 precipitates from seawater: Geology, v. 25, no. 1, p. 85-87.

Morse, J. W., Wang, Q., and Tsio, M. Y., 1997b, Influences of temperature and Mg:Ca ratio on CaCO3 precipitates from seawater: Geology, v. 25, no. 1, p. 85-87.

Mucci, A., and Morse, J. W., 1983, The incorporation of Mg2+ and Sr2+ into calcite overgrowths: influences of growth rate and solution composition: Geochimica et Cosmochimica Acta, v. 47, no. 2, p. 217-233.

Ries, J. B., Cohen, A. L., and McCorkle, D. C., 2009, Marine calcifiers exhibit mixed responses to CO2-induced ocean acidification: Geology, v. 37, no. 12, p. 1131-1134.

Rodriguez-Blanco, J. D., Shaw, S., Bots, P., Roncal-Herrero, T., and Benning, L. G., 2012, The role of pH and Mg on the stability and crystallization of amorphous calcium carbonate: Journal of Alloys and Compounds, v. 536, p. S477-S479.

Saenger, C., and Wang, Z., 2014, Magnesium isotope fractionation in biogenic and abiogenic carbonates: implications for paleoenvironmental proxies: Quaternary Science Reviews, v. 90, p. 1-21.

Sandberg, P. A., 1983, An oscillating trend in Phanerozoic non-skeletal carbonate mineralogy: Nature, v. 305, p. 19.

Walter, L. M., 1983, An oscillating trend in Phanerozoic non-skeletal carbonate mineralogy: Nature, v. 305, p. 19.

-, 1986, Relative efficiency of carbonate dissolution and precipitation during diagenesis: a progress report on the role of solution chemistry.

Wang, Z., Hu, P., Gaetani, G., Liu, C., Saenger, C., Cohen, A., and Hart, S., 2013, Experimental calibration of Mg isotope fractionation between aragonite and seawater: Geochimica et Cosmochimica Acta, v. 102, p. 113-123.

Wilkinson, B. H., and Given, R. K., 1986, Secular Variation in Abiotic Marine Carbonates: Constraints on Phanerozoic Atmospheric Carbon Dioxide Contents and Oceanic Mg/Ca Ratios: The Journal of Geology, v. 94, no. 3, p. 321-333.

Young, E. D., and Galy, A., 2004, The Isotope Geochemistry and Cosmochemistry of Magnesium: Reviews in Mineralogy and Geochemistry, v. 55, no. 1, p. 197-230.

Chapter 2
Literature Review

2.1. Chemical evolution of seawater during the Phanerozoic

The chemical evolution of seawater during the Phanerozoic (≈ 541 m.y.) is still a matter of debate. Over the past two decades, a number of models suggested that the chemistry of the oceans, rather than remaining constant, has oscillated significantly over at least the past 541 m.y. (Hardie, 1991; Hardie, 1996; Spencer and Hardie, 1990). Chemical analyses of ancient ooids and cements as well as of fluid inclusions in marine halites showed that the major composition of seawater (Mg, Ca, K, Na, SO_4 and Cl) has varied during the Phanerozoic (Horita et al., 2002; Lowenstein et al., 2001). Secular changes in the mineralogy of marine non-skeletal limestones (Sandberg, 1983b) and late-state evaporites (Hardie, 1996) occur on a 100-200 m.y. time scale. Within this cycle, periods termed "aragonite seas" are believed to have been dominated by primarily aragonite precipitation and synchronized with $MgSO_4$ evaporites while periods believed to have been dominated by primarily calcite precipitation were termed "calcite seas" and coincided with KCl evaporites. The 'aragonite' and 'calcite' seas also correlate with variation in seawater Mg:Ca (Figure 2.1) (Hardie, 1996; Holland et al., 1996; Stanley and Hardie, 1998; Wallmann, 2001; Wilkinson and Algeo, 1989).

Such secular variations in seawater Mg:Ca are supported by synchronized secular variations in:

(1) The ionic composition of fluid inclusions in primary marine halite (Horita et al., 2002; Lowenstein et al., 2003; Lowenstein et al., 2001; Volodymyr M. Kovalevich et al., 1998; Zimmermann, 2000).

(2) The mineralogy of late stage marine evaporites, abiogenic carbonates, as well as carbonates formed by reef and sediment-forming marine calcifiers (Hardie, 1996; Sandberg, 1983b).

(3) The Mg:Ca ratios of fossil echinoderms, molluscs, rugose corals, and abiogenic carbonates (Coggon et al., 2010; de Villiers et al., 2005; Dickson, 2002; Martin, 1995).

(4) Global rates of mid-ocean ridge production, which drive the preferential removal of Mg versus Ca via hydrothermal circulation (Morse et al., 1997b; Stanley, 2006).

(5) Additional proxies of seawater including Sr:Ca ratios of abiogenic carbonates, Sr:Ca ratios of biogenic carbonates, and Br concentrations in marine halite (Coggon et al., 2010; Cohen et al., 2002; Lear et al., 2000; Lear et al., 2002).

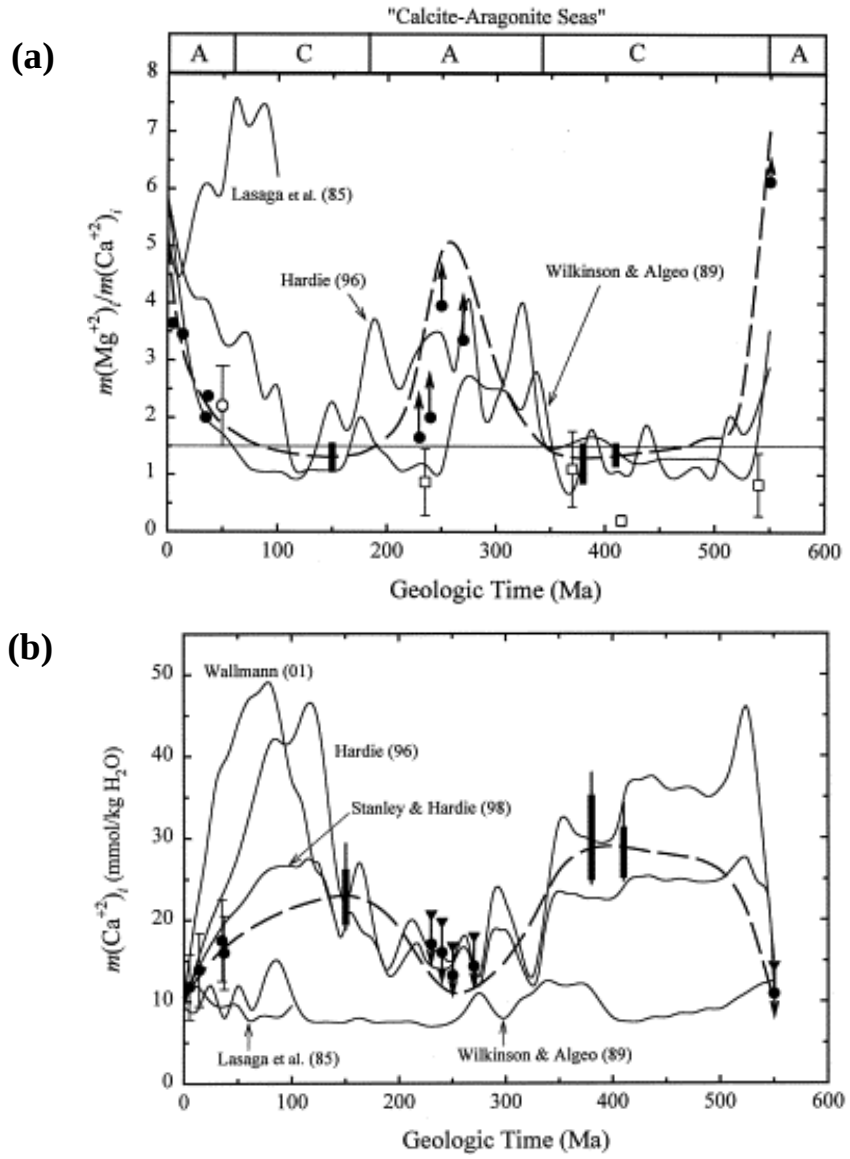

Figure 2. 1: *Seawater Mg (a) and Ca (b) concentration during the Phanerozoic as determined from halite fluid inclusions from: Horita et al. (2002, dashed lines); the solid lines represent models from Hardie (1996), Stanley and Hardie (1998), Wallmann (2001) and Wilkinson and Algeo (1989); figure reprinted from Horita et al. (2002).*

Although experimental evidence supports seawater Mg:Ca as a control on carbonate mineralogy, it is clear that many other interacting factors such as temperature (Burton and Walter, 1987; Morse et al., 1997b), concentration of SO_4 (Figure 2.2) (Bots et al., 2011; Railsback and Anderson, 1987), saturation state and therefore atmospheric pCO_2 (Morse et al., 2007; Sandberg, 1983b; Wilkinson et al., 1984), phosphate, etc. must also influence the switch between the various $CaCO_3$ polymorphs.

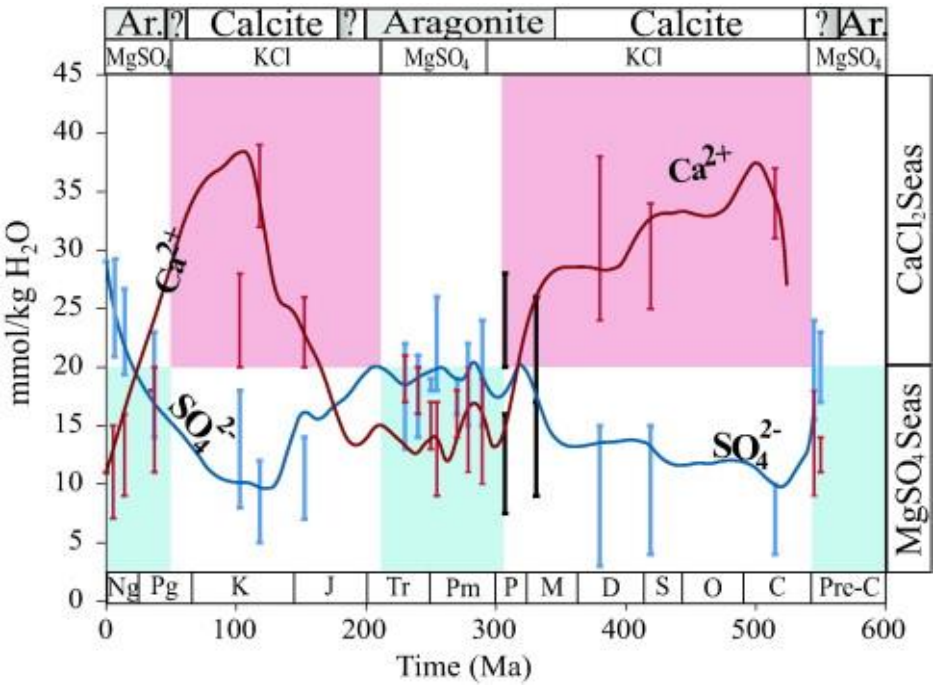

Figure 2. 2: *Secular variation in concentration of Ca and SO_4 (millimolal, mmol/kg H_2O) in seawater during the Phanerozoic estimated from primary fluid inclusions in marine halite (red and blue bars). Black bars are Ca and SO_4 concentrations for Mississippian and Pennsylvanian seawater estimated from this study. Curves for Ca and SO_4 from model of Phanerozoic seawater composition (Demicco et al., 2005). "$CaCl_2$ seas" have seawater mCa > mSO_4 and "$MgSO_4$" seas have mCa < mSO_4. KCl and $MgSO_4$ evaporites (Hardie, 1996) are plotted at the top of the diagram along with distributions of primary Phanerozoic nonskeletal carbonates (Sandberg, 1983b); figure reprinted from Holt et al. 2014.*

The current hypothesis for these ~100-200 m.y. cycles in carbonate and evaporite mineralogy involve secular variation in the major ion chemistry of seawater produced by:

(1) The selective removal of calcium ions from the oceans as a consequence of the appearance and rise of calcareous nannoplankton and planktonic foraminifera (Folk, 1974; Sandberg, 1983b).

(2) The position of global sea level (emergent or submergent modes) (Wilkinson and Given, 1986).

(3) Changes in the steady-state mixing of the two major contributors to ocean chemistry, river water input (RW) and hydrothermal brines from mid-ocean ridge (MOR), coupled with precipitation of solid $CaCO_3$ and amorphous SiO_2 phases (Hardie, 1991; Spencer and Hardie, 1990).

(4) Secular variations in the flux of mid-ocean ridge (MOR) hydrothermal fluids driven by secular variation in the rate of ocean crust production, which causes variation in cation exchange between mid ocean ridge basalts and seawater (Berner, 2004; Holland, 2005; Stanley and Hardie, 1998; Wilkinson et al., 1985).

(5) Seawater-driven dolomitization (Holland, 2005; Holland et al., 1996; Lowenstein et al., 2001).

2.1.1. Calcite - Aragonite seas

As mentioned above during the Phanerozoic there were two periods when the primary mineralogy of ooids and early marine cements were either dominated by calcitic mineralogy and three periods which were aragonitic (Figure 2.3) (Sandberg, 1983b).

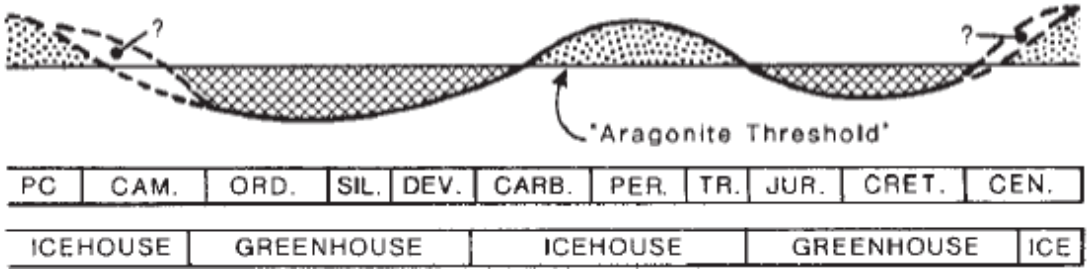

Figure 2. 3: *Oscillations between aragonite and calcite seas as estimated by Sandberg (1983).*

Studies of late-stage salts in marine evaporites reveal that periods when potash deposits included abundant $MgSO_4$ salts, alternate with periods when potash

deposits were characterized mainly by KCl salts, with SO_4 minerals being rare or totally absent (Hardie, 1990; Hardie, 1991; Hardie, 1996). What is rather significant is that these secular changes in ooid and cement mineralogy and evaporites occurred in phase, such that periods termed “aragonite seas” were synchronous with $MgSO_4$ – rich evaporites and periods termed “calcite seas” were synchronous with KCl - rich evaporites (Figure 2.4). However, the geologic records nevertheless documents that the calcium carbonate formed during the Phanerozoic was rarely purely calcite or aragonite. The definition simply refers to “calcite seas” as periods when calcite was the dominant calcium carbonate phase, and “aragonite seas” as those periods when aragonite was the predominant polymorph (Adabi, 2004; Bots et al., 2011; Wilkinson et al., 1985; Zhuravlev and Wood, 2009).

As mentioned above, different chemical and physical parameters were suggested as the cause of these mineralogical changes. Among these seawater Mg:Ca ratios has been suggested as the primary factor controlling seawater calcium carbonate mineralogy, because in the Phanerozoic geologic record, the range and patterns of seawater Mg:Ca variations match (Figure 2.4), in a general way, both those predicted by existing mass balance models (Hardie, 1996; Wilkinson and Algeo, 1989) and those Mg:Ca estimates from fluid inclusions in halite (Lowenstein et al., 2001). Furthermore, more recent studies demonstrated that the seawater Mg:Ca ratio is an important factor in determining the primary calcium carbonate polymorph formed from seawater (Stanley, 2006).

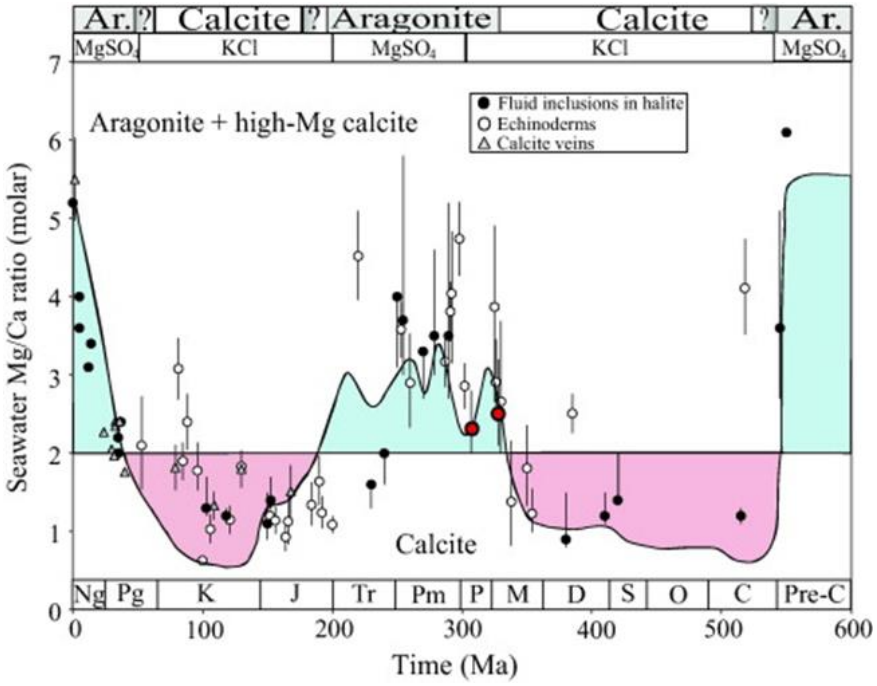

Figure 2. 4: *Secular variation in the Mg:Ca ratio of seawater during the Phanerozoic. Red points data from Holt et al., 2014. Horizontal line at Mg:Ca= 2 represents the approximate divide between aragonite + high-Mg calcite (Mg:Ca> 2) and calcite (Mg:Ca< 2) nucleation fields in seawater at 25ºC. Closed circles data from Lowenstein et al., 2001, 2003, 2005; Horita et al., 2002; Brennan and Lowenstein, 2002; Brennan et al., 2004; Satterfield et al., 2005; Timofeeff et al., 2006. Open circles show data from Dickson, 2002. Triangles show data from Coggon et al., 2010. Curve is Mg:Ca of seawater estimated using model of Demicco et al. (2005).*

Despite all these findings the precise magnesium to calcium ratio that determined the switch from calcite to aragonite during the Phanerozoic is still a topic of debate. Initial studies proposed ratios between 1 and 2 (Hardie, 1996; Morse et al., 1997b; Wilkinson and Algeo, 1989). It has been documented experimentally that temperature may be an important factor controlling calcium carbonate mineralogy, as it might influence the Mg:Ca ratio at which the switch form calcite to aragonite occurs (Morse et al., 1997b). A first combined quantification of the effects that both SO_4 and the Mg:Ca ratio have on $CaCO_3$ mineralogy was carried out by (Bots et al., 2011). Their results indicated that at 21°C, an increase in dissolved SO_4 decreased the Mg:Ca ratio at which calcite becomes less stable and aragonite becomes the dominant calcium carbonate polymorph. A recent proposed threshold for calcite presence at Mg:Ca> 0.6-0.7 (Bots et al., 2011), was at the lower end of those proposed before (~1-2). Recently, new experiments allowed for temperature to be included as an important factor controlling calcium carbonate mineralogy (Balthasar and Cusack, 2015). This study, in contradiction of previous work, showed that there

is a gradual change in the proportion of mineral phases with variation in Mg:Ca and temperature rather than an absolute threshold at which mineral phases change. All these studies indicate that several competing or complementing parameters control calcite and aragonite precipitation and that we still lack a good constraint on their formation pathways, both in time and space. These studies also highlight that further experiments designed to test many of the important factors that may influence polymorph selection or dominance must be carried out.

2.2. Carbonate mineralogy

Calcium carbonate minerals are found in nature as nominally anhydrous phases (aragonite, calcite and vaterite), and as hydrated phases (ikaite and monohydrocalcite). Vaterite, which has the largest molar volume of the three anhydrous polymorphs, is metastable, while the relative stabilities of the anhydrous aragonite and calcite are dependent on pressure and temperature (MmxcRAF and Rrnnrn, 1985; Plummer and Busenberg, 1982). Among the three anhydrous phases, calcite is the most stable under ambient conditions while vaterite is the least stable (Plummer and Busenberg, 1982). Similarly, aragonite is the most stable phase at high pressure and low temperatures, while vaterite is thought to be stable at low temperature and pressure (Albright, 1971).

Not surprising, the stability of these phases is influenced by their structure. The structure of calcite is characterized by layers of alternating 6-fold coordinated calcium ions with layers of carbonate ions (Graf, 1961; MmxcRAF and Rrnnrn, 1985). The structure of aragonite resemblances a hexagonal close packed structure, where the calcium ions are 9-fold coordinated. Hence, the aragonite structure is denser compared to the calcite structure (Appelo and Postma, 2005). In contrast, vaterite has a less dense structure compared to calcite and aragonite. However, the exact nature of the vaterite crystal system is still debated. The calcium ions in the vaterite structure have been determined to be either 6 or 8-fold coordinated in a hexagonal sub-lattice (Kamhi, 1963; Le Bail et al., 2011; Meyer, 1969) with carbonate planes aligned roughly parallel to the c-axis (Kamhi, 1963; Meyer, 1969). However, the carbonate ions in the vaterite structure have a high degree of disorder (Le Bail et al., 2011; Medeiros et al., 2007; Meyer, 1969; Wang and Becker, 2009).

Finally, the least stable calcium carbonate phase that has been identified is amorphous calcium carbonate (ACC). Research suggested that nanoparticulate ACC preferentially forms over nanoparticulate crystalline calcium carbonate phases due to a low energetic barrier for ACC nucleation and growth (Raiteri and Gale, 2010; Tribello et al., 2009). However, in nature, ACC has so far predominantly been identified as an intermediate phase during biomineralization (Addadi et al., 2003; Cusack and Freer, 2008; Meldrum and Cölfen, 2008; Weiner and Dove, 2003). Structural characterization of ACC indicates that this phase has no long range (>15 Å) (Goodwin et al., 2010; Michel et al., 2008; Quigley and Rodger, 2008; Rodriguez-Blanco et al., 2008; Rodriguez-Blanco et al., 2011) order and is characterized by calcium rich and carbonate rich regions . The short range order (<15 Å) resembles the short range order of either one or multiple crystalline calcium carbonate phases (Gebauer et al., 2010; Lam et al., 2007; Tribello et al., 2009). When magnesium is in part exchanged for calcium other Ca-Mg phases form (see Table 2.1). Among these, dolomite ($Ca_{0.5}Mg_{0.5}CO_3$) has the same crystal system as calcite but with alternating layers of calcium (and magnesium) and carbonate ions. However, in dolomite every second calcium layer is exchanged for a magnesium layer (Alruopn, 1977).

In seawater reactions, the most important carbonate minerals are the $CaCO_3$ polymorphs aragonite and calcite. The solubility of some carbonate minerals are given in Table 2.1.

Aragonite is both denser and more soluble than calcite. These two phases also differ in their tendency to accept divalent cations other than Ca in solid solution. The general pattern of coprecipitation is governed by the following rule. Cations such as Sr and Ba, whose ionic radii exceed that of Ca (1.00 Å, assuming 6-fold coordination with oxygen) are more frequently accommodated in the orthorhombic aragonite structure, in which cations are in a 9-fold coordination to carbonate oxygens. Conversely, smaller cations such as Mg are found more frequently in the hexagonal calcite structure, in which the cations are in a octahedral (6-fold) coordination with oxygen, each of which belongs to a distinct carbonate phase (Morse et al., 2007).

Table 2. 1: *Stabilities of common carbonate minerals under STP conditions.*

Phase	Formula	$K'_{sp\ (stoich)}$ ($(mol^2kg^{-2}) \times 10^{-7}$)	pK
Aragonite	$CaCO_3$	6.65[7]	8.30[155]
Calcite	$CaCO_3$	4.39[7]	8.48[155]
Magnesite	$MgCO_3$		8.04[9]
Siderite	$FeCO_3$		10.52[9]
Rhodochrosite	$MnCO_3$		10.08[9]
Dolomite	$CaMg(CO_3)_2$		18.15[9]
Kutnahorite	$CaMn(CO_3)_2$		21.81±0.07[10.39]

[a] K´sp (stoich) is the stoichiometric solubility product in seawater. pK values are thermodynamic - $\log K_{sp.}$

2.3. Influence of solution chemistry and physical factors on the formation and stability of $CaCO_3$

Over the last two decades, there has been a continued interest in the effect that chemistry of "foreign" ions present in the common carbonate minerals have on their formation pathways; this is particularly especially true for calcite and aragonite due to their implications for interpreting the chemistry of the Phanerozoic oceans (Burton, 1991; Katz, 1973; Kitano et al., 1971; Lorens and Bender, 1980). As mentioned above, solution chemistry and other physical factors such as temperature have a significant influence on $CaCO_3$ polymorph and crystal morphology of carbonate minerals precipitated from natural waters, and particularly seawater (Morse and Mackenzie, 1990). The carbonate polymorphs that are observed to commonly precipitate are commonly not those which would be predicted via straightforward equilibrium thermodynamic considerations, and in many cases the pathways for formation are a result of complex reaction kinetics (Morse and Casey, 1988). In this context, the role played by foreign ions in the crystallization of minerals can be a consequence of different factors, ranging from their incorporation

in the structure of the crystal during the growth process, both in lattice and non-lattice positions, to their adsorption onto specific sites on crystal surfaces and to modifications of the solvent structure. On the basis of such relationships, variation in abiotic marine (cements and ooids) carbonate-mineral content of marine sediments has been used extensively as a major tool in attempting to unravel the historical dependence of the Earth's global climate on changes in marine and atmospheric chemistry (Berner, 1994; Dickson, 2004; Mackenzie and Morse, 1992; Sandberg, 1985; Wilkinson et al., 1984).

The general interpretation of variation in the dominant carbonate polymorph is that it may reflect changes in the pCO_2 (partial pressure of carbon dioxide) of the paleo-atmosphere, which significantly altered the saturation state of near-surface seawater and global climate, and/or change in the seawater Mg:Ca ratio that was driven by variation in the production rate of oceanic ridges. However, the distribution of carbonate minerals in recent marine sediments appears to be strongly influenced by water temperature: aragonite and high-Mg calcite are dominantly associated with warm tropic to subtropic waters, and low-Mg calcite occurs more abundantly in cooler waters generally found at higher latitudes or in cool deep waters.

Below, the state of the knowledge base around the roles and effects of these main parameters (Mg, SO_4, temperature, pH, and pCO_2) will be reviewed each in turn, to set the scene for the experimental work presented later in this thesis.

2.3.1. Magnesium

Magnesium has a significant influence on calcium carbonate precipitation. In the presence of magnesium in solution, calcium can be exchanged for magnesium in the calcite structure. The amount of Mg incorporated into the calcite structure appears to be primarily controlled by the Mg:Ca ratio in solution and is otherwise largely independent of saturation state and precipitation rate (Burton, 1991; Morse et al., 2007; Morse and Bender, 1990; Mucci and Morse, 1983). However, two recent studies (De Choudens-Sánchez and González, 2009; Lee and Morse, 2010), have shown that both solution Mg:Ca ratio and the saturation state of the solution with respect to calcium carbonate influence the polymorph mineralogy of the calcium carbonate minerals that precipitate from the solution. The Mg ion is more strongly hydrated than Ca and is strongly absorbed onto the surface of growing calcite

crystals. Dehydration of the Mg ions prior to incorporation in the calcite lattice creates a barrier to the growth of calcite nuclei (Lippmann, 2012; Loste et al., 2003b). Magnesian calcite (calcite with magnesium incorporated) is more soluble than pure calcite, which renders this phase energetically less stable (Busenberg and Plummer, 1989; Davis et al., 2004; Lippmann, 1973). The decrease in calcite stability is caused by the introduction of a disorder in the calcite lattice due to the difference in size between the calcium and magnesium ions (Berner, 1975; Mucci and Morse, 1983). However, because the magnesium content, geometry and growth rate, aragonite is less influenced by solution Mg:Ca ratio. Since magnesium incorporation into aragonite is negligible, aragonite will be kinetically favoured when solution Mg:Ca ratios are high (Appelo, 2005; Davis et al., 2000a; Mucci et al., 1985). This observations provides mechanistic support for the experimental and geological evidence that a seawater Mg:Ca ratio about 1-2 divides the calcite (Mg:Ca<1-2) and aragonite (Mg:Ca>1-2) predominance fields. Although vaterite only forms at very low magnesium concentrations, any Mg incorporation into the vaterite structure leads to a significant decrease of its unit cell parameters (0.3 mol% Mg decreases the a-axis by 0.06% and the c-axis by 0.03%) (Bots et al., 2011).

Magnesium becomes preferentially incorporated during growth onto calcite crystal growth steps that propagate in specific crystallographic directions, which causes magnesium incorporation to also alter the morphology and habit of calcite crystals (Davis et al., 2004). Thus, in the presence of magnesium, calcite rhombohedrals have a more rounded appearance than without magnesium (Loste et al., 2003b) .

Magnesium has also shown a significant effect on the pathways and mechanisms of the transformation of ACC into crystalline $CaCO_3$, increasing the stability of ACC and inhibiting vaterite crystallization, favouring the direct transformation of ACC to calcite (Rodriguez-Blanco et al., 2012). The magnesium content of ACC is defined by the Mg:Ca ration in solution, and increases systematically with increasing Mg:Ca (Loste et al., 2003b). In turn, ACC occluding higher magnesium concentrations was significantly more stable than low magnesium ACC.

2.3.2. Sulphate

Sulphate is recognized as a significant coprecipitating anion in marine abiogenic and biogenic calcites. In the presence of sulphate in solution, carbonate is substituted by sulphate in the calcite structure leading to an anisotropic change in its unit cell parameters (1.5 mol% SO_4 incorporation causes the c-axis to increase by 0.22% and the a-axis to decrease by 0.035%) (Bots et al., 2011), which is indicative of the substitution of a planar carbonate for a tetragonal sulphate ion (Busenberg and Niel Plummer, 1985; Kontrec et al., 2004a; Pingitore et al., 1995). Calcite thermodynamic stability decreases when sulphate is incorporated into its structure and its solubility increases (Busenberg and Plummer, 1989; Fernández-Díaz et al., 2010). In magnesium free solutions, sulphate incorporation by calcite tends to increase with the precipitation rate, with increasing inhibition as a function of saturation state (Busenberg and Niel Plummer, 1985). By comparison, relatively little sulphate is taken up in aragonite, and natural marine aragonites typically contain less than 6000 ppm SO_4 (Land and Hoops, 1973; Mucci and Morse, 1983). The effect of sulphate on the aragonite structure is negligible (1.5 mol% SO_4 incorporation causes the c-axis to increase by ~0.07% and the b-axis to increase by ~0.02%) (Bots et al., 2011). Thus, SO_4 ions promote the formation of aragonite with respect to calcite (Bischoff, 1968). Finally, vaterite is the $CaCO_3$ polymorph that best accommodates sulphate groups into its structure (Fernández-Díaz et al., 2010). Interestingly, however the incorporation of sulphate into the vaterite structure does not significantly affect its unit cell parameters (Bots et al., 2011). When sulphate becomes incorporated into the vaterite structure, its thermodynamic stability is enhanced and a decrease in its lattice energy promotes its formation. The incorporation of sulphate into vaterite is linearly correlated with the SO_4:CO_3 ratio in solution (Adabi, 2004). Furthermore, the presence of sulphate has a retarding and inhibiting effect on the transformation of vaterite into aragonite and of aragonite into calcite (Bischoff and Fyfe, 1968; Gleeson et al., 2011; Lippmann, 1973). Thus, an increase in the sulphate concentration promotes the precipitation and stability of either vaterite or aragonite (Bots et al., 2012; Doner and Pratt, 1969; Fernández-Díaz et al., 2010; Yasushi, 1962).

Finally, there is also some evidence that the presence of sulphate in solution has a strong influence on calcium carbonate polymorph crystal size, which decreases as

the relative SO_4 concentration with respect to CO_3^{2-} increases. However, the combined effects, for example between magnesium and sulphate on polymorph composition and predominance, incorporation rates, or polymorph shapes and sizes, are still little understood.

2.3.3. Temperature

Temperature is also known to exert an influence on the polymorph mineralogy of marine carbonates (Burton, 1991; Morse et al., 1997b). The growth rates of aragonite or calcite at equivalent degrees of supersaturation are strong functions of temperature. With increasing temperature and at equivalent saturation states, aragonite growth rates outpace those of calcite. However with decreasing temperatures, the difference between these two rates diminishes and at 5°C calcite and aragonite have similar precipitation rates (Figure. 2.5) (Burton and Walter, 1987).

Experimental evidence seems to also suggest that at any given temperature, variation in precipitation rates have no significant effect on the incorporation of Mg into calcites (Burton and Walter, 1987; Mucci and Morse, 1983). On the other hand, the magnesium incorporation into calcite increases simultaneously with an increase in temperature (Figure 2.6) (Burton, 1991). This increase in magnesium incorporation with increasing temperature will lead to a decrease in calcite stability with respect to aragonite (Busenberg and Niel Plummer, 1989). Hence, the magnesium to calcium ratio at which aragonite precipitation is preferred, decreases as temperature increases (Morse et al., 1997b).

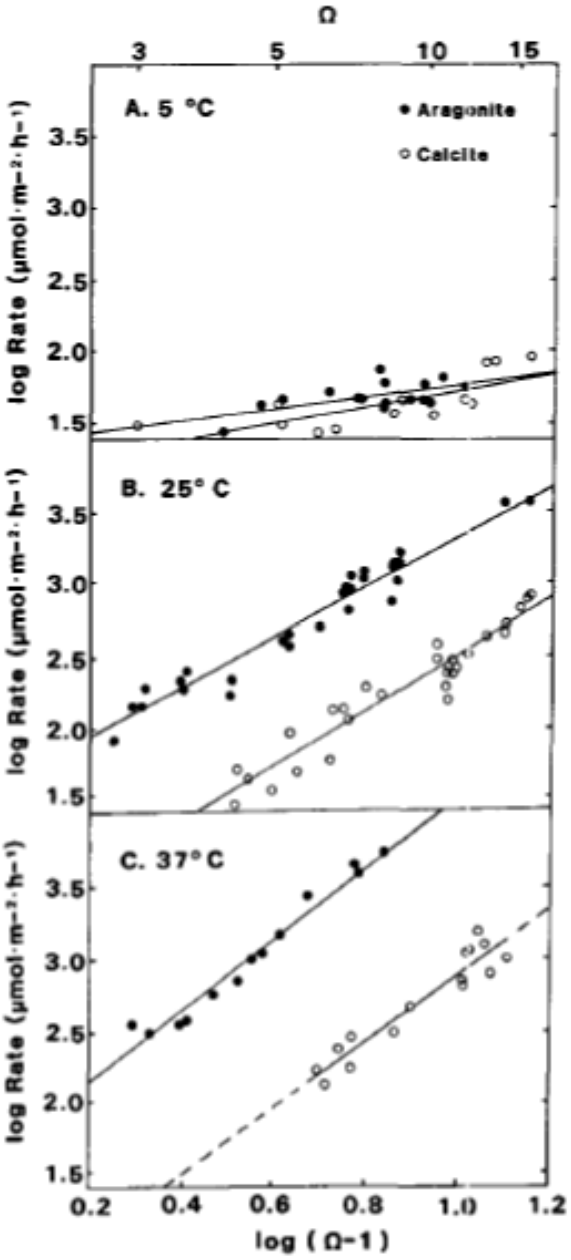

Figure 2. 5: *Precipitation rates of aragonite and calcite normalized to seed surface area as a function of aragonite or calcite saturation state at (A) 5°C, (B) 25°C and (C) 37°C in seawater (Burton and Walter, 1987).*

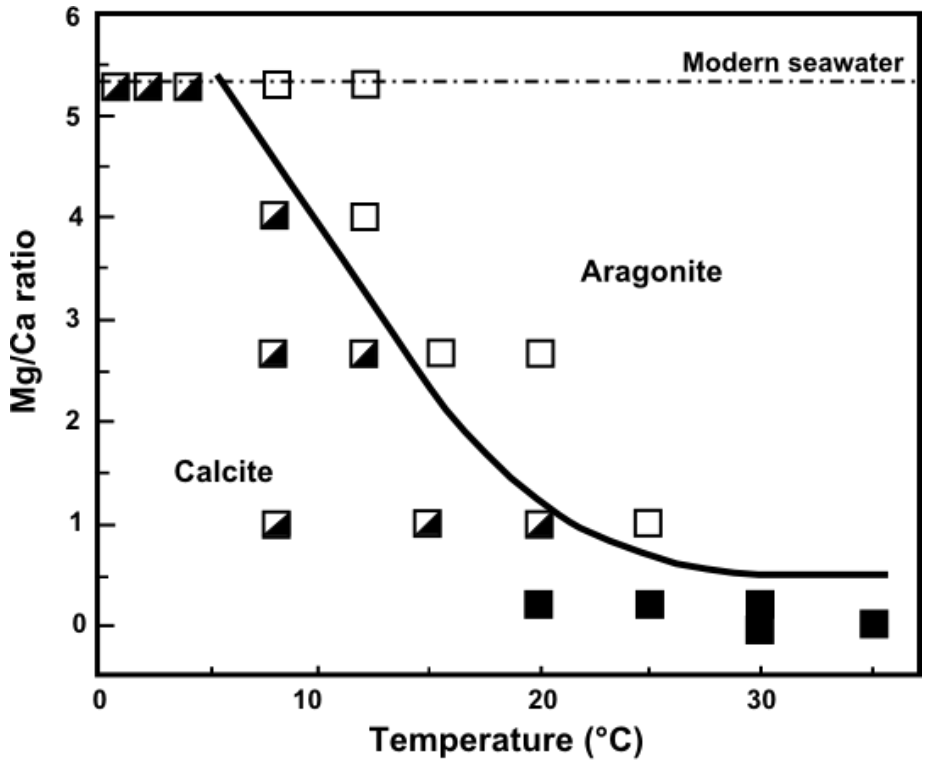

Figure 2. 6: *Influence of temperature and Mg/Ca on the calcium carbonate mineralogy (Morse et al. 1997). White squares are aragonite, black squares are calcite, and split squares are situations in which calcite initially precipitates but then aragonite grows on calcite.*

Experimental studies in general confirm the overall distribution patterns of carbonate cement mineralogies observed in nature. They correctly predict that aragonite cements should be most abundant in warm (shallow, equatorial) to hot (tidal flat) marine environments and that the percentage of Mg incorporated into calcite should decline rapidly with increasing latitude and depth (Burton and Walter, 1987). However, predictive tools that can be used as a quantitative proxy to link analyses of geologic samples with formation palaeo-temperatures are still poorly validated.

2.3.4. pH and pCO_2

At current seawater condition, the percentage of dissolved carbonate species is $[CO_2]$: $[HCO_3^-]$:$[CO_3^{2-}] \approx 0.5\% : 86.5\% : 13\%$. Thus, bicarbonate is the dominant species, followed by the carbonate ion. Dissolved carbon dioxide is present only in small concentrations. This is illustrated in Figure 2.7 by the crossover between the concentration curves and the dashed vertical line at pH= 8.1. Because Figure 2.7

shows the concentration of the carbonate species as a function of pH, one might be tempted to believe that the pH is controlling the concentrations and relative proportions of the carbonate species in the ocean. However, the reverse is true; the carbonate system is the natural buffer for the seawater pH.

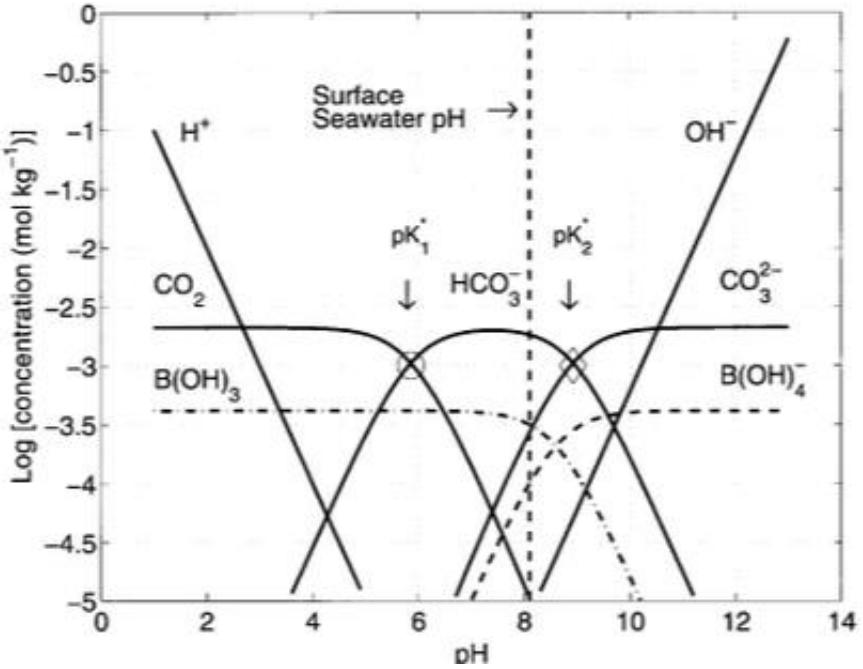

Figure 2. 7: *Carbonate system: Bjerrum plot. DIC= 2.1 mmol/kg; S=35; T= 25°C. The circle and the diamond indicate pK_1*= 5.85 and pK_2*= 8.92 of carbonic acid.*

The current rate of anthropogenic CO_2 release leads to a surface ocean environment characterized not only by elevated dissolved CO_2 and decreased pH (Caldeira and Wickett, 2003) but, critically, by a decreased saturation with respect to calcium carbonates ($CaCO_3$), the compound widely used by marine organisms for the construction of their shells and skeletons. In contrast, slower rates of CO_2 release lead to a different balance in carbonate chemical changes and a smaller seawater $CaCO_3$ saturation response, which may induce differential biotic responses or even no response at all. The reason for a lower saturation response to slow CO_2 release is that alkalinity released by rock weathering on land must ultimately be balanced by the preservation and burial of $CaCO_3$ in marine sediments, which itself is controlled by the calcium carbonate saturation state of the oceans (Ridgwell and Zeebe, 2005). Hence, $CaCO_3$ saturation is ultimately regulated primarily by weathering on long time scales, not atmospheric partial pressure of CO_2 (pCO_2). While weathering itself

is related to atmospheric pCO_2 (Archer et al., 1997), it is related much more weakly than ocean pH, which allows pH and $CaCO_3$ saturation to be almost completely decoupled for slowly increasing atmospheric pCO_2.

So far, several studies have addressed different influences of pH on calcium carbonate precipitation. It has been showed that at pH< 7, bicarbonate is the dominant carbonate species absorbed on calcite surface (Plummer, 1979). In contrast, at pH ≈8.3 carbonate is the dominant species absorbed on calcite structure (Stack and Grantham, 2010). Changes in the pH and alkalinity can also affect the incorporation of sulphate and magnesium. The incorporation of sulphate into calcite is thought to be a function of the aqueous sulphate to carbonate ratio (Busenberg and Niel Plummer, 1985; Takano, 1985). Hence, a change in calcite growth via either carbonate or bicarbonate (due to variations in pH) could also change the incorporation of sulphate into calcite and affect calcite growth kinetics. Additionally, an increase in the concentration of bicarbonate decreases the amount of magnesium incorporated into the calcite structure (Burton, 1991), which could also destabilize calcite with respect to aragonite (Davis et al., 2000a).

As discussed above, many experimental studies have identified various effects of changes in solution chemistry (Mg:Ca ratio and SO_4 concentration) or changes in physical parameters such as temperature have on the formation, transformation and structure of calcium carbonate phases. However, the lack of a synergistic and deterministic approach in currently used experimental approaches and thus also models about the role such parameters have in controlling carbonate mineralogy is a big gap in our knowledge and hinders our predictive capabilities. Thus the relative influence and effects of each of these parameters must be determined in order to assess the total influence of solution chemistry, temperature and pCO_2 on calcium carbonate precipitation.

References

Adabi, M. H., 2004, A re-evaluation of aragonite versus calcite seas: Carbonates and Evaporites, v. 19, no. 2, p. 133.

Addadi, L., Raz, S., and Weiner, S., 2003, Taking Advantage of Disorder: Amorphous Calcium Carbonate and Its Roles in Biomineralization: Advanced Materials, v. 15, no. 12, p. 959-970.

Albright, J. N., 1971, Mineralogical notes vaterite stability: American Mineralogist: Journal of Earth and Planetary Materials, v. 56, no. 3-4_Part_1, p. 620-624.

Alruopn, P. L., 1977, Structural refinements of dolomite and a magnesian calcite and implications for dolomite formation in the marine environment: American Mineralogist, v. 62, p. 772-783.

Appelo, C., and Postma, D., 2005, Geochemistry, groundwater and pollution, CRC: Balkema, Roterdam.

Appelo, C., Postma, D., Appelo, C., 2005, Geochemistry, Groundwater and Pollution: London: CRC Press.

Archer, D., Kheshgi, H., and Maier-Reimer, E., 1997, Multiple timescales for neutralization of fossil fuel CO2: Geophysical Research Letters, v. 24, no. 4, p. 405-408.

Balthasar, U., and Cusack, M., 2015, Aragonite-calcite seas—Quantifying the gray area: Geology, v. 43, no. 2, p. 99-102.

Berner, R. A., 1975, The role of magnesium in the crystal growth of calcite and aragonite from sea water: Geochimica et Cosmochimica Acta, v. 39, no. 4, p. 489-504.

Berner, R. A., 1994, GEOCARB II: A revised model of atmospheric CO[sub 2] over phanerozoic time: American Journal of Science; (United States), p. Medium: X; Size: Pages: 56-91.

Berner, R. A., 2004, A model for calcium, magnesium and sulfate in seawater over Phanerozoic time: American Journal of Science, v. 304, no. 5, p. 438-453.

Bischoff, J. L., 1968, Catalysis, inhibition, and the calcite-aragonite problem; [Part] 2, The vaterite-aragonite transformation: American Journal of Science, v. 266, no. 2, p. 80-90.

Bischoff, J. L., and Fyfe, W., 1968, Catalysis, inhibition, and the calcite-aragonite problem;[Part] 1, The aragonite-calcite transformation: American Journal of Science, v. 266, no. 2, p. 65-79.

Bots, P., Benning, L., Rickaby, R., and Shaw, S., 2011, The role of SO4 in the switch from calcite to aragonite seas: Geology, v. 39, no. 4, p. 331-334.

Bots, P., Benning, L. G., Rodriguez-Blanco, J.-D., Roncal-Herrero, T., and Shaw, S., 2012, Mechanistic insights into the crystallization of amorphous calcium carbonate (ACC): Crystal Growth & Design, v. 12, no. 7, p. 3806-3814.

Bots P. , B. L. G., Rickaby R. E. M., and Shaw S., 2011, The role of SO4 in the switch from calcite to aragonite seas: Geology, v. 39, no. 4, p. 331-334.

Burton, E. A., and Walter, L. M., 1987, Relative precipitation rates of aragonite and Mg calcite from seawater: Temperature or carbonate ion control?: Geology, v. 15, no. 2, p. 111-114.

-, 1991, The effects of PCO2 and temperature on magnesium incorporation in calcite in seawater and MgCl2-CaCl2 solutions: Geochimica et Cosmochimica Acta, v. 55, no. 3, p. 777-785.

Busenberg, E., and Niel Plummer, L., 1985, Kinetic and thermodynamic factors controlling the distribution of SO32− and Na+ in calcites and selected aragonites: Geochimica et Cosmochimica Acta, v. 49, no. 3, p. 713-725.

-, 1989, Thermodynamics of magnesian calcite solid-solutions at 25°C and 1 atm total pressure: Geochimica et Cosmochimica Acta, v. 53, no. 6, p. 1189-1208.

Busenberg, E., and Plummer, L. N., 1989, Thermodynamics of magnesian calcite solid-solutions at 25 C and 1 atm total pressure: Geochimica et Cosmochimica Acta, v. 53, no. 6, p. 1189-1208.

Caldeira, K., and Wickett, M. E., 2003, Anthropogenic carbon and ocean pH: Nature, v. 425, p. 365.

Coggon, R. M., Teagle, D. A. H., Smith-Duque, C. E., Alt, J. C., and Cooper, M. J., 2010, Reconstructing Past Seawater Mg/Ca and Sr/Ca from Mid-Ocean Ridge Flank Calcium Carbonate Veins: Science, v. 327, no. 5969, p. 1114-1117.

Cohen, A. L., Owens, K. E., Layne, G. D., and Shimizu, N., 2002, The Effect of Algal Symbionts on the Accuracy of Sr/Ca Paleotemperatures from Coral: Science, v. 296, no. 5566, p. 331-333.

Cusack, M., and Freer, A., 2008, Biomineralization: Elemental and Organic Influence in Carbonate Systems: Chemical Reviews, v. 108, no. 11, p. 4433-4454.

Davis, K. J., Dove, P. M., and De Yoreo, J. J., 2000, The role of Mg2+ as an impurity in calcite growth: Science, v. 290, no. 5494, p. 1134-1137.

Davis, K. J., Dove, P. M., Wasylenki, L. E., and De Yoreo, J. J., 2004, Morphological consequences of differential Mg2+ incorporation at structurally distinct steps on calcite: American Mineralogist, v. 89, no. 5-6, p. 714-720.

De Choudens-Sánchez, V., and González, L. A., 2009, Calcite and Aragonite Precipitation Under Controlled Instantaneous Supersaturation: Elucidating the Role of CaCO3 Saturation State and Mg/Ca Ratio on Calcium Carbonate Polymorphism: Journal of Sedimentary Research, v. 79, no. 6, p. 363-376.

de Villiers, S., Dickson, J. A. D., and Ellam, R. M., 2005, The composition of the continental river weathering flux deduced from seawater Mg isotopes: Chemical Geology, v. 216, no. 1, p. 133-142.

Dickson, J. A. D., 2002, Fossil Echinoderms As Monitor of the Mg/Ca Ratio of Phanerozoic Oceans: Science, v. 298, no. 5596, p. 1222-1224.

-, 2004, Echinoderm Skeletal Preservation: Calcite-Aragonite Seas and the Mg/Ca Ratio of Phanerozoic Oceans: Journal of Sedimentary Research, v. 74, no. 3, p. 355-365.

Doner, H. E., and Pratt, P. F., 1969, Solubility of Calcium Carbonate Precipitated in Aqueous Solutions of Magnesium and Sulfate Salts1: Soil Science Society of America Journal, v. 33, no. 5, p. 690-693.

Fernández-Díaz, L., Fernández-González, Á., and Prieto, M., 2010, The role of sulfate groups in controlling CaCO3 polymorphism: Geochimica et Cosmochimica Acta, v. 74, no. 21, p. 6064-6076.

Folk, R. L., 1974, The natural history of crystalline calcium carbonate; effect of magnesium content and salinity: Journal of Sedimentary Research, v. 44, no. 1, p. 40-53.

Gebauer, D., Gunawidjaja, P. N., Ko, J. Y. P., Bacsik, Z., Aziz, B., Liu, L., Hu, Y., Bergström, L., Tai, C.-W., Sham, T.-K., Edén, M., and Hedin, N., 2010, Proto-Calcite and Proto-Vaterite in Amorphous Calcium Carbonates: Angewandte Chemie International Edition, v. 49, no. 47, p. 8889-8891.

Gleeson, D. F., WILLIAMSON, C., GRASBY, S. E., PAPPALARDO, R. T., SPEAR, J. R., and TEMPLETON, A. S., 2011, Low temperature S0 biomineralization at a supraglacial spring system in the Canadian High Arctic: Geobiology, v. 9, no. 4, p. 360-375.

Goodwin, A. L., Michel, F. M., Phillips, B. L., Keen, D. A., Dove, M. T., and Reeder, R. J., 2010, Nanoporous Structure and Medium-Range Order in Synthetic Amorphous Calcium Carbonate: Chemistry of Materials, v. 22, no. 10, p. 3197-3205.

Graf, D. L., 1961, Crystallographic tables for the rhombohedral carbonates: American Mineralogist: Journal of Earth and Planetary Materials, v. 46, no. 11-12, p. 1283-1316.

Hardie, L. A., 1990, The roles of rifting and hydrothermal CaCl 2 brines in the origin of potash evaporites; an hypothesis: American Journal of Science, v. 290, no. 1, p. 43-106.

Hardie, L. A., 1991, On the Significance of Evaporites: Annual Review of Earth and Planetary Sciences, v. 19, no. 1, p. 131-168.

Hardie, L. A., 1996, Secular variation in seawater chemistry: An explanation for the coupled secular variation in the mineralogies of marine limestones and potash evaporites over the past 600 m.y: Geology, v. 24, no. 3, p. 279-283.

Holland, H. D., 2005, Sea level, sediments and the composition of seawater: American Journal of Science, v. 305, no. 3, p. 220-239.

Holland, H. D., Horita, J., and Seyfried, J. W. E., 1996, On the secular variations in the composition of Phanerozoic marine potash evaporites: Geology, v. 24, no. 11, p. 993-996.

Horita, J., Zimmermann, H., and Holland, H. D., 2002, Chemical evolution of seawater during the Phanerozoic: Implications from the record of marine evaporites: Geochimica et Cosmochimica Acta, v. 66, no. 21, p. 3733-3756.

Kamhi, S. R., 1963, On the structure of vaterite CaCO3: Acta Crystallographica, v. 16, no. 8, p. 770-772.

Katz, A., 1973, The interaction of magnesium with calcite during crystal growth at 25–90°C and one atmosphere: Geochimica et Cosmochimica Acta, v. 37, no. 6, p. 1563-1586.

Kitano, Y., Kanamori, N., and Oomori, T., 1971, Measurements of distribution coefficients and barium between carbonate precipitate —Abnormally high values of distribution measured at early stages of carbonate of strontium and solution coefficients formation: GEOCHEMICAL JOURNAL, v. 4, no. 4, p. 183-206.

Kontrec, J., Kralj, D., Brečević, L., Falini, G., Fermani, S., Noethig-Laslo, V., and Mirosavljević, K., 2004, Incorporation of Inorganic Anions in Calcite: European Journal of Inorganic Chemistry, v. 2004, no. 23, p. 4579-4585.

Lam, R. S. K., Charnock, J. M., Lennie, A., and Meldrum, F. C., 2007, Synthesis-dependant structural variations in amorphous calcium carbonate: CrystEngComm, v. 9, no. 12, p. 1226-1236.

Land, L. S., and Hoops, G. K., 1973, Sodium in carbonate sediments and rocks; a possible index to the salinity of diagenetic solutions: Journal of Sedimentary Research, v. 43, no. 3, p. 614-617.

Le Bail, A., Ouhenia, S., and Chateigner, D., 2011, Microtwinning hypothesis for a more ordered vaterite model: Powder Diffraction, v. 26, no. 1, p. 16-21.

Lear, C. H., Elderfield, H., and Wilson, P. A., 2000, Cenozoic Deep-Sea Temperatures and Global Ice Volumes from Mg/Ca in Benthic Foraminiferal Calcite: Science, v. 287, no. 5451, p. 269-272.

Lear, C. H., Rosenthal, Y., and Slowey, N., 2002, Benthic foraminiferal Mg/Ca-paleothermometry: a revised core-top calibration: Geochimica et Cosmochimica Acta, v. 66, no. 19, p. 3375-3387.

Lee, J., and Morse, J. W., 2010, Influences of alkalinity and pCO2 on CaCO3 nucleation from estimated Cretaceous composition seawater representative of “calcite seas”: Geology, v. 38, no. 2, p. 115-118.

Lippmann, F., 1973, Sedimentary Carbonate Minerals: Springer.

-, 2012, Sedimentary Carbonate Minerals: Science & Business Media.

Lorens, R. B., and Bender, M. L., 1980, The impact of solution chemistry on Mytilus edulis calcite and aragonite: Geochimica et Cosmochimica Acta, v. 44, no. 9, p. 1265-1278.

Loste, E., Wilson, R. M., Seshadri, R., and Meldrum, F. C., 2003, The role of magnesium in stabilising amorphous calcium carbonate and controlling calcite morphologies: Journal of Crystal Growth, v. 254, no. 1, p. 206-218.

Lowenstein, T. K., Hardie, L. A., Timofeeff, M. N., and Demicco, R. V., 2003, Secular variation in seawater chemistry and the origin of calcium chloride basinal brines: Geology, v. 31, no. 10, p. 857-860.

Lowenstein, T. K., Timofeeff, M. N., Brennan, S. T., Hardie, L. A., and Demicco, R. V., 2001, Oscillations in Phanerozoic Seawater Chemistry: Evidence from Fluid Inclusions: Science, v. 294, no. 5544, p. 1086-1088.

Mackenzie, F. T., and Morse, J. W., 1992, Sedimentary carbonates through Phanerozoic time: Geochimica et Cosmochimica Acta, v. 56, no. 8, p. 3281-3295.

Martin, R. E., 1995, Cyclic and secular variation in microfossil biomineralization: clues to the biogeochemical evolution of Phanerozoic oceans: Global and Planetary Change, v. 11, no. 1, p. 1-23.

Medeiros, S., Albuquerque, E., Maia Jr, F., Caetano, E., and Freire, V., 2007, First-principles calculations of structural, electronic, and optical absorption properties of CaCO3 Vaterite: Chemical Physics Letters, v. 435, no. 1-3, p. 59-64.

Meldrum, F. C., and Cölfen, H., 2008, Controlling Mineral Morphologies and Structures in Biological and Synthetic Systems: Chemical Reviews, v. 108, no. 11, p. 4332-4432.

Meyer, H., 1969, Struktur und fehlordnung des vaterits: Zeitschrift für Kristallographie-Crystalline Materials, v. 128, no. 1-6, p. 183-212.

Michel, F. M., MacDonald, J., Feng, J., Phillips, B. L., Ehm, L., Tarabrella, C., Parise, J. B., and Reeder, R. J., 2008, Structural Characteristics of Synthetic Amorphous Calcium Carbonate: Chemistry of Materials, v. 20, no. 14, p. 4720-4728.

MmxcRAF, S., and Rrnnrn, R., 1985, High-temperature structure refinements of calcite and magnesite: American Mineralogist, v. 70, p. 590400.

Morse, J. W., Arvidson, R. S., and Lüttge, A., 2007, Calcium Carbonate Formation and Dissolution: Chemical Reviews, v. 107, no. 2, p. 342-381.

Morse, J. W., and Bender, M. L., 1990, Partition coefficients in calcite: Examination of factors influencing the validity of experimental results and their application to natural systems: Chemical Geology, v. 82, p. 265-277.

Morse, J. W., and Casey, W. H., 1988, Ostwald processes and mineral paragenesis in sediments: American Journal of Science, v. 288, no. 6, p. 537-560.

Morse, J. W., and Mackenzie, F. T., 1990, Geochemistry of sedimentary carbonates, Elsevier.

Morse, J. W., Wang, Q., and Tsio, M. Y., 1997, Influences of temperature and Mg:Ca ratio on CaCO3 precipitates from seawater: Geology, v. 25, no. 1, p. 85-87.

Mucci, A., and Morse, J. W., 1983, The incorporation of Mg2+ and Sr2+ into calcite overgrowths: influences of growth rate and solution composition: Geochimica et Cosmochimica Acta, v. 47, no. 2, p. 217-233.

Mucci, A., Morse, J. W., and Kaminsky, M. S., 1985, Auger spectroscopy analysis of magnesian calcite overgrowths precipitated from seawater and solutions of similar composition: Am. J. Sci.; (United States), p. Medium: X; Size: Pages: 289-305.

Pingitore, N. E., Meitzner, G., and Love, K. M., 1995, Identification of sulfate in natural carbonates by x-ray absorption spectroscopy: Geochimica et Cosmochimica Acta, v. 59, no. 12, p. 2477-2483.

Plummer, L. N., 1979, Critical review of the kinetics of calcite dissolution and precipitation: Chemical Modeling in Aqueous Systems., p. 539-573.

Plummer, L. N., and Busenberg, E., 1982, The solubilities of calcite, aragonite and vaterite in CO2-H2O solutions between 0 and 90 C, and an evaluation of the aqueous model for the system CaCO3-CO2-H2O: Geochimica et Cosmochimica Acta, v. 46, no. 6, p. 1011-1040.

Quigley, D., and Rodger, P. M., 2008, Free energy and structure of calcium carbonate nanoparticles during early stages of crystallization: The Journal of Chemical Physics, v. 128, no. 22, p. 221101.

Railsback, L. B., and Anderson, T. F., 1987, Control of Triassic seawater chemistry and temperature on the evolution of post-Paleozoic aragonite-secreting faunas: Geology, v. 15, no. 11, p. 1002-1005.

Raiteri, P., and Gale, J. D., 2010, Water is the key to nonclassical nucleation of amorphous calcium carbonate: Journal of the American Chemical Society, v. 132, no. 49, p. 17623-17634.

Ridgwell, A., and Zeebe, R. E., 2005, The role of the global carbonate cycle in the regulation and evolution of the Earth system: Earth and Planetary Science Letters, v. 234, no. 3, p. 299-315.

Rodriguez-Blanco, J., Shaw, S., and Benning, L., 2008, How to make 'stable'ACC: protocol and preliminary structural characterization: Mineralogical Magazine, v. 72, no. 1, p. 283-286.

Rodriguez-Blanco, J. D., Shaw, S., and Benning, L. G., 2011, The kinetics and mechanisms of amorphous calcium carbonate (ACC) crystallization to calcite, via vaterite: Nanoscale, v. 3, no. 1, p. 265-271.

Rodriguez-Blanco, J. D., Shaw, S., Bots, P., Roncal-Herrero, T., and Benning, L. G., 2012, The role of pH and Mg on the stability and crystallization of amorphous calcium carbonate: Journal of Alloys and Compounds, v. 536, p. S477-S479.

Sandberg, P. A., 1983, An oscillating trend in Phanerozoic non-skeletal carbonate mineralogy: Nature, v. 305, p. 19.

Sandberg, P. A., 1985, Nonskeletal Aragonite and pCO2 in the Phanerozoic and Proterozoic, The Carbon Cycle and Atmospheric CO2: Natural Variations Archean to Present, p. 585-594.

Spencer, R., and Hardie, L., 1990, Control of seawater composition by mixing of river waters and mid-ocean ridge hydrothermal brines: Fluid-mineral interactions: A tribute to HP Eugster: Geochemical Society Special Publication, v. 19, p. 409-419.

Stack, A. G., and Grantham, M. C., 2010, Growth Rate of Calcite Steps As a Function of Aqueous Calcium-to-Carbonate Ratio: Independent Attachment and Detachment of Calcium and Carbonate Ions: Crystal Growth & Design, v. 10, no. 3, p. 1409-1413.

Stanley, S. M., 2006, Influence of seawater chemistry on biomineralization throughout phanerozoic time: Paleontological and experimental evidence: Palaeogeography, Palaeoclimatology, Palaeoecology, v. 232, no. 2, p. 214-236.

Stanley, S. M., and Hardie, L. A., 1998, Secular oscillations in the carbonate mineralogy of reef-building and sediment-producing organisms driven by tectonically forced shifts in seawater chemistry: Palaeogeography, Palaeoclimatology, Palaeoecology, v. 144, no. 1, p. 3-19.

Takano, B., 1985, Geochemical implications of sulfate in sedimentary carbonates: Chemical Geology, v. 49, no. 4, p. 393-403.

Tribello, G. A., Bruneval, F., Liew, C., and Parrinello, M., 2009, A Molecular Dynamics Study of the Early Stages of Calcium Carbonate Growth: The Journal of Physical Chemistry B, v. 113, no. 34, p. 11680-11687.

Volodymyr M. Kovalevich, Tadeusz Marek Peryt, and Oleg I. Petrichenko, 1998, Secular Variation in Seawater Chemistry during the Phanerozoic as Indicated by Brine Inclusions in Halite: The Journal of Geology, v. 106, no. 6, p. 695-712.

Wallmann, K., 2001, Controls on the cretaceous and cenozoic evolution of seawater composition, atmospheric CO2 and climate: Geochimica et Cosmochimica Acta, v. 65, no. 18, p. 3005-3025.

Wang, J., and Becker, U., 2009, Structure and carbonate orientation of vaterite (CaCO3): American Mineralogist, v. 94, no. 2-3, p. 380-386.

Weiner, S., and Dove, P. M., 2003, An Overview of Biomineralization Processes and the Problem of the Vital Effect: Reviews in Mineralogy and Geochemistry, v. 54, no. 1, p. 1-29.

Wilkinson, B. H., and Algeo, T. J., 1989, Sedimentary carbonate record of calcium-magnesium cycling: American Journal of Science, v. 289, no. 10, p. 1158-1194.

Wilkinson, B. H., Buczynski, C., and Owen, R. M., 1984, Chemical control of carbonate phases; implications from Upper Pennsylvanian calcite-aragonite ooids of southeastern Kansas: Journal of Sedimentary Research, v. 54, no. 3, p. 932-947.

Wilkinson, B. H., and Given, R. K., 1986, Secular Variation in Abiotic Marine Carbonates: Constraints on Phanerozoic Atmospheric Carbon Dioxide Contents and Oceanic Mg/Ca Ratios: The Journal of Geology, v. 94, no. 3, p. 321-333.

Wilkinson, B. H., Owen, R. M., and Carroll, A. R., 1985, Submarine hydrothermal weathering, global eustasy, and carbonate polymorphism in Phanerozoic marine oolites: Journal of Sedimentary Research, v. 55, no. 2, p. 171-183.

Yasushi, K., 1962, The Behavior of Various Inorganic Ions in the Separation of Calcium Carbonate from a Bicarbonate Solution: Bulletin of the Chemical Society of Japan, v. 35, no. 12, p. 1973-1980.

Zhuravlev, A. Y., and Wood, R. A., 2009, Controls on carbonate skeletal mineralogy: Global CO2 evolution and mass extinctions: Geology, v. 37, no. 12, p. 1123-1126.

Zimmermann, H., 2000, Tertiary seawater chemistry; implications from primary fluid inclusions in marine halite: American Journal of Science, v. 300, no. 10, p. 723-767.

Chapter 3
Material and Methods

In this chapter, the experimental and analytical methods are described. The descriptions here overlap with the method descriptions in later chapters. This is done to keep the results chapters self-explanatory.

3.1. Laboratory based experimental methods

The two mineral synthesis methods described below were designed and used to examine the interaction between solution chemistry, temperature and pCO_2 and the precipitated calcium carbonate mineralogy. The results from the constant addition experiments at different temperatures are described in Chapter 4 and Appendix A and the results from constant addition experiments at different pCO_2 values are described in Chapter 5 and Appendix B.

3.1.1. Constant addition experiments at different temperatures

Calcium carbonate precipitation was performed using constant addition experiments ranging the sulfate and magnesium concentrations suggested for Phanerozoic seawater (Horita et al., 2002) and at three different temperatures (5, 21 and 35°C). At 21 °C (± 1°C), a constant addition batch reactor set-up was used (Bots P. , 2011), while at 5 and 35 °C, the whole experimental setup (Figure 3.1) was placed in a cooling / heating incubator (Binder). Calcium carbonate precipitation was induced by continuous injection of two separate $CaCl_2 \cdot 2H_2O$ (250 mM) + $MgCl_2 \cdot 6H_2O$ (0 – 110 mM) and Na_2CO_3 (230 mM) + Na_2SO_4 (0 – 220 mM) solutions into an atmospherically pre-equilibrated seawater solution. Injection was done via a syringe pump at a flow rate of 1.0 ml/h for 48 hours (see A.6 for justification of these experimental conditions). The initial seawater was prepared by dissolving NaCl to reach seawater salinity (Kester et al., 1967) and 10 mM $CaCl_2 \cdot 2H_2O$. In addition, we varied the concentrations of magnesium and sulfate by adding adequate amounts of $MgCl_2 \cdot 6H_2O$ (0-55 mM) and Na_2SO_4 (0-110 mM) to the batch solution. Finally, in order to mimic oöid formation in seawater, we added glass spheres (BioSpec Products 2g/l) as precipitation substrates. Once prepared, each seawater batch

solution was equilibrated with the atmosphere for at least 3 days in an open beaker (with a porous plug), while shaking at 270 rpm on an orbital shaker to ensure homogeneous conditions. Before injection, the pH of the seawater solution was adjusted by adding 2N NaOH drop wise until a pH ≈8.1 and an alkalinity of ≈1.6 mM was reached. The pH profile of the whole experiments (prior and during injection) was recorded at a rate of ≈1 measurement every 10 minutes.

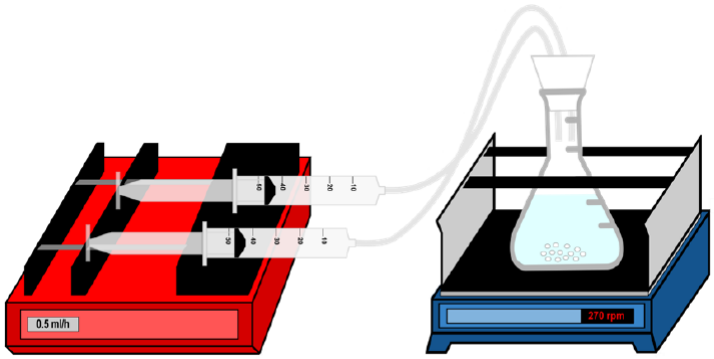

Figure 3.1: *Schematic representation of constant addition experiments at different temperatures*

Sample aliquots (≈5ml) were extracted from the reacting solutions throughout each experiment and immediately filtered through 0.2 µm syringe filters. Solutions were diluted and acidified with HCl 1%, stored cooled (5°C) for analyses of the aqueous sulfate, calcium and magnesium concentrations. After either, 48 or 96 hour post injection initiation, the whole batch was filtered through 0.2 µm polycarbonate track etch membrane filters using a vacuum pump to separate the precipitated $CaCO_3$ from the aqueous solutions for analyses. The solid samples were washed (using Milli-Q water equilibrated with $CaCO_3$), dried at 35 °C and stored at room temperature until further analyses. When experiments were carried out at 5 or 35 °C the separated solution and solid samples were filtered, dried and stored at their respective experimental temperatures.

3.1.2. Constant addition experiments at different pCO_2 values.

Calcium carbonate ($CaCO_3$) precipitation was performed using constant addition experiments at a range of CO_2 concentrations spanning modern and ancient values (pCO_2= 400, 1500 and 3000 ppm), at 21°C (± 1°C) and a representative range of Phanerozoic Mg:Ca ratios and SO_4 seawater concentrations (Horita et al., 2002).

The experimental set-up is shown in Figure 3.2. $CaCO_3$ precipitation is induced by continuous injection of two separate $CaCl_2 \cdot 2H_2O$ (250 mM) + $MgCl_2 \cdot 6H_2O$ (0 – 110 mM) and Na_2CO_3 (230 mM) + Na_2SO_4 (0 – 220 mM) solutions into a seawater solution. Injection was done using two peristaltic pumps at a flow rate of 1.0 ml/h for 48 hours. The initial seawater solution was prepared by dissolving 10 mM $CaCl_2 \cdot 2H_2O$, and appropriate amounts of $MgCl_2 \cdot 6H_2O$ (0-55 mM) and Na_2SO_4 (0-110 mM) to produce the required Mg:Ca ratio and SO_4 concentration, and NaCl to produce a salinity of 35‰ (Kester et al., 1967). In order to mimic oöid formation in seawater, we added glass spheres (BioSpec Products 2g/l) as precipitation substrates. Before injection, the initial seawater solution and the two inlet solutions ($CaCl_2 \cdot 2H_2O$ + $MgCl_2 \cdot 6H_2O$ and Na_2CO_3 + Na_2SO_4) were allowed to equilibrate with the given pCO_2 for at least 3 days. Pumping of the inlet solutions at a constant rate together with continuous bubbling of an air/CO_2 gas mixture in the reactor (P≈ 1 bar) lead to the attainment of a steady-state pH (± 0.05) during $CaCO_3$ precipitation. To minimize evaporation, the air/CO_2 gas mixture is bubbled in a 0.4 M NaCl solution prior to its introduction in the reactor vessel and in the inlet solutions vessels. Once steady-state was reached, the pH of the seawater solution equilibrated with an air/CO_2 gas of 400 ppm pCO_2 was 8.2 ± 0.05. When the pCO_2 of the air/CO_2 gas was 1500 and 3000 ppm, the pH of the seawater solution was 7.8 ± 0.05 and 7.6 ± 0.05 respectively (Figure B.1). To ensure homogeneous conditions, the reactor vessel is shaken at 270 rpm on an orbital shaker during the course of a run. Sample aliquots (≈5ml) were extracted from the reacting solutions throughout each experiment and immediately filtered through 0.2 μm syringe filters. Sub-samples were diluted and acidified with HCl 1%, and stored cooled (5°C) for analyses of the aqueous sulfate, calcium and magnesium concentrations. pH and alkalinity were determined in a second sub-sample. To get a more detailed pH profile of the whole experiment (prior and during injection) for each given pCO_2, the pH was recorded at a rate of ≈1 measurement every 10 minutes in two of each set of experiments at a given pCO_2 (Figure B.1). After 48 hour post injection initiation, the whole batch was filtered through 0.2 μm polycarbonate track etch membrane filters using a vacuum pump to separate the precipitated $CaCO_3$ from the aqueous solutions for analyses. The solid samples were washed (using Milli-Q water equilibrated with $CaCO_3$), dried at 35 °C and stored at room temperature until further analyses.

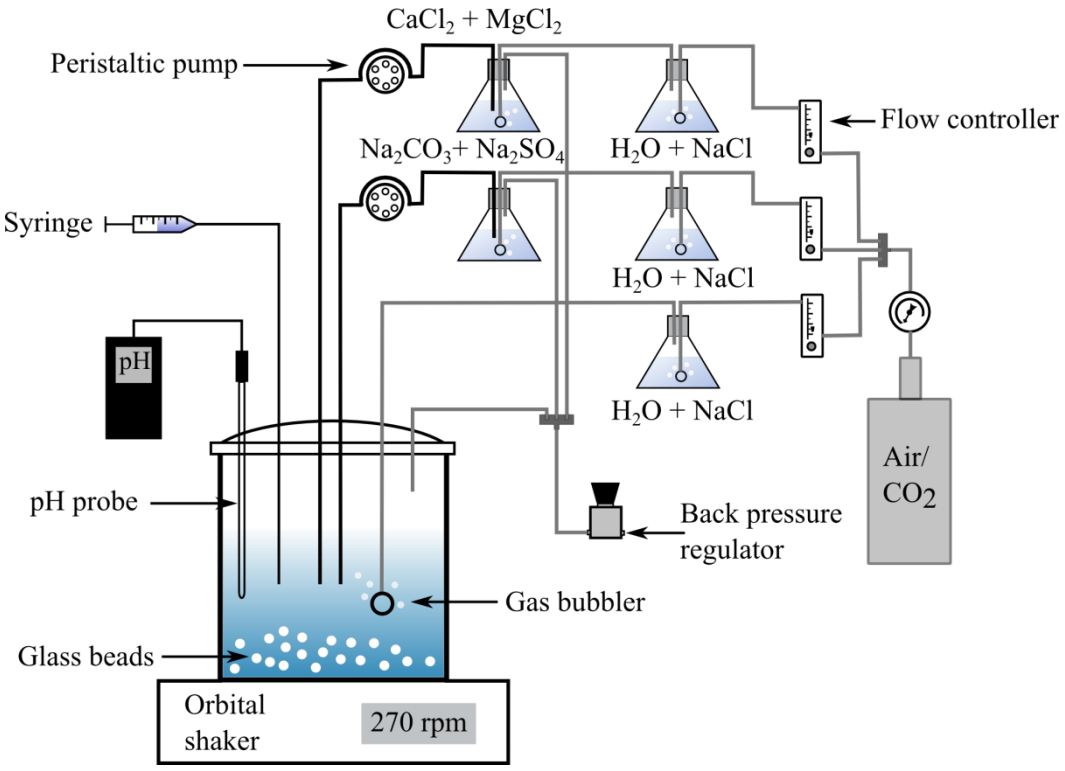

Figure 3.2: *Experimental set-up for constant addition experiments at different pCO_2 values.*

3.2. Laboratory based analytical methods

This section briefly describes the analytical methods used in this thesis.

3.2.1. X-ray diffraction

Solid samples were mineralogically characterized by X-ray powder diffraction (XRD) with a silicon internal standard, using a Bruker D8 X-Ray Diffractometer (Cu kα_1). Scans were collected from 2 to 85° (2θ) and a quantitative estimate of the relative proportion of the precipitated $CaCO_3$ polymorphs and their unit cell parameters were performed with Topas 4-2®.

3.2.2. Scanning Electron Microscopy

The solid reaction products were mounted on Scanning Electron Microscopy stubs using conducting carbon tape and were sputter-coated with a ≈20 nm layer of carbon prior to viewing. Morphology and size of the precipitated $CaCO_3$ particles were characterized by SEM using a field emission gun scanning electron microscope

(FEG SEM, FEI Quanta 650) operating at 10 keV. From each SEM image, size parameters of the precipitated particles were evaluated using ImageJ software.

3.2.3. Electron Microprobe Analysis

To analyse the concentration of Ca, Mg and S in each of the polymorphs present in the solid reaction products, powder aliquots were embedded in epoxy, polished, carbon-coated and analysed by electron probe microanalysis (EPMA) using a JEOL Hyperprobe JXA-8500F with a thermal field-emission cathode. Si analysis were also performed in order to obtain a parameter which allowed us to detect whether we were analysing only $CaCO_3$ crystals or when part of a glass bead was also present in the selected area of interest. For quantitative chemical analysis the electron probe was operated at 15 kV acceleration voltage, 5 nA beam current and 1 µm spot size. Standardization was done with dolomite (for Mg and Ca), ZnS (for S) and tugtupite (for Si). Counting times on peak and background were 30 and 15 seconds respectively for Mg and S and 10 and 5 seconds respectively for Ca and Si.

The detection limits of our EPMA were approximately 312 ppm for Ca, 164 ppm for Mg, 272 ppm for S and 345 ppm for Si. To have a reliable statistical study at least 10 different crystals of each polymorph present in each sample were analysed. Those analyses with anomalously high concentrations of Si were assumed to have been contaminated by matrix silicates and so were removed from the datasets.

3.2.4. Dissolved Mg, Ca and S by Inductively-Coupled Plasma Mass Spectrometry and Optical Emission Spectroscopy (ICP-MS/OES)

The ICP-MS/OES is an analytical technique used for elemental determination that combines a high temperature ICP source with a mass spectrometer or an optical emission spectrometer. The instrument is capable to detect metals and several non-metals at very low concentrations (often at parts per trillion levels). Samples are introduced, and then atoms within the samples are ionized by the ICP source. These ions are then separated and detected by the mass spectrometer (Jarvis et al., 1992). The analysis of dissolved metals was performed using a Thermo Scientific iCAP7400 ICP-OES with an analytical uncertainty $\leq 3\%$ and a detection limit of

0.007, 0.04 and 0.005 for Mg, Ca and S respectively. Precipitates were digested by dissolving a powder aliquot in HCl 1% and diluting with Milli-Q water.

3.3. Scanning Transmission X-ray Microscopy (STXM)

A NEXAFS spectrum measures the absorption of X-rays at and above (to +150 eV) the ionization energy (or "absorption edge") of an element. Specific elements within a sample can be targeted because of their unique ionization energies.

The position of the absorption edge is influenced by the electronic structure of the atom, and features of the post absorption edge region are defined by multiple scattering from the atom´s next-nearest-neighbours. For example, the features of a NEXAFS Mg-spectrum are determined by the Mg coordination: the number, arrangement and species of its nearest-neighbour atoms, and in turn their environment (what else they are bonded to) – everything that influences the local electronic structure around the atom of interest. In the consideration of these Mg spectra, it is important to note that only the immediate environment around the Mg is relevant, and not the long-range structure of the whole phase.

3.3.1. Sample preparation

Calcite, vaterite, aragonite or mixtures were synthesized using a constant addition approach detailed above. Mixed phases were produced at Mg:Ca ratios of 1 to 6, SO_4 concentrations between 0 and 110 mM, temperature from 5 to 35°C and at a partial pressure of CO_2 of 400, 1500 and 3000 ppm using the above described methods.

In brief, prior to STXM analyses, the bulk mineralogical composition and phase distribution was determined by X-Ray diffraction (XRD) with a silicon internal standard, using a Bruker D8 X-Ray Diffractometer (Cu kα_1). Scans were collected from 2 to 85° (2θ) and a quantitative estimate of the relative proportion of the precipitated $CaCO_3$ polymorphs and their unit cell parameters were performed with Topas 4-2®. Samples were dissolved and analysed with inductively coupled optical emission spectroscopy (ICP-OES) to determine bulk elemental contents, with a focus specifically on Mg and SO_4. For spatially resolved analyses, samples were embedded in epoxy resin and polished to expose the edges of the $CaCO_3$ particles.

The polished surfaces were carbon coated and analysed by electron microprobe (EPMA) as described in detail in this chapter and specifically with respect to Mg, Ca and S to determine their spatial distributions. Focused ion beam (FIB) foils were cut from the samples and analysed by transmission electron microscopy (TEM) together with energy dispersive X-Ray spectroscopy (EDS). Several trials with highly-spatially resolved electron energy loss spectroscopy (EELS) analyses were attempted but this was not feasible due to beam damage issues even after short exposures.

For the subsequent STXM analyses, we selected 20 samples (See Table 7.1 in Chapter 7) representing relevant seawater conditions. These samples were pre-imaged with a scanning electron microscope to cross-confirm the mineralogy of the polymorphs in each section and to find adequate STXM analyses areas. Then the selected areas were analysed by EPMA as described above. Following this pre-analyses, the FIB foils were cut from adjacent crystals. Depending on the element to be analysed the FIB foils were cut to different thicknesses. For Mg FIB foils of ≈ 2μm were cut, while for S ≈ 10μm to ≈ 25μm were cut, depending on total concentration as analysed by EMPA. The adequate thickness of the FIB foils depending on their use for either, Mg or S analysis, was determined through a Rapid Access test we did at Diamond Light Source previously to our first STXM beamtime. FIB sections were deposited on 3 mm Si_3N_4 membranes and were imaged and analysed spectrally across the Mg and S edges. In addition to the FIB foils, we also analysed powdered samples (See Table 7.1 in Chapter 7). In such cases for STXM analysis, the powdered sample was mixed with isopropanol and dispersed in an ultrasonic bath. A small quantity of these samples were pipetted onto 3 mm EM Au grids, transferred to a STXM sample holder and mounted on the beamline for analyses.

3.3.2. STXM data acquisition and pre-analysis

X-Ray absorption near structure spectroscopy (XANES) was used to characterize magnesium and sulphur incorporation in the series of synthetic $CaCO_3$ samples.

Data were collected at Canadian Light Source (beamline 10ID-1) and Diamond Light Source (beamline I08). Mg μ-XANES energy stacks were collected over the full Mg K-edge from 1305 to 1360 eV and at a spectral resolution of 0.1 – 0.2 eV.

We used a dwell time of 10 ms and a spatial resolution of 400 nm/pixel resolution. We collected S μ-XANES energy stacks over the full S K-edge from 2460 to 2520 eV, at a spatial resolution of 0.2 eV, dwell time of 10 ms and a spatial resolution of 200 – 600 nm/pixel. Data were processed using Mantis and PyMca software.

References

Bots P. , B. L. G., Rickaby R. E. M., and Shaw S., 2011, The role of SO4 in the switch from calcite to aragonite seas: Geology, v. 39, no. 4, p. 331-334.

Horita, J., Zimmermann, H., and Holland, H. D., 2002, Chemical evolution of seawater during the Phanerozoic: Implications from the record of marine evaporites: Geochimica et Cosmochimica Acta, v. 66, no. 21, p. 3733-3756.

Jarvis, K. E., Gray, A. L., Houk, R. S., Jarvis, I., McLaren, J., and Williams, J. G., 1992, Handbook of inductively coupled plasma mass spectrometry, Blackie Glasgow.

Kester, D. R., Duedall, I. W., Connors, D. N., and Pytkowicz, R. M., 1967, PREPARATION OF ARTIFICIAL SEAWATER1: Limnology and Oceanography, v. 12, no. 1, p. 176-179.

Chapter 4

Temperature does not affect $CaCO_3$ polymorph distribution in the Phanerozoic "aragonite" and "calcite" seas.

M.P. Ramírez-García[1], Robert J. Newton[1] and Liane G. Benning[1,2]

[1]School of Earth and Environment, University of Leeds

[2] German Research Centre for Geosciences, GFZ, Potsdam, Germany

Abstract

Oscillations in seawater composition during the Phanerozoic Eon are believed to have controlled the dominant inorganic carbonate mineral polymorph, leading to the concept of "aragonite" and "calcite" seas (Holt et al., 2014; Horita et al., 2002). These variations are important for understanding the evolution of marine calcifiers, the controls on the marine Ca isotope system and the vulnerability of the marine biodiversity to global warming and ocean acidification. Mg:Ca ratio (Burton and Walter, 1987) and sulfate (Bots et al., 2011) have been taken as the main drivers by previous works. Here, we examine the role of dissolved Mg and SO_4 as well as seawater temperature in these processes. We demonstrate that temperature does not play any role in regulating the secular oscillations in seawater compositions and thus prevalent $CaCO_3$ polymorphs mineralogy. We also experimentally validate Mg:Ca ratio in inorganic calcite as a paleotemperature proxy and show that it is seawater Mg:Ca ratio dependent and seawater SO_4 independent.

4.1. Introduction

During the Phanerozoic, oscillations in seawater composition are believed to have controlled the synchronized transitions in the dominant $CaCO_3$ polymorph mineralogy of the major reef-building and sediment-producing calcareous marine organisms and abiotic $CaCO_3$ precipitates (ooids, marine cements), leading to the

concept of “aragonite” and “calcite” seas (Sandberg, 1983a). The cyclicity of the dominant $CaCO_3$ mineral type broadly also coincides with oscillations in the major ion composition of the Phanerozoic oceans (Hardie, 1996; Lowenstein et al., 2001) and the extent of greenhouse and icehouse periods (Holt et al., 2014). These variations are important for understanding the evolution of marine calcifiers, the controls on the marine Ca isotope system and the vulnerability of the marine biodiversity to ocean acidification and climate change. The composition of abiotic carbonates precipitated from seawater can inform us about the chemical state of past oceans. Previous work on the drivers of these variations has focused mainly on the Mg:Ca ratio, not only in the mineralogy of abiotic $CaCO_3$ but also in sediment-producing calcifiers and reef builders (Stanley and Hardie, 1998). How and if other parameters (e,g., temperature or sulfate concentrations), affect $CaCO_3$ polymorph distributions are scarce. In a landmark study, it has been suggested that the Mg:Ca ratio influences $CaCO_3$ polymorph formation as a function of temperature (Morse et al., 1997b); and a more recent study showed a proportional increase of aragonite compared to calcite as temperature and Mg:Ca ratio in solution increase (Balthasar and Cusack, 2015). Finally, another recent quantification of the effects of SO_4 on $CaCO_3$ mineralogy (Bots et al., 2011) indicated that at 21°C, an increase in dissolved SO_4 decreases the Mg:Ca threshold at which the shift from calcite to aragonite occurs. Although temperature has been suggested as an important factor controlling calcium carbonate mineralogy in Aptian bivalves (Pascual-Cebrian et al., 2016), so far the relative influence and effects of temperature and solution chemistry in todays and past oceans is still poorly constrained, making it difficult to predict the responses of modern carbonate-producing biota to climate change. To close this gap we experimentally investigated the effect of temperature, seawater Mg:Ca ratio and SO_4 concentration on abiotic $CaCO_3$ precipitation and provide a new predictive framework for interpreting observations of primary $CaCO_3$ mineralogy in Phanerozoic rocks. Our data also experimentally shows that the use of Mg:Ca ratio in abiogenic calcite as paleotemperature proxy should be interpreted with care.

4.2. Methods

Calcium carbonate precipitation was performed using constant addition experiments ranging the sulfate and magnesium concentrations suggested for Phanerozoic seawater (Horita et al., 2002) and at three different temperatures (5, 21 and 35°C). At 21 °C (± 1°C), a constant addition batch reactor set-up was used (Bots et al., 2011), while at 5 and 35 °C, the whole experimental setup was placed in a cooling / heating incubator (Binder). Calcium carbonate precipitation was induced by continuous injection of two separate $CaCl_2 \cdot 2H_2O$ (250 mM) + $MgCl_2 \cdot 6H_2O$ (0 – 110 mM) and Na_2CO_3 (230 mM) + Na_2SO_4 (0 – 220 mM) solutions into an atmospherically pre-equilibrated seawater solution. Injection was done via a syringe pump at a flow rate of 1.0 ml/h for 48 hours (see A.6 for justification of these experimental conditions). The initial seawater was prepared by dissolving NaCl to reach seawater salinity (Kester et al., 1967) and 10 mM $CaCl_2 \cdot 2H_2O$. In addition, we varied the concentrations of magnesium and sulfate by adding adequate amounts of $MgCl_2 \cdot 6H_2O$ (0-55 mM) and Na_2SO_4 (0-110 mM) to the batch solution. Finally, in order to mimic oöid formation in seawater, we added glass spheres (BioSpec Products 2g/l) as precipitation substrates. Once prepared, each seawater batch solution was equilibrated with the atmosphere for at least 3 days in an open beaker (with a porous plug), while shaking at 270 rpm on an orbital shaker to ensure homogeneous conditions. Before injection, the pH of the seawater solution was adjusted by adding 2N NaOH drop wise until a pH ≈8.1 and an alkalinity of ≈1.6 mM was reached. The pH profile of the whole experiments (prior and during injection) was recorded at a rate of ≈1 measurement every 10 minutes. Sample aliquots (≈5ml) were extracted from the reacting solutions throughout each experiment and immediately filtered through 0.2 μm syringe filters. Solutions were diluted and acidified with HCl 1%, stored cooled (5°C) for analyses of the aqueous sulfate, calcium and magnesium concentrations. After either, 48 or 96 hour post injection initiation, the whole batch was filtered through 0.2 μm polycarbonate track etch membrane filters using a vacuum pump to separate the precipitated $CaCO_3$ from the aqueous solutions for analyses. The solid samples were washed (using Milli-Q water equilibrated with $CaCO_3$), dried at 35 °C and stored at room temperature until further analyses. When experiments were carried out at 5 or 35 °C the separated solution and solid samples were filtered, dried and stored at their respective experimental temperatures. Solid samples were mineralogically

characterized by X-ray powder diffraction (XRD) with a silicon internal standard, using a Bruker D8 X-Ray Diffractometer (Cu $k\alpha_1$). Scans were collected from 2 to 85° (2θ) and a quantitative estimate of the relative proportion of the precipitated $CaCO_3$ polymorphs and their unit cell parameters were performed with Topas 4-2®. Ca, Mg and S concentrations in solution and in acid digested solid reaction products were determined by inductively coupled optical emission spectroscopy (ICP-OES) using a Thermo Scientific iCAP7400 ICP-OES. Precipitates were digested by dissolving a powder aliquot in HCl 10% and diluting with Milli-Q water. To analyse the concentration of Ca, Mg and S in each of the polymorphs present in the solid reaction products, powder aliquots were embedded in epoxy, polished, carbon-coated and analysed by electron probe microanalysis (EPMA) using a JEOL Hyperprobe JXA-8500F with a thermal field-emission cathode. Si analysis were also performed in order to obtain a parameter which allowed us to detect whether we were analysing only $CaCO_3$ crystals or when part of a glass bead was also present in the selected area of interest. For quantitative chemical analysis the electron probe was operated at 15 kV acceleration voltage, 5 nA beam current and 1 µm spot size of crystal-free glassy areas. Standardization was done with dolomite (for Mg and Ca), ZnS (for S) and tugtupite (for Si). Counting times on peak and background were 30 and 15 seconds respectively for Mg and S and 10 and 5 seconds respectively for Ca and Si.

4.3. Results and discussion

Our experiments revealed only minor effects of temperature on primary $CaCO_3$ polymorph mineralogy at conditions representing the “calcite seas” and “aragonite seas” (Figure 4.1a & Table A.1). As a general trend, our data shows that pure calcite precipitated only in Mg and SO_4 free seawater. Pure aragonite precipitated at high Mg:Ca ratios and SO_4 concentrations (Mg:Ca> 0.65; SO_4> 10 mM) and in SO_4 free conditions when Mg:Ca was higher than 1.00 molar. Vaterite precipitated only in Mg free seawater and at very low Mg:Ca ratios (Mg:Ca≤ 0.10), and it was as a mixture of calcite-vaterite up to SO_4 concentration of 15 mM and as a mixture of aragonite-vaterite at SO_4 concentration higher than 15 mM. Hence in most experimental conditions, a mixture of polymorphs precipitated. We have considered as predominant polymorph which its presence in the sample is higher than 50%. Our

data elucidate that calcite, aragonite and vaterite predominance fields are almost equivalent at all studied temperatures (5, 21 and 35°C; Figure 4.1a). XRD analyses revealed that aragonite dominates at high Mg and SO_4 contents (Mg:Ca> 0.65 ± 0.1; SO_4> 10 mM), and calcite dominates at low Mg and SO_4 concentrations. Vaterite only forms at low Mg concentrations conditions and at SO_4 concentrations of up to ≈60 mM. The only difference in polymorph predominance distribution with temperature is a small change in the Mg:Ca threshold at which aragonite became the predominant polymorph (>50%) in the absence of SO_4 (Figure 4.1b). The boundary between the calcite and aragonite predominance fields increases slightly as temperature decreases, from Mg:Ca= 0.55 at 35°C to Mg:Ca= 0.75 at 5°C.

Quantitative EPMA of the solid products and ICP-OES analyses of the digested polymorphs indicate that SO_4 became incorporated into all three polymorphs, while Mg became only incorporated into calcite (Table A.1 & A.2). In the absence of SO_4, the change in $CaCO_3$ polymorph composition was a consequence of the increases incorporation of Mg into calcite with increasing Mg:Ca ratio in solution, reducing the thermodynamic stability of aragonite, while simultaneously increases the solubility of calcite (Busenberg and Niel Plummer, 1989; Davis et al., 2000b) . At low Mg:Ca ratios (≤ 0.22 molar) and at all the studied temperatures, the shift from calcite to aragonite predominance occurs at a SO_4 threshold of 10 mM (Figure 4.1c), yet this threshold decreases rapidly at Mg:Ca ratios above 0.22.

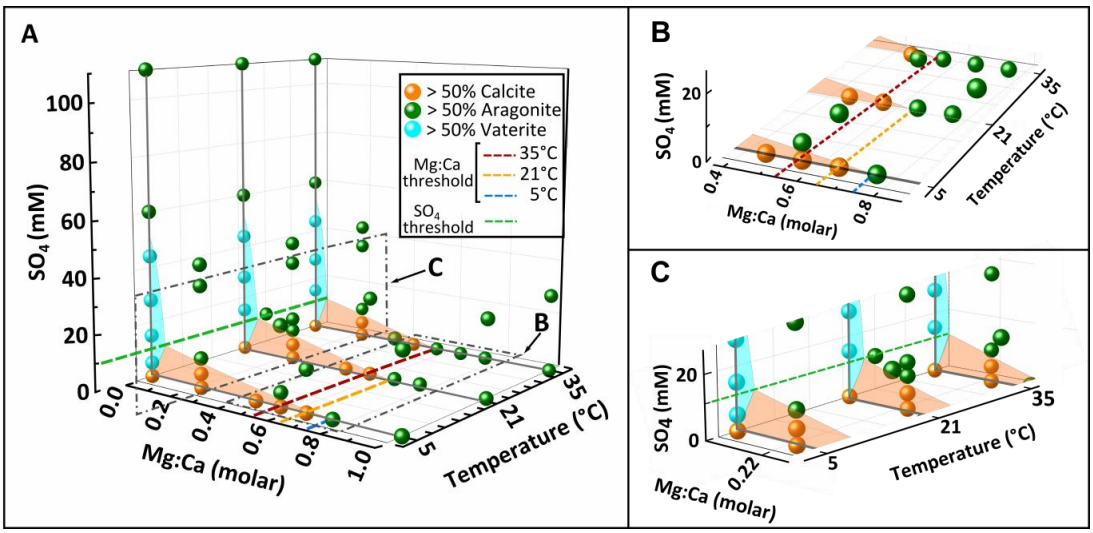

Figure 4. 1: *a) Polymorph distribution as a function of solution chemistry and temperature; b) Expanded area of the main figure showing the Mg:Ca threshold at the three temperatures and seawater SO_4= 0 mM; c) Expanded area of the main figure showing the SO_4 threshold at low Mg:Ca ratios (Mg:Ca ≤ 0.22 molar).*

Our EPMA data revealed a clear dependence between the incorporation of Mg into calcite and its formation temperature. On average, ≈4 times more Mg became incorporated in calcite at 35°C than at 5°C (Figure 4.2 & Table A.2). Incorporation of Mg into calcite is, however, not solely dependent on temperature, but also on seawater Mg:Ca ratio. Our results showed that the increase of the Mg incorporation into calcite with temperature is approximately 3 times higher when Mg:Ca ratio in seawater is higher than 0.22 (Figure 4.2a) . These trends appear to be unaffected by the presence of SO_4 with the solution Mg:Ca ratio and temperature exerting the overriding control on Mg incorporation into calcite (Figure 4.2 B). Mg content in calcite has been previously reported as positively correlated to temperature increasing but independent of solution saturation state and the kinetic mechanism of calcite growth (Lopez et al., 2009). EPMA and ICP-OES data also confirmed that the influence of temperature on SO_4 incorporation into calcite is insignificant when seawater SO_4 concentration is ≤5 mM. Nevertheless, when SO_4 concentration in seawater is ≥5 mM, the influence of temperature on SO_4 incorporation into calcite is quite denoting, decreasing the SO_4 content in calcite about 65% when temperature increases from 5 to 35°C (Figure 4.2 D and Figure A.2. A). Our EPMA results also elucidated that the effect of temperature in SO_4 incorporation into aragonite is negligible (Figure A.2 B & C).

Nevertheless, the large increase in Mg incorporation into calcite with temperature did not lead to significant differences in the predominant polymorph distribution with increasing temperature (Figure 4.1). Therefore, the slightly lower Mg:Ca threshold at 35°C relative to that at 5°C is likely to be due to the combination of the increase in the incorporation of magnesium into calcite (Figure 4.2 and (Mucci, 1987), and the well-known increase in aragonite precipitation rate relative to calcite at higher temperatures (Davis et al., 2000b; Elizabeth A. Burton, 1987).

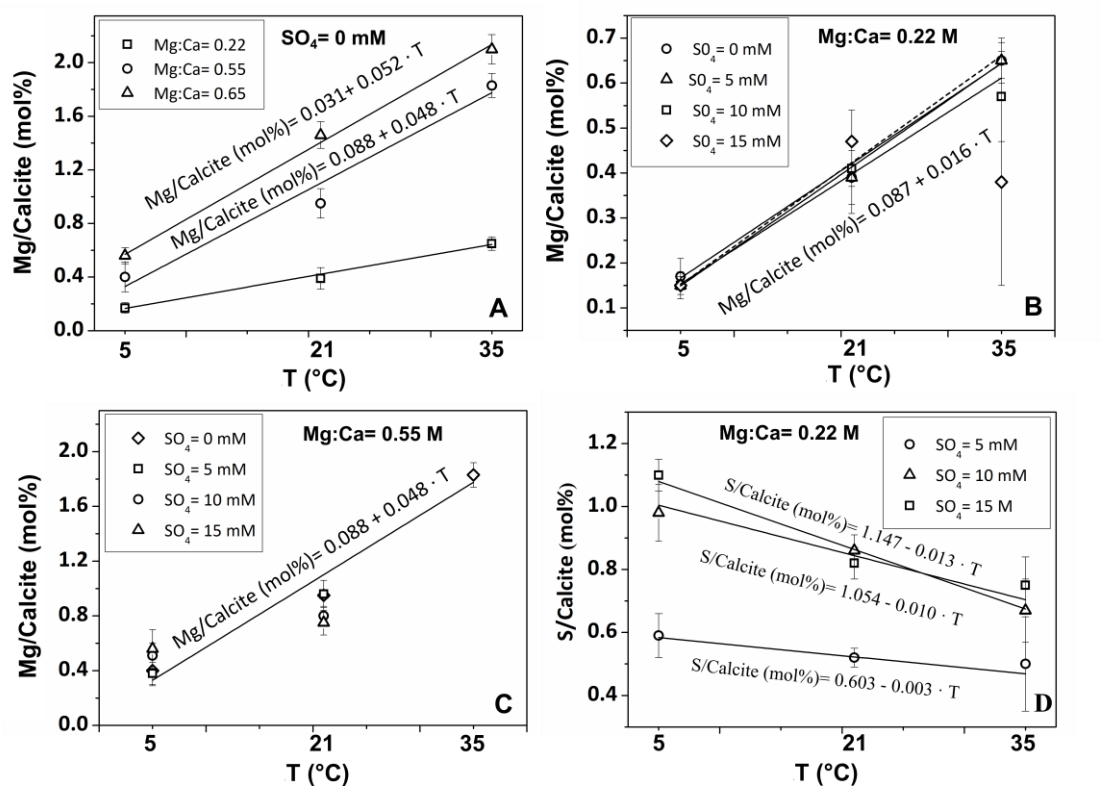

Figure 4. 2: *Mg incorporation into calcite vs. temperature. Solution chemistry: a) SO_4= 0 mM; b) Mg:Ca= 0.22 (molar); c) Mg:Ca= 0.55 (molar); d) S incorporation into calcite for seawater Mg:Ca= 0.22 and as a function of temperature and SO_4 concentration. Dashed line represents predicted correlations. Error bars equivalent to 95% confidence interval. Additional information about the source of the higher errors at 35°C is shown in Appendix A.5 & Figure A.1.*

Our data also confirm that aragonite precipitation was indeed favoured at high Mg:Ca ratios (> 0.65 molar) and with increasing temperature (Figure 4.3 A). Combining our data with previous studies allows us to show the gradual shift in $CaCO_3$ polymorph proportions between exclusive calcite and aragonite precipitation fields (Figure 4.3). Important to note however, is that our aragonite-calcite co-precipitation field derived from experiments that spanned the range of Phanerozoic Mg:Ca ratios (0 – 5.2 molar) and temperatures (5 - 35°C) was much narrower than proposed in previous studies (Figure 4.3). This significant difference is in part explainable due to the different experimental $CaCO_3$ precipitation methods. Our constant addition experiments were designed so that we keep the solution chemistry constant throughout the course of each experiment, as also confirmed by the analyses of the fluid compositions throughout the experiments (Table A.4). Moreover, and as mentioned in chapter 3, the experiment time was also tested to assure that the $CaCO_3$ phases precipitated were the stable ones at each experimental

condition. However in the experiments of previous work (Balthasar and Cusack, 2015; Morse et al., 1997b), $CaCO_3$ precipitation was induced through degassing of CO_2, which lead to changing precipitation conditions throughout the run. Although in Balthasar and Cusack´s work it was suggested that an insignificant amount of Ca was removed from solution due to $CaCO_3$ precipitation; Morse and co-workers using the same experimental setup, reported some artefacts in their experiments due to aragonite crystals growing over initially precipitated calcite crystals as the reaction progressed. This was explained as a continuous increase of the solution Mg:Ca ratio throughout the experiment due to $CaCO_3$ precipitation, which made aragonite more likely to form.

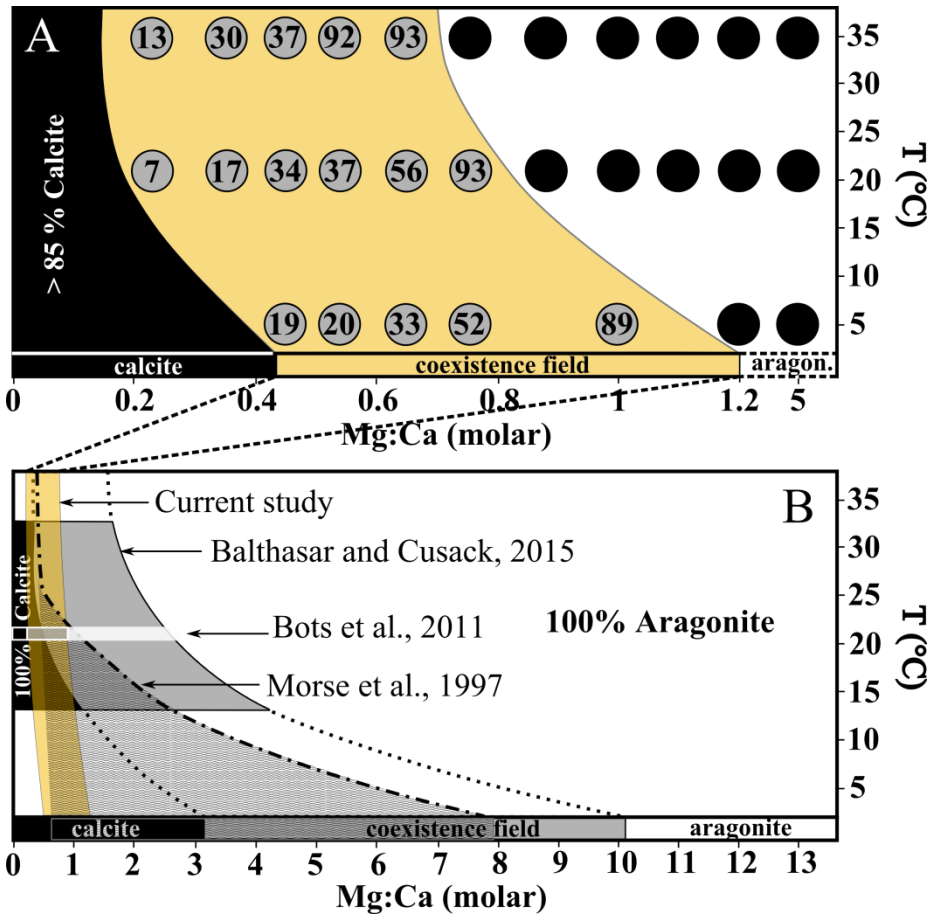

Figure 4. 3: *Average proportions of aragonite in the solid reaction products as a function of Mg:Ca ratio and temperature and from sulfate free experiments; a) Data as measured in current study; b) Data from (Balthasar and Cusack, 2015) and from (Morse et al., 1997b). Numbers in circles represent the proportion of aragonite present in the sample; black circles represent 100 % aragonite samples; black shaded areas represent the >85% calcite field in A and the 100% calcite field in B; the yellow shaded areas represents the aragonite-calcite coexistence field of the current study; grey shaded areas represent the aragonite-calcite coexistence field of (Balthasar and Cusack, 2015); wavy shaded area represents the aragonite-calcite co-precipitation field of Morse et al., 1997; dotted and dashed line indicates position of the boundary between aragonite and calcite precipitation of Morse et al., 1197; dotted lines in B represent the extrapolation of the boundary of the aragonite-calcite co-existence field of Balthasar and Cusack, 2015 up to the temperature range under study (5 – 35 °C).*

Together with seawater Mg:Ca ratio and temperature, we have also studied the influence of seawater SO_4 concentration in the proportion of aragonite against calcite in our precipitates (Figure A.3), showing that for a fixed Mg:Ca ratio, the proportion of aragonite in the sample increases as SO_4 increases and the differences in the polymorphs proportion with temperature are more significant. With increasing SO_4 in solution, the pure calcite and aragonite-calcite co-existence fields are narrower while the pure aragonite field gets wider.

4.4. Implications for Phanerozoic aragonite-calcite seas.

Outlining the role of temperature on aragonite-calcite seas, our experimental data elucidate that changes in seawater temperature (5 - 35°C) did not lead to variations in the secular oscillations between predominant aragonite and calcite precipitation. Temperature changes from 5 to 35°C, only caused a variation of 0.2 units in the value of the Mg:Ca threshold (Mg:Ca ≈0.65±0.1) and did not affect the SO_4 threshold which was ≈10 mM at the three studied temperatures (when Mg:Ca≤ 0.22). Thus, the synchronized oscillations between calcite and aragonite sea states seen in the geological record are separated by distinct seawater Mg:Ca ratio and SO_4 boundaries which are independent of temperature. Hence, our data show that temperature should not be included in any existing models relating seawater chemistry to $CaCO_3$ mineralogy throughout the Phanerozoic. In agreement with earlier experimental studies (Balthasar and Cusack, 2015; Morse et al., 1997b), the existence of an aragonite-calcite co-existence field and a relationship between the polymorph proportion present in the sample, the Mg:Ca ratio and SO_4 concentration in solution and temperature is demonstrated. However, our aragonite-calcite co-precipitation area is much narrower than previously proposed. Although cold waters kinetically favour the precipitation of calcite, the framework shown in this study would be globally homogeneous states of seawater compositions through Earth history that would vary due to temperature and latitude change only in times characterized by low seawater Mg:Ca ratios (between 0.22 and 1). Independently of temperature, calcite seas dominated when seawater Mg:Ca ratio was ≤ 0.65 and seawater SO_4 concentration ≤ 5 mM and when SO_4 concentration was ≤ 10 mM and Mg:Ca ratio ≤ 0.22. Our proposed calcite-Mg:Ca threshold is in agreement with Mg:Ca ratios suggested by previous experimental studies (Mg:Ca≈ 0.6 – 0.7) (Bots et al., 2011) and with the estimated Mg:Ca ratios of ≈ 0.2 – 0.3 for the early Mississippian seawater from abiotic marine $CaCO_3$ records (Hasiuk and Lohmann, 2008) but it is much lower than the Mg:Ca ratio of ≈2 determined from marine halite fluid inclusions (Horita et al., 2002; Lowenstein et al., 2003). Our proposed calcite SO_4 threshold is in accordance with SO_4 concentrations suggested for the Early Jurassic (<5 mM) and Cretaceous (<4 mM) from sulfur isotope records (Newton et al., 2011; Wortmann and Chernyavsky, 2007). On the other hand, aragonite seas dominated when Mg:Ca ratios were >1. Considering the lower range of the Phanerozoic seawater Mg:Ca ratios proposed by the geological record (2 – 0.7)

(Dickson, 2002; Holt et al., 2014), the only times when Mg:Ca ratio was lower or equal to 1, were during Cretaceous and Cambrian eras. Hence, according to our results, it could have been during these periods of time when variations in the proportions of $CaCO_3$ polymorphs formed in seawater would have varied due to changes in temperature and latitude. However these two eras overlap with calcite predominance seas. Comparing our aragonite-calcite seas pattern with the one suggested by the geological record, our view of the aragonite-calcite sea concept would be unrealistic for Phanerozoic seawater because of the low probability of calcite seas to form. However, the overall match among $CaCO_3$ polymorphs, the inferred oceanic state and climate change is still quite controversial. Past calcite-seas are mainly coincident with warm global climate (Crowley and Berner, 2001), low Mg:Ca ratios, high sea levels and weak latitudinal temperature gradients (Huber et al., 2002), whereas in the present ocean, dominated by aragonite and high-Mg calcite, low-Mg calcite is associated with cool waters. Although aragonite-seas and high-Mg calcite are dominantly found in present warm water environments, past aragonite-sea times are associated with a more varied climate history including icehouse and greenhouse periods (Brand et al., 2012). Correlations between changes in skeletal mineralogy of Aptian rudist bivalves with changing temperature have been made, showing an inverse correlation between calcite-aragonite ratio in polyconitid rudist bivalves and temperature (Pascual-Cebrian et al., 2016). The Aptian era was characterized by low and stable Mg:Ca ratios but also by high and variable pCO_2 concentrations what could have been a driver of these mineralogical changes observed in bivalves as well. This latter hypothesis has remains to be tested. Even though, due to the important role that physiology plays in biomineralization (e.g. specific demands of a mode of life, metabolic costs, ecological factors, etc.), it is difficult to transfer results from abiogenic $CaCO_3$ studies to organisms and vice versa.

Our study confirms the strong correlation of the partition coefficient of Mg into abiogenic calcite with temperature and also reveals that this relationship is also controlled by the Mg:Ca ratio in seawater but is independent on SO_4 concentration in seawater. There are many studies on benthic and planktonic foraminifera (Elderfield et al., 1996; Lear et al., 2002; Nürnberg et al., 1996; Rosenthal et al., 1997) and a few on corals (Reynaud et al., 2007; Wei et al., 2000; Yu et al., 2005) and ostracods (Dwyer, 1995) which have made use of Mg:Ca ratios in calcite as a

marine paleothermometer. As it is revealed in this study for abiotic marine $CaCO_3$, Mg:Ca ratios in corals and ostracods also show a positive linear correlation with temperature. However, due to thermodynamic considerations, Mg:Ca–temperature relationship in benthic and planktonic foraminifera are best described by an exponential fit. Mg:Ca–temperature calibration equations have been suggested for each genus of benthic and planktonic foraminifera, corals, ostracods, etc., and that variations in trace-element contents in seawater affect the control in the intake of trace elements into marine calcifiers, the strong biological control on the incorporation of Mg and the species-specific temperature sensitivity, it is not accurate to provide a single Mg:Ca – temperature calibration equation for marine calcifiers species. Support for this Mg:Ca paleotemperature proxy has been also found in laboratory experiments, showing a positive and linear response of the Mg incorporation into abiogenic calcite to temperature (Elizabeth A. Burton, 1991; Katz, 1973). It has been suggested that at room temperature, the incorporation of Mg into inorganically precipitated magnesian calcite overgrowths on calcite seeds is controlled by the seawater Mg:Ca ratio from which they formed (Mucci et al., 1985). Nevertheless, no dependence of the relationship between the amount of Mg incorporated into abiogenic marine calcite and temperature on seawater Mg:Ca ratios has been shown so far. After all, changes in seawater Mg:Ca remain one of the largest uncertainties in using Mg:Ca in marine carbonates as paleothermometry to determine seawater temperature over long timescales. EPMA data showed that the Mg incorporation into calcite was directly proportional to seawater temperature over the seawater Mg:Ca range where calcite precipitation was possible (Mg:Ca= 0.00 – 1.00) but that the nature of this relationship is also dependent on seawater Mg:Ca ratio. Our results indicated that the proportion of Mg incorporated into calcite increases with temperature ≈3 times more rapidly when seawater Mg:Ca ratio was ≥ 0.55 than when seawater Mg:Ca ratio was ≤0.55. This fact suggests that for the abiotic marine $CaCO_3$ system, it is not possible to provide a single Mg thermometry calibration and the use of seawater Mg:Ca-specific equations should provide a more accurate translation to paleotemperature.

4.5. Conclusions

Our work evaluating and quantifying the influence of seawater Mg:Ca ratio, SO_4 concentration and temperature in abiotic seawater $CaCO_3$ mineralization, demonstrates that there is not a significant response of abiotic marine $CaCO_3$ mineralogy to changing temperature. Hence, the view of Phanerozoic aragonite-calcite seas should not be temperature corrected. We confirm seawater Mg:Ca ratio and SO_4 concentration as dominant drivers since small differences in their values can be invoked as controlling the variation in abiotic $CaCO_3$ polymorphs. We propose lower Mg:Ca and SO_4 thresholds on seawater chemistry for calcite predominance seas (Mg:Ca$\leq$ 0.65, $SO_4\leq$ 10 mM) (Bots et al., 2011) than those suggested by the geological records (Mg:Ca$\approx$ 2) (Horita et al., 2002; Lowenstein et al., 2003). This mismatch between our experimental and the aragonite-calcite sea pattern from the records may mean: (1) more solid data on Phanerozoic seawater Mg:Ca ratios and SO_4 concentrations are needed to accurately predict Mg contents of ancient marine abiogenic and biogenic carbonates and to better constrain current models, (2) Mg:Ca ratios and SO_4 concentrations were lower as suggested by recent studies (Newton et al., 2011; Wortmann and Chernyavsky, 2007) or that (3) an additional parameter other than Mg:Ca ratio and SO_4 concentration in seawater (e.g., seawater saturation state, partial pressure of carbon dioxide or dissolve organics) could have played a more dominant role in regulating the secular oscillations in seawater composition and thus prevalent $CaCO_3$ polymorphs mineralogy. We also validate abiogenic calcite Mg:Ca as a reliable and quantitative proxy for past global seawater temperature change if its dependence on both the temperature and the Mg:Ca ratio of the seawater is considered. We propose the use of seawater Mg:Ca-specific equations to provide more accurate temperature estimates instead of a single calibration equation since the relationship between Mg:Ca in calcite and temperature varies with only small variations in the seawater Mg:Ca ratio.

References

Balthasar, U., and Cusack, M., 2015, Aragonite-calcite seas—Quantifying the gray area: Geology, v. 43, no. 2, p. 99-102.

Bots, P., Benning, L., Rickaby, R., and Shaw, S., 2011, The role of SO4 in the switch from calcite to aragonite seas: Geology, v. 39, no. 4, p. 331-334.

Bots P. , B. L. G., Rickaby R. E. M., and Shaw S., 2011, The role of SO4 in the switch from calcite to aragonite seas: Geology, v. 39, no. 4, p. 331-334.

Brand, U., Posenato, R., Came, R., Affek, H., Angiolini, L., Azmy, K., and Farabegoli, E., 2012, The end-Permian mass extinction: A rapid volcanic CO2 and CH4-climatic catastrophe: Chemical Geology, v. 322–323, p. 121-144.

Burton, E. A., and Walter, L. M., 1987, Relative precipitation rates of aragonite and Mg calcite from seawater: Temperature or carbonate ion control?: Geology, v. 15, no. 2, p. 111-114.

Busenberg, E., and Niel Plummer, L., 1989, Thermodynamics of magnesian calcite solid-solutions at 25°C and 1 atm total pressure: Geochimica et Cosmochimica Acta, v. 53, no. 6, p. 1189-1208.

Crowley, T. J., and Berner, R. A., 2001, CO₂ and Climate Change: Science, v. 292, no. 5518, p. 870-872.

Davis, K. J., Dove, P. M., and De Yoreo, J. J., 2000, The Role of Mg²⁺ as an Impurity in Calcite Growth: Science, v. 290, no. 5494, p. 1134-1137.

Dickson, J. A. D., 2002, Fossil Echinoderms As Monitor of the Mg/Ca Ratio of Phanerozoic Oceans: Science, v. 298, no. 5596, p. 1222-1224.

Dwyer, G. S., Cronin, T. M., Baker, P. A., Raymo, M. E., Buzas, J. S., Corrège. T., 1995, North atlantic deepwater temperature change during late pliocene and late quaternary climatic cycles, Science, Volume 270, p. 1347 - 1351.

Elderfield, H., Bertram, C. J., and Erez, J., 1996, A biomineralization model for the incorporation of trace elements into foraminiferal calcium carbonate: Earth and Planetary Science Letters, v. 142, no. 3, p. 409-423.

Elizabeth A. Burton, a. L. M. W., 1991, The effects of PCO2 and temperature on magnesium incorporation in calcite in seawater and MgCl2-CaCl2 solutions: Geochimica et Cosmochimica Acta, v. 55, no. 3, p. 777-785.

Elizabeth A. Burton, L. M. W., 1987, Relative precipitation rates of aragonite and Mg calcite from seawater: Temperature or carbonate ion control?: Geology, v. 15, no. 2, p. 111-114.

Hardie, L. A., 1996, Secular variation in seawater chemistry: An explanation for the coupled secular variation in the mineralogies of marine limestones and potash evaporites over the past 600 m.y: Geology, v. 24, no. 3, p. 279-283.

Hasiuk, F. J., and Lohmann, K. C., 2008, Mississippian Paleocean Chemistry from Biotic and Abiotic Carbonate, Muleshoe Mound, Lake Valley Formation, New Mexico, U.S.A: Journal of Sedimentary Research, v. 78, no. 2, p. 147-164.

Holt, N. M., García-Veigas, J., Lowenstein, T. K., Giles, P. S., and Williams-Stroud, S., 2014, The major-ion composition of Carboniferous seawater: Geochimica et Cosmochimica Acta, v. 134, p. 317-334.

Horita, J., Zimmermann, H., and Holland, H. D., 2002, Chemical evolution of seawater during the Phanerozoic: Implications from the record of marine evaporites: Geochimica et Cosmochimica Acta, v. 66, no. 21, p. 3733-3756.

Huber, B. T., Norris, R. D., and MacLeod, K. G., 2002, Deep-sea paleotemperature record of extreme warmth during the Cretaceous: Geology, v. 30, no. 2, p. 123-126.

Katz, A., 1973, The interaction of magnesium with calcite during crystal growth at 25–90°C and one atmosphere: Geochimica et Cosmochimica Acta, v. 37, no. 6, p. 1563-1586.

Kester, D. R., Duedall, I. W., Connors, D. N., and Pytkowicz, R. M., 1967, PREPARATION OF ARTIFICIAL SEAWATER1: Limnology and Oceanography, v. 12, no. 1, p. 176-179.

Lear, C. H., Rosenthal, Y., and Slowey, N., 2002, Benthic foraminiferal Mg/Ca-paleothermometry: a revised core-top calibration: Geochimica et Cosmochimica Acta, v. 66, no. 19, p. 3375-3387.

Lopez, O., Zuddas, P., and Faivre, D., 2009, The influence of temperature and seawater composition on calcite crystal growth mechanisms and kinetics:

Implications for Mg incorporation in calcite lattice: Geochimica et Cosmochimica Acta, v. 73, no. 2, p. 337-347.

Lowenstein, T. K., Hardie, L. A., Timofeeff, M. N., and Demicco, R. V., 2003, Secular variation in seawater chemistry and the origin of calcium chloride basinal brines: Geology, v. 31, no. 10, p. 857-860.

Lowenstein, T. K., Timofeeff, M. N., Brennan, S. T., Hardie, L. A., and Demicco, R. V., 2001, Oscillations in Phanerozoic Seawater Chemistry: Evidence from Fluid Inclusions: Science, v. 294, no. 5544, p. 1086-1088.

Morse, J. W., Wang, Q., and Tsio, M. Y., 1997, Influences of temperature and Mg:Ca ratio on CaCO3 precipitates from seawater: Geology, v. 25, no. 1, p. 85-87.

Mucci, A., 1987, Influence of temperature on the composition of magnesian calcite overgrowths precipitated from seawater: Geochimica et Cosmochimica Acta, v. 51, no. 7, p. 1977-1984.

Mucci, A., Morse, J. W., and Kaminsky, M. S., 1985, Auger spectroscopy analysis of magnesian calcite overgrowths precipitated from seawater and solutions of similar composition: Am. J. Sci.; (United States), p. Medium: X; Size: Pages: 289-305.

Newton, R. J., Reeves, E. P., Kafousia, N., Wignall, P. B., Bottrell, S. H., and Sha, J.-G., 2011, Low marine sulfate concentrations and the isolation of the European epicontinental sea during the Early Jurassic: Geology, v. 39, no. 1, p. 7-10.

Nürnberg, D., Bijma, J., and Hemleben, C., 1996, Assessing the reliability of magnesium in foraminiferal calcite as a proxy for water mass temperatures: Geochimica et Cosmochimica Acta, v. 60, no. 5, p. 803-814.

Pascual-Cebrian, E., Götz, S., Bover-Arnal, T., Skelton, P. W., Gili, E., Salas, R., and Stinnesbeck, W., 2016, Calcite/aragonite ratio fluctuations in Aptian rudist bivalves: Correlation with changing temperatures: Geology, v. 44, no. 2, p. 135-138.

Reynaud, S., Ferrier-Pagès, C., Meibom, A., Mostefaoui, S., Mortlock, R., Fairbanks, R., and Allemand, D., 2007, Light and temperature effects on Sr/Ca and Mg/Ca ratios in the scleractinian coral Acropora sp: Geochimica et Cosmochimica Acta, v. 71, no. 2, p. 354-362.

Rosenthal, Y., Boyle, E. A., and Slowey, N., 1997, Temperature control on the incorporation of magnesium, strontium, fluorine, and cadmium into benthic foraminiferal shells from Little Bahama Bank: Prospects for thermocline paleoceanography: Geochimica et Cosmochimica Acta, v. 61, no. 17, p. 3633-3643.

Sandberg, P. A., 1983, An oscillating trend in Phanerozoic non-skeletal carbonate mineralogy: Nature, v. 305, no. 5929, p. 19-22.

Stanley, S. M., and Hardie, L. A., 1998, Secular oscillations in the carbonate mineralogy of reef-building and sediment-producing organisms driven by tectonically forced shifts in seawater chemistry: Palaeogeography, Palaeoclimatology, Palaeoecology, v. 144, no. 1, p. 3-19.

Wei, G., Sun, M., Li, X., and Nie, B., 2000, Mg/Ca, Sr/Ca and U/Ca ratios of a porites coral from Sanya Bay, Hainan Island, South China Sea and their relationships to sea surface temperature: Palaeogeography, Palaeoclimatology, Palaeoecology, v. 162, no. 1–2, p. 59-74.

Wortmann, U. G., and Chernyavsky, B. M., 2007, Effect of evaporite deposition on Early Cretaceous carbon and sulphur cycling: Nature, v. 446, no. 7136, p. 654-656.

Yu, K.-F., Zhao, J.-X., Wei, G.-J., Cheng, X.-R., Chen, T.-G., Felis, T., Wang, P.-X., and Liu, T.-S., 2005, δ18O, Sr/Ca and Mg/Ca records of Porites lutea corals from Leizhou Peninsula, northern South China Sea, and their applicability as paleoclimatic indicators: Palaeogeography, Palaeoclimatology, Palaeoecology, v. 218, no. 1–2, p. 57-73.

Chapter 5

The role of pCO_2 on switching between calcite and aragonite seas

M.P. Ramírez-García[1], Robert J. Newton[1] and Liane G. Benning[1,2]

[1]School of Earth and Environment, University of Leeds

[2] German Research Centre for Geosciences, GFZ, Potsdam, Germany

Abstract

Since industrialisation (Doney et al., 2009), global CO_2 levels have increased significantly with 33% entering the oceans and reducing pH (Raven et al., 2005), accelerating climate change and influencing marine calcification (Addadi et al., 2003; Bach, 2015; Garrard et al., 2014; Zhao et al., 2017). Observations in the rock record give evidence that environmental changes such as partial pressure of carbon dioxide (pCO_2) and global warming have impacts on calcification and marine biota (Hönisch et al., 2012). Therefore together with Mg:Ca ratio in seawater and SO_4 concentration, pCO_2 might be a potential driver controlling marine calcium carbonate precipitation. Experiments were conducted on $CaCO_3$ precipitation in seawater of estimated Phanerozoic Eon composition and at 3 different partial pressures of carbon dioxide (400, 1500 and 3000 ppm) to determine the influence of seawater chemistry and pCO_2 on abiotic marine $CaCO_3$ mineralogy. Our experimental data reveal that $CaCO_3$ precipitation in the ocean occurs even at extreme atmospheric partial pressures of carbon dioxide (up to pCO_2 of 3000 ppm). It is also shown that pCO_2 and seawater pH do not need to be considered as major controls on the Phanerozoic oscillations between aragonite and calcite seas. We confirm seawater Mg:Ca ratio and SO_4 concentration as the main driving forces controlling $CaCO_3$ precipitation. Here, we prove a clear relationship among abiogenic calcite SO_4 content, seawater SO_4 concentration and seawater pH. We propose SO_4 content in abiogenic calcite as a reliable and quantitative proxy for past seawater pH and atmospheric pCO_2, but our results indicate that it is not possible to provide a single SO_4–pH calibration and the use of seawater SO_4-specific equations is needed.

5.1. Introduction

Continuous anthropogenic emissions of CO_2 to the atmosphere and uptake of part of this CO_2 by oceans will result not only in an elevated dissolved CO_2 and decreased pH (Caldeira and Wickett, 2003) but, critically, in a decreased saturation with respect to calcium carbonates ($CaCO_3$), the compound widely used by marine organisms for the construction of their shells and skeletons. Ocean acidification has raised serious concerns about the potential effects on marine organisms and ecosystems, especially those organisms producing shells, tests or skeletons out of calcium carbonate. Several studies have addressed different influences of pH on calcium carbonate precipitation. (Plummer, 1979) showed that at pH< 7, bicarbonate is the dominant carbonate species absorbed on calcite surface. In contrast, at pH ≈8.3 carbonate is the dominant species absorbed on calcite structure (Stack and Grantham, 2010). Changes in the pH and alkalinity can also affect the incorporation of sulphate and magnesium into calcium carbonate. The incorporation of sulphate into calcite is thought to be a function of the aqueous sulphate to carbonate ratio (Busenberg and Niel Plummer, 1985; Takano, 1985). Hence, a change in calcite growth via either carbonate or bicarbonate (due to variations in pH) could also change the incorporation of sulphate into calcite and affect calcite growth kinetics. Additionally, an increase in the concentration of bicarbonate decreases the amount of magnesium incorporated into the calcite structure (Burton, 1991), which could also destabilize calcite with respect to aragonite (Davis et al., 2000a).

Many experimental studies have identified various effects of changes in solution chemistry (Mg:Ca ratio and SO_4 concentration) (Bots et al., 2011; Morse et al., 2007) or changes in physical parameters such as temperature (Balthasar and Cusack, 2015; Burton and Walter, 1987; Morse et al., 1997a) have on the formation, transformation and structure of calcium carbonate phases . Strong links between the carbon cycle and climate change observed in the rock record give evidence that environmental changes such as pCO_2 and global warming have impacts on calcification and marine biota (Hönisch et al., 2012). However, there is lack of a synergistic and deterministic approach in currently used experimental approaches and thus also models about the role such parameters have in controlling carbonate mineralogy is a big gap in our knowledge and hinders our predictive capabilities. Thus the relative influence and effects of each of these parameters must be

determined in order to assess the total influence of solution chemistry, temperature and pCO_2 on calcium carbonate precipitation.

5.2. Methods

5.2.1. Experimental set-up

Calcium carbonate ($CaCO_3$) precipitation was performed using constant addition experiments at a range of CO_2 concentrations spanning modern and ancient values (pCO_2= 400, 1500 and 3000 ppm), at 21°C (± 1°C) and a representative range of Phanerozoic Mg:Ca ratios and SO_4 seawater concentrations (Horita et al., 2002). The experimental set-up is shown in Figure 5.1. $CaCO_3$ precipitation is induced by continuous injection of two separate $CaCl_2{\cdot}2H_2O$ (250 mM) + $MgCl_2{\cdot}6H_2O$ (0 – 110 mM) and Na_2CO_3 (230 mM) + Na_2SO_4 (0 – 220 mM) solutions into a seawater solution. Injection was done using two peristaltic pumps at a flow rate of 1.0 ml/h for 48 hours. The initial seawater solution was prepared by dissolving 10 mM $CaCl_2{\cdot}2H_2O$, and appropriate amounts of $MgCl_2{\cdot}6H_2O$ (0-55 mM) and Na_2SO_4 (0-110 mM) to produce the required Mg:Ca ratio and SO_4 concentration, and NaCl to produce a salinity of 35‰ (Kester et al., 1967). In order to mimic oöid formation in seawater, we added glass spheres (BioSpec Products 2g/l) as precipitation substrates. Before injection, the initial seawater solution and the two inlet solutions ($CaCl_2{\cdot}2H_2O$ + $MgCl_2{\cdot}6H_2O$ and Na_2CO_3 + Na_2SO_4) were allowed to equilibrate with the given pCO_2 for at least 3 days. Pumping of the inlet solutions at a constant rate together with continuous bubbling of an air/CO_2 gas mixture in the reactor (P≈ 1 bar) lead to the attainment of a steady-state pH (± 0.05) during $CaCO_3$ precipitation. To minimize evaporation, the air/CO_2 gas mixture is bubbled in a 0.4 M NaCl solution prior to its introduction in the reactor vessel and in the inlet solutions vessels. Once steady-state was reached, the pH of the seawater solution equilibrated with an air/CO_2 gas of 400 ppm pCO_2 was 8.2 ± 0.05. When the pCO_2 of the air/CO_2 gas was 1500 and 3000 ppm, the pH of the seawater solution was 7.8 ± 0.05 and 7.6 ± 0.05 respectively (Figure B.1). To ensure homogeneous conditions, the reactor vessel is shaken at 270 rpm on an orbital shaker during the course of a run. Sample aliquots (≈5ml) were extracted from the reacting solutions throughout each experiment and immediately filtered through 0.2 μm syringe filters. Sub-samples

were diluted and acidified with HCl 1%, and stored cooled (5°C) for analyses of the aqueous sulfate, calcium and magnesium concentrations. pH and alkalinity were determined in a second sub-sample. To get a more detailed pH profile of the whole experiment (prior and during injection) for each given pCO_2, the pH was recorded at a rate of ≈1 measurement every 10 minutes in two of each set of experiments at a given pCO_2 (Figure B.1). After 48 hour post injection initiation, the whole batch was filtered through 0.2 µm polycarbonate track etch membrane filters using a vacuum pump to separate the precipitated $CaCO_3$ from the aqueous solutions for analyses. The solid samples were washed (using Milli-Q water equilibrated with $CaCO_3$), dried at 35 °C and stored at room temperature until further analyses.

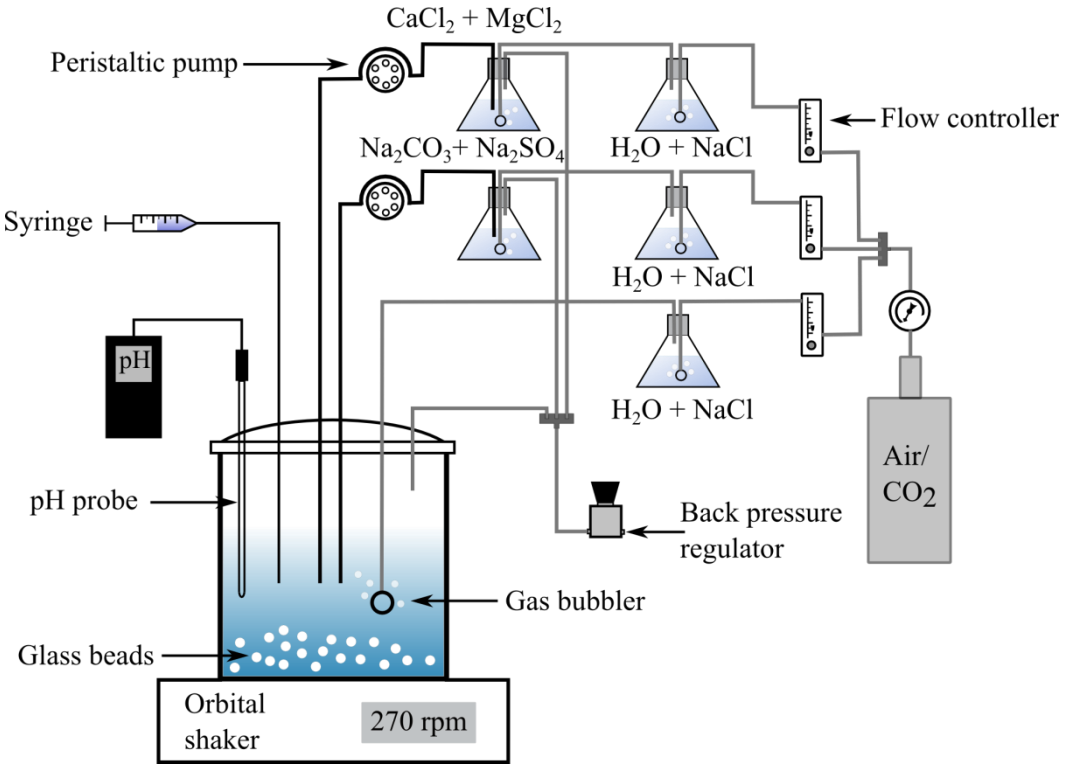

Figure 5. 1: *Experimental set-up*

5.2.2. Analytical methods

Ca, Mg and S concentrations in solution and in acid digested solid reaction products were determined by inductively coupled optical emission spectroscopy (ICP-OES) using a Thermo Scientific iCAP7400 ICP-OES with an analytical uncertainty ≤ 3% and a detection limit of 0.007, 0.04 and 0.005 for Mg, Ca and S respectively.

Precipitates were digested by dissolving a powder aliquot in HCl 10% and diluting with Milli-Q water. Solid samples were mineralogically characterized by X-ray powder diffraction (XRD) with a silicon internal standard, using a Bruker D8 X-Ray Diffractometer (Cu kα1). Note that the detection limit of the X-ray diffraction technique is ≈ 3% of the mass of the analysed sample. Scans were collected from 2 to 85° (2θ) and a quantitative estimate of the relative proportion of the precipitated $CaCO_3$ polymorphs and their unit cell parameters were performed with Topas 4-2® (Table B.1). To analyse the concentration of Ca, Mg and S in each of the polymorphs present in the solid reaction products, powder aliquots were embedded in epoxy, polished, carbon-coated and analysed by electron probe microanalysis (EPMA) using a JEOL Hyperprobe JXA-8500F with a thermal field-emission cathode. Si analysis were also performed in order to obtain a parameter which allowed us to detect whether we were analysing only $CaCO_3$ crystals or when part of a glass bead was also present in the selected area of interest. For quantitative chemical analysis the electron probe was operated at 15 kV acceleration voltage, 5 nA beam current and 1 µm spot size of crystal-free glassy areas. Standardization was done with dolomite (for Mg and Ca), ZnS (for S) and tugtupite (for Si). Counting times on peak and background were 30 and 15 seconds respectively for Mg and S and 10 and 5 seconds respectively for Ca and Si. Morphology and size of the precipitated $CaCO_3$ particles were characterized by SEM using a field emission gun scanning electron microscope (FEG SEM, FEI Quanta 650) operating at 10 keV. Size parameters of the precipitated particles were evaluated from each SEM image using ImageJ software.

5.3. Results

Our experiments were designed to study how changes in pCO_2 together with changes in seawater Mg:Ca ratio and SO_4 concentration affect the mineralogy of abiotic $CaCO_3$. Our results show that an increase in pCO_2 significantly favoured calcite precipitation at low Mg:Ca ratios (< 0.65 molar) (Figure 5.2). Overall, with increasing pCO_2 from 400 to 3000 ppm, the predominant calcite field (≥ 85% calcite) got wider, the calcite-aragonite co-precipitation field got narrower and the pure aragonite field kept constant. At 400 ppm of pCO_2, calcite presence in the samples was higher than 85% up to a Mg:Ca ratio of 0.22 and SO_4 concentration of

5 mM. More than 95% of the solid sample was calcite up to a Mg:Ca ratio of 0.35 and SO_4 concentration of 10 mM at 1500 ppm of pCO_2. At the highest studied pCO_2 (3000 ppm), pure calcite samples precipitated up to Mg:Ca ratio of 0.65 and SO_4 concentration of 10 mM. However, vaterite precipitation was less favoured with increasing pCO_2 (Table B.1). At current pCO_2 (400 ppm), vaterite formed in Mg free seawater conditions and at very low Mg:Ca ratios ($\leq$ 0.10) where SO_4 concentrations were up to 110 mM and 60 mM respectively. At 1500 ppm of pCO_2, vaterite still precipitated but only in Mg free seawater and at SO_4 concentrations from 10 to 36 mM. At 3000 ppm of pCO_2, vaterite did not precipitate at all.

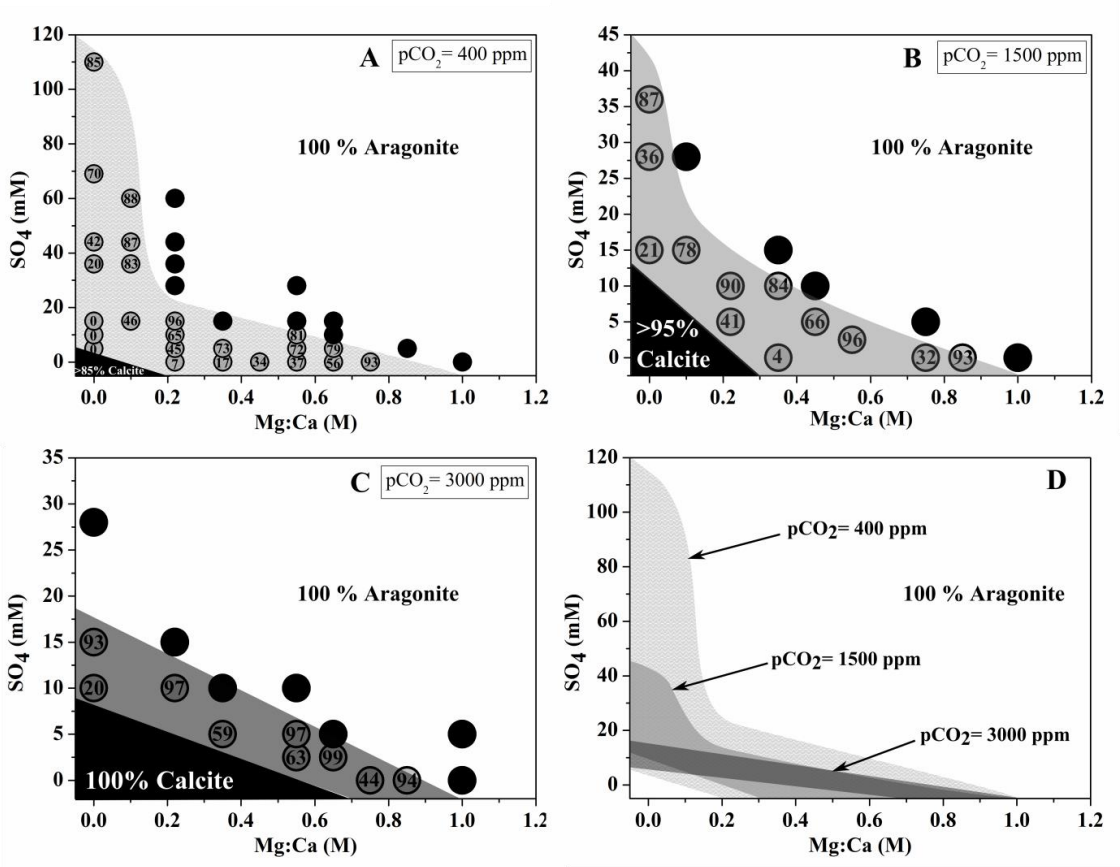

Figure 5. 2: *Schematic diagrams of the average proportion of aragonite in the solid reaction products as a function of Mg:Ca ratio, SO_4 concentration and pCO_2; A) pCO_2= 400 ppm; B) pCO_2= 1500 ppm; C) pCO_2= 3000 ppm; D) Comparison of the calcite-aragonite co-existence field at the 3 studied atmospheric pCO_2 . Numbers in circles represent the proportion of aragonite present in the sample; black circles represent 100% aragonite samples; grey shaded areas represent the aragonite-calcite coexistence fields; black shaded areas represent the >85% calcite field in A, the >95% calcite field in B and the 100 % calcite field in C.*

As mentioned above, the pure aragonite field mostly stayed the same, but at seawater Mg:Ca ratios lower than 0.22, pure aragonite precipitated at lower SO_4

concentrations at 3000 ppm of pCO_2 than at 1500 ppm. At the current atmospheric pCO_2 composition (400 ppm), pure aragonite did not precipitate when the Mg:Ca ratio was lower than 0.22.

Both, ICP-OES analyses of the digested polymorphs and quantitative EPMA of the solid products confirmed that Mg became incorporated only into calcite while SO_4 became incorporated into all the three polymorphs (calcite, aragonite and vaterite) (Table A.2 & B.2). Our EPMA data revealed that changes in pCO_2 and therefore in pH, influence the Mg incorporation into calcite as pCO_2 increases (Figure 5.3 A). At low Mg:Ca ratios in solution (Mg:Ca< 0.55), the incorporation of Mg into calcite is quite similar at the three studied pCO_2. However, at high Mg:Ca ratios in solution (Mg:Ca≥ 0.55), Mg incorporation into calcite is approximately 1.6 – 2.0 times higher at 400 ppm than at either 1500 or 3000 ppm of pCO_2. Surprisingly, the Mg incorporation into calcite is pretty similar at 1500 and 3000 ppm pCO_2 and for the whole range of seawater SO_4 concentrations and Mg:Ca ratios studied. As a general trend and for the 3 studied partial pressures of carbon dioxide, Mg incorporation into calcite increases as Mg:Ca ratio in solution increases, and decreases as SO_4 concentration in solution increases. On the contrary, SO_4 incorporation into calcite decreases as Mg:Ca ratio in solution decreases and increases as SO_4 concentration in solution increases (Figure 5.3 B, E & F). Our data indicate that the incorporation of SO_4 into calcite is significantly affected by changes in pCO_2 (Figure 5.3 B, C & D), being ≈ 1.5 ± 0.2 higher at high pCO_2 (1500 and 3000 ppm) than at the current one (400 ppm). SO_4 incorporation into calcite seems to be also higher at 1500 ppm than at 3000 ppm of pCO_2, but from this set of experiments, only EPMA data from samples precipitated at seawater Mg:Ca= 0 are available to quantify this relationship (Figure 5.3 C). On the other hand, our data showed a negligible influence of pCO_2 on SO_4 content in aragonite (Figure 5.3 E & F).

Solid material recovered after the end of the experiments at high pCO_2 (1500 and 3000 ppm) exhibits a similar morphology to that at current pCO_2 (400 ppm) for the three anhydrous $CaCO_3$ phases: calcite, aragonite and vaterite. Hence, $CaCO_3$ morphology is not affected by changes in atmospheric pCO_2 and therefore in seawater pH. At the three studied pCO_2 but depending on the solution chemistry, calcite precipitated as rhombohedra, rod-like particles and trigonal prims. In most of the experimental conditions, aragonite precipitated with a needle like morphology. At very high seawater Mg:Ca ratios (Mg:Ca= 5.2) and SO_4 concentrations (110

mM), the needles branched into dumbbell structures. Vaterite always precipitated in "pan-cake" like plates, with the plates aggregated together to form flaky-floret structures.

Changes in pCO_2 also strongly influenced particle size. $CaCO_3$ particles grown at high pCO_2 conditions (1500 and 3000 ppm) were significantly smaller than the particles grown under current atmospheric pCO_2 conditions (Figure 5.4). While at current pCO_2 most calcite particles (97%) are bigger than 3 μm, at 1500 ppm of pCO_2 only 28% of the calcite crystals are bigger than 3 μm. At the highest studied partial pressure of carbon dioxide (3000 ppm), calcite particles were always smaller than 4 μm, with 75% of the particles smaller than 3 μm. This decrease of particle size with increasing pCO_2 was also observed for aragonite and vaterite particles.

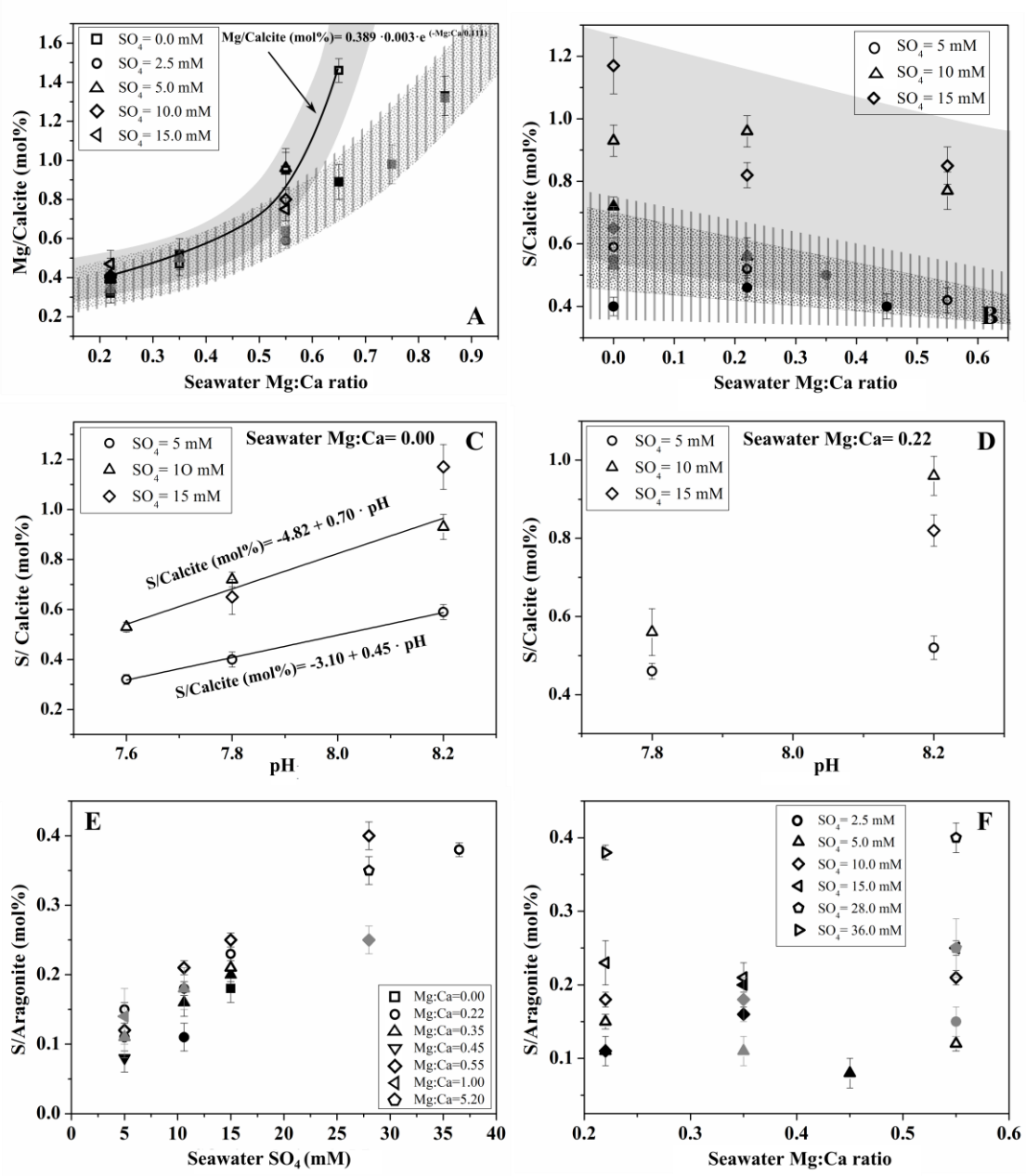

Figure 5. 3: *a) Mg incorporation into calcite as a function of Mg:Ca ratio and SO_4 concentration in solution for the 3 studied pCO_2 (400, 1500 and 3000 ppm); b) S incorporation into calcite as a function of Mg:Ca ratio and SO_4 concentration in solution for the 3 studied pCO_2 (400, 1500 and 3000 ppm); c) S incorporation into calcite as a function of pH and SO_4 concentration in solution for a seawater Mg:Ca ratio= 0; d) S incorporation into calcite as a function of pH and SO_4 concentration in solution for a seawater Mg:Ca ratio= 0.22; e) S incorporation into aragonite as a function of Mg:Ca ratio and SO_4 concentration in solution for the 3 studied pCO_2 (400, 1500 and 3000 ppm); f) e) S incorporation into aragonite as a function of Mg:Ca ratio and SO_4 concentration in solution at pCO_2 =400 ppm. Open black symbols represent data at 400 ppm of pCO_2; closed black symbols represent data at 1500 ppm of pCO_2; closed grey symbols represent data from experiments at 3000 ppm of pCO_2; grey shaded area highlights the trend of the incorporation of Mg or S into calcite, or S incorporation into aragonite at 400 ppm of pCO_2; stripes shaded area highlights the trend of the incorporation of Mg or S into calcite, or S incorporation into aragonite at 1500 ppm of pCO_2; dot shaded area highlights the trend of the incorporation of Mg or S into calcite, or S incorporation into aragonite at 3000 ppm of pCO_2.*

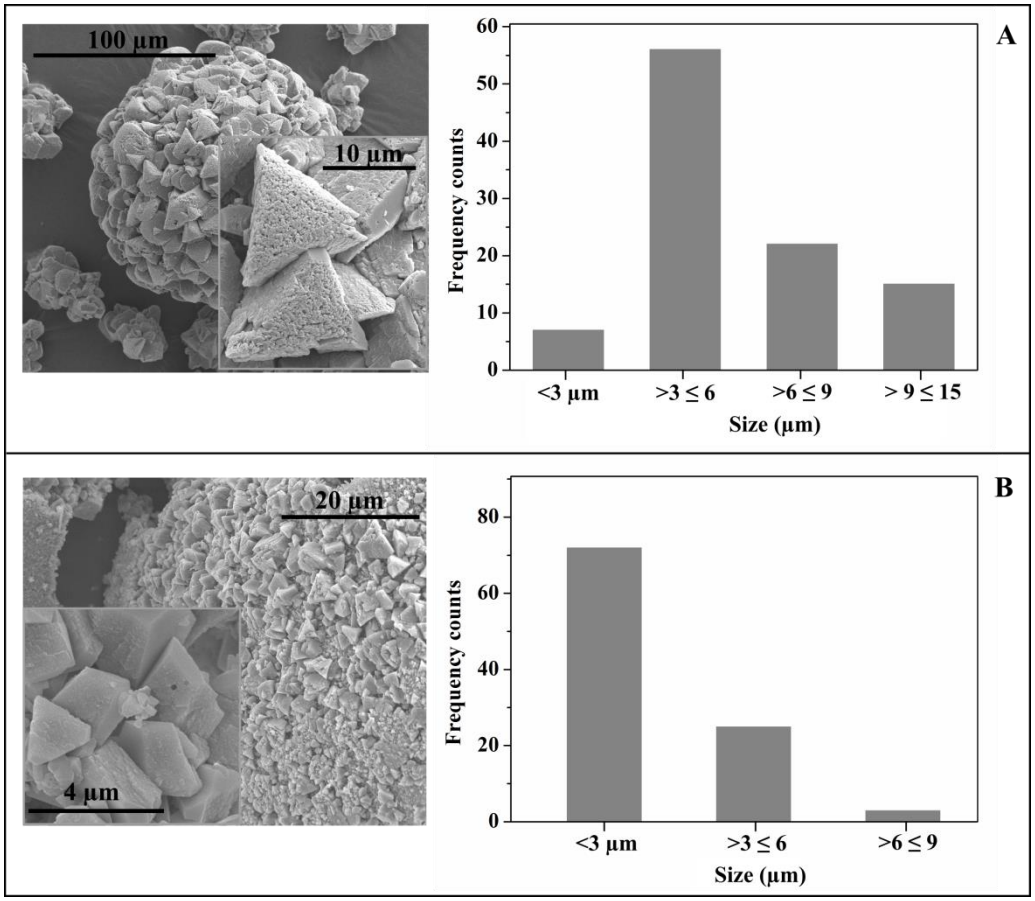

Figure 5. 4: *Influence of pCO_2 on calcite crystal size. Solution chemistry: Mg:Ca= 0.22 M; SO_4= 0 mM; T= 21°C. a) pCO_2= 400 ppm; b) pCO_2= 1500 ppm.*

5.4. Implications of ocean acidification on abiogenic marine $CaCO_3$ mineralogy and on Phanerozoic aragonite-calcite seas.

The results of this study indicate that calcium carbonate precipitation in the ocean occurs even at extreme atmospheric partial pressures of carbon dioxide (up to pCO_2 of 3000 ppm) (Janie Lee, 2010). Therefore, an increase in ocean acidification due to an increase in the atmospheric pCO_2 resulting from anthropogenic emissions of CO_2 may not have severe consequences for inorganic marine carbonates as the current projections related to increased rates of dissolution as pH declines. However, increased atmospheric pCO_2 would impact on the calcite-aragonite co-precipitation range, the Mg incorporation into calcite and SO_4 incorporation into both calcite and aragonite, and the calcite particle size.

An increase of atmospheric pCO_2 from 400 ppm to 3000 ppm and its consequent decrease of seawater pH from 8.2 to 7.6 would cause a decrease of the seawater

Mg:Ca ratio and SO_4 concentration ranges that limit the current aragonite-calcite co-precipitation field. This downsizing of the aragonite-calcite co-precipitation area with decreasing pH is because lower pH favours calcite precipitation. Lower seawater pH scenarios would be characterized by having a wider pure calcite precipitation field and higher proportion of calcite with respect to aragonite in the aragonite-calcite co-precipitation field, but these variations in abiotic marine $CaCO_3$ mineralogy with pH would be only manifested in the seawater Mg:Ca ratio range from 0 to 1. The stability field for pure aragonite would remain constant. Thus, under future increasingly acidic seawater conditions, abiotic carbonate minerals such as calcite and low Mg-calcite could become increasingly dominant but only in ocean environments of very low seawater Mg:Ca ratios (Mg:Ca$\leq$ 1).

Although elevated pCO_2 levels and lower carbonate ion (CO_3^{2-}) concentrations have been suggested to be responsible of making calcite the dominate polymorph in the Phanerozoic Eon (Wilkinson and Given, 1986), our work shows that acidic seawater conditions contribute to higher ratios of calcite but only when seawater Mg:Ca ratio is lower than 1. It is therefore possible to confirm that past changes in atmospheric pCO_2 and hence in seawater pH did not play an important role in the secular oscillations between predominant aragonite and calcite seas during the Phanerozoic Eon.

Mg content in calcite generally decreases with increasing water depth, decreasing carbonate ion concentration and decreasing temperature (Videtich, 1985) (Chapter 4). Carbonate ion concentration is influenced by variations in any of the other species of the carbonic acid system (HCO_3^-, pCO_2 and H^+). The influence of pCO_2 on the incorporation of Mg in calcite has been studied extensively so far (Hartley and Mucci, 1996; Katz, 1973; Morse et al., 1997b; Mucci and Morse, 1983). Although the literature on this subject is abundant, it is marked by controversy. An inverse linear correlation between the Mg content of calcite overgrowths and $\log_{10}pCO_2$ of the gas phase in equilibrium with the parent solutions has been shown in some studies (Elizabeth A. Burton, 1991). However, other studies suggest that the Mg content of the calcite overgrowths is independent of the pCO_2 (Hartley and Mucci, 1996).

Our results indicate that the dependence of Mg incorporation into calcite on pH varies depending on whether atmospheric pCO_2 is low (current one, 400 ppm) or

high (1500 and 3000 ppm) and whether seawater Mg:Ca ratio is lower or higher than 0.55. Atmospheric pCO_2 and therefore seawater pH do not influence Mg incorporation into calcite when seawater Mg:Ca ratio is < 0.55, that is, in the aragonite-calcite co-precipitation range where calcite is the predominant polymorph at current pCO_2. However, the incorporation of Mg into calcite exponentially decreases as pH decreases from 8.2 to 7.8 (400 ppm and 1500 ppm of pCO_2 respectively) when seawater Mg:Ca is ≥ 0.55, that is, in the aragonite-calcite co-precipitation range where aragonite is the predominant $CaCO_3$ phase at current pCO_2. When pCO_2 is equal or higher than 1500 ppm (pH≤ 7.8), there is not an influence of pH on Mg incorporation into calcite at any seawater Mg:Ca range. Hence, the Mg content of abiotic calcitic minerals will decrease in more acidic conditions due to changes in surface seawater chemistry (ocean acidification and decreasing seawater carbonate saturation), but only in ocean environments of 0.55≤ Mg:Ca <1.

It has been extensively reported that ocean acidification due to anthropogenic emissions of CO_2 may have severe consequences for some marine calcifying organisms, but specially for low Mg-calcite, high latitude and cold-water calcifiers (Andreas J. Andersson, 2008). Also, it is predicted that the magnesium content of calcitic hard parts will decrease both kinetically and thermodynamically due to these changes in surface seawater chemistry (lower CO_3^{2-} concentration and consequently lower carbonate saturation state) (Fred T. Mackenzie, 1983). On the other hand, there are some species of algae such as crustose coralline algae which show no significant effect of pCO_2 on their Mg content (M. C. Nash, 2015). Because the response of organisms to ocean acidification is species specific since they have the ability to influence the polymorph formation and control the intake of trace elements, the growth parameters of non-biogenic polymorph formation grown from artificial seawater cannot be used for biogenic applications. However, it could be used to predict how far from equilibrium their carbonate is and therefore the energy that they will need to expend to control its precipitation.

Biogeochemical sulfur cycling has varied widely over geologic time, mainly in response to environmental factors that includes changes in pyrite burial driven by organic carbon supply, volcanism, weathering and evaporite deposition. In conjunction, these processes are linked to numerous oceanic anoxic events (OAEs) that are marked by intervals of enhanced organic carbon burial which are attributed

to increased primary production under greenhouse conditions; this means under elevated temperatures, elevated atmospheric carbon dioxide concentrations, rising sea level and lower oxygen solubility in seawater. Studies based on sulfur isotope records from carbonate-associated sulfate and pyrite have asserted that during the two most globally significant OAEs (OAE1 and OAE2) marine sulfate concentrations were much lower than modern concentrations (Adams et al., 2010; Gomes et al., 2016; Paris et al., 2014; Poulton et al., 2015). Our work shows that changes in atmospheric pCO_2 and consequently changes in seawater pH affect significantly the incorporation of SO_4 into calcite. In Mg free seawater and 5 mM of SO_4 concentration, the SO_4 content in calcite decreased from 0.59 mol% at pH= 8.2 to 0.32 mol% at pH= 7.6 (Figure 5.3 C). SO_4 incorporation into calcite showed a similar dependence on pH at other seawater Mg:Ca ratios, but trends are offset by seawater SO_4 concentration effects on SO_4 incorporation into calcite (Figure 5.3 B & D). Hence, our results evidences that lower SO_4 contents in marine calcitic carbonates can be attributed to the relative contribution of high atmospheric carbon dioxide concentrations (>400 ppm), low seawater SO_4 concentrations and high temperatures (≥35°C) (Chapter 4), which are environmental conditions characteristic of oceanic anoxic events. Here, we prove a clear relationship among abiogenic calcite SO_4 content, seawater SO_4 concentration and seawater pH. Therefore, we propose abiogenic calcite SO_4 content as a reliable quantitative proxy for past global seawater pH if its dependence on both pH and seawater SO_4 concentration is considered. The use of SO_4 content in abiogenic calcite as a paleo-pH proxy would help to constrain ancient marine pH and therefore ancient atmospheric carbon dioxide concentrations.

This work together with that presented in the Chapter 4 on how temperature, seawater Mg:Ca ratio and SO_4 concentration could have affected the $CaCO_3$ primary mineralogy during the Phanerozoic Eon, provide a multi-variable approach to better understand the mechanisms that facilitate the dominant $CaCO_3$ mineralogy and hence the secular oscillation between aragonite and calcite seas. Previous work on the drivers of these variations has focused mainly on seawater Mg:Ca ratio, not only in the mineralogy of abiotic $CaCO_3$ but also in sediment-producing calcifiers and reef builders (Morse et al., 2007; Stanley and Hardie, 1998). However, other parameters such as temperature (Balthasar and Cusack, 2015; Elizabeth A. Burton, 1987; Morse et al., 1997b), pCO_2 (Janie Lee, 2010; Morse et al., 2007) and SO_4

(Bots et al., 2011) (Chapter 4) are also known to influence $CaCO_3$ polymorph formation but are often overlooked in the context of aragonite-calcite seas.

Now, from our extensive experimental data set of characterized $CaCO_3$ samples precipitated at a wide range of seawater Mg:Ca ratios, SO_4 concentrations, temperature and atmospheric pCO_2 values, it can be concluded that neither temperature nor atmospheric pCO_2 lead to large variations in the predominant $CaCO_3$ polymorph distribution. Note that it has been considered as predominant polymorph which its presence in the sample is $\geq$ 50%. The main driving forces controlling the precipitation of $CaCO_3$ polymorphs are seawater Mg:Ca ratio and SO_4 concentration (Bots et al., 2011) (Chapter 4).

Our proposed Mg:Ca ratio at which aragonite predominance seas switch to calcite predominance seas is 0.65±0.1, which is in agreement with Mg:Ca ratios suggested by previous experimental studies (Mg:Ca$\approx$ 0.6 – 0.7) (Bots et al., 2011) but is far lower than the Mg:Ca ratio of 2 determined from marine halite fluid inclusions (Horita et al., 2002; Lowenstein et al., 2003) (Figure 5.5 B).

Combining literature data (Demicco et al., 2005; Hardie, 1996; Lowenstein et al., 2003; Sandberg, 1983b) with our experimental data revealed that to have a similar aragonite-calcite seas scenario over time to that shown in the literature, during the Phanerozoic there must have been periods when seawater SO_4 concentration was lower than 10 mM, reaching the lowest possible values suggested by the geological record (Figure 5.5 A. Note that our seawater SO_4 concentration trend would be the red dashed line) (Adams et al., 2010; Berner, 2004; Holland, 2005; Newton et al., 2011; Poulton et al., 2015; Wortmann and Chernyavsky, 2007). Even though considering the lowest values of seawater SO_4 concentration prescribed in literature and from our experimental data, the first and second periods of aragonite seas must have been slightly longer (Figure 5.5 A). However, taking into account only the trend suggested in literature for seawater SO_4 concentration and assuming a minimum SO_4 concentration of just under 10 mM in some of the time periods, would lead to very extensive periods of aragonite predominance seas and very constricted periods of calcite predominance seas (Figure B.2 A & B).

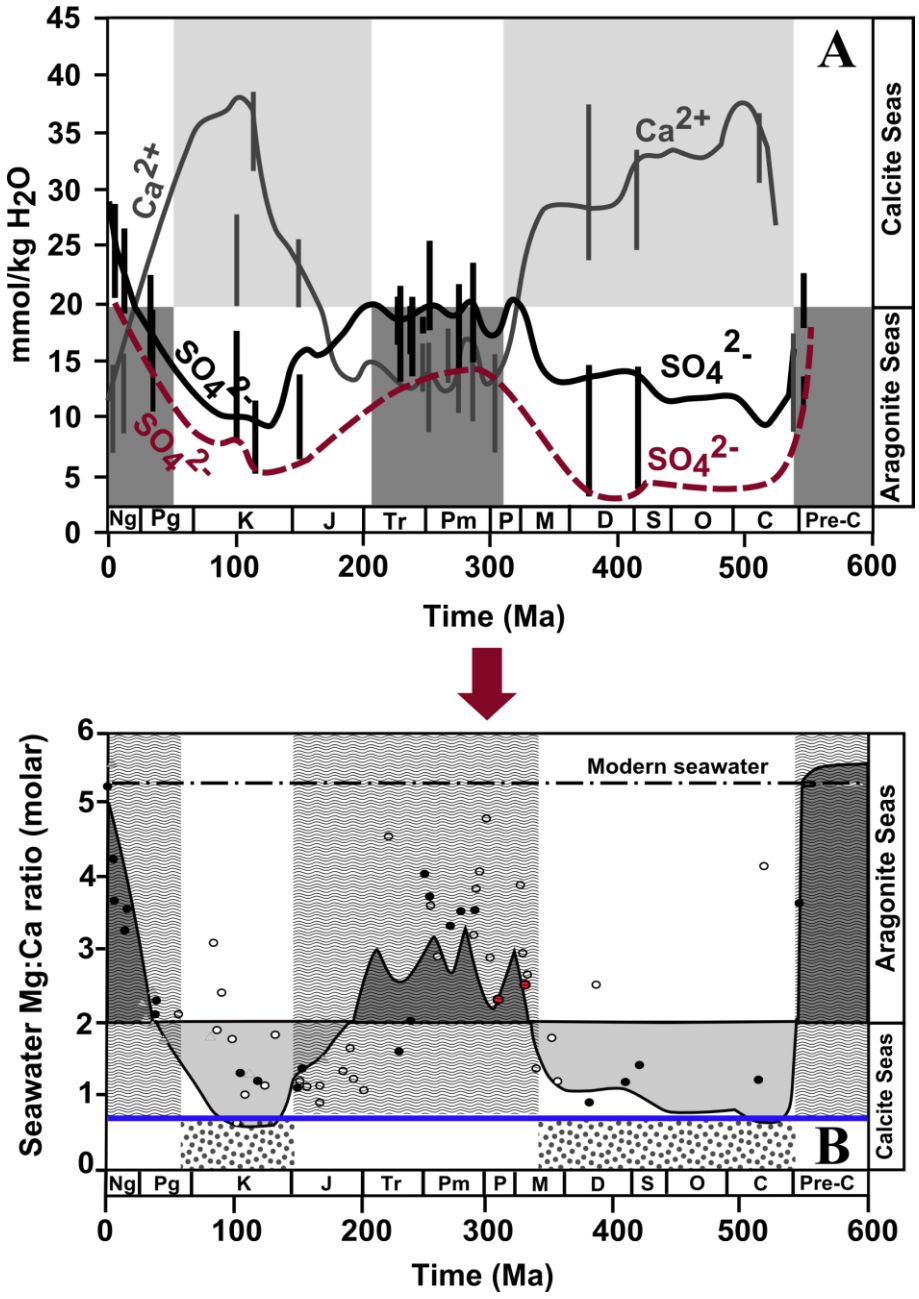

Figure 5. 5: *A) Secular variation in concentration of Ca^{2+} and SO_4^{2-} in seawater during the Phanerozoic from primary fluid inclusions in marine halite (grey and black bars). Ca^{2+} and SO_4^{2-} curves are from model of Phanerozoic seawater composition (Robert V. Demicco, 2005). Figure modified after Holt et al., 2014. Dashed red line represents our proposed curve for SO_4^{2-}Phanerozoic seawater concentrations. B) Secular variation in the Mg:Ca ratio of seawater during Phanerozoic. Horizontal black line at Mg:Ca= 2 represents the approximate divide between aragonite and calcite nucleation fields in seawater at 25ºC; .Figure modified after Holt et al., 2014. Horizontal dashed black line represent the current seawater Mg:Ca. Horizontal blue line represents the seawater Mg:Ca ratio (Mg:Ca≈ 0.65±0.1) proposed from this study and M.P. Ramírez-García et al., 2018. Wavy grey shaded areas and dotted grey shaded areas represent our proposed periods of time for aragonite and calcite seas respectively.*

5.5. Conclusions

Our experimental data reveal that neither changes in pCO_2 in the range 400 to 3000 ppm, or their respective changes in seawater pH (8.2, to 7.6) lead to major variations in the stability fields for aragonite and calcite precipitation. Hence, pCO_2 and seawater pH do not need to be considered as major controls on the Phanerozoic oscillations between aragonite and calcite seas and the dominant controls can be considered to be Mg:Ca and SO_4 concentration alone.

In the future, ocean acidification due to anthropogenic emissions of CO_2 will not cause a significant response of the primary abiogenic marine $CaCO_3$ mineralogy to decreasing seawater pH.

We propose SO_4 content in abiogenic calcite as a reliable and quantitative proxy for past seawater pH and atmospheric pCO_2, but our results indicated that it is not possible to provide a single SO_4–pH calibration and the use of seawater SO_4-specific equations is needed.

It can also be concluded that switches between aragonite and calcite seas calculated from the stability fields from our experimental results would only match the proxy data for seawater chemistry in the geological record if the lowest suggested seawater SO_4 concentrations are considered ($[SO_4] \leq 10$ mM) (Adams et al., 2010; Newton et al., 2011; Poulton et al., 2015; Wortmann and Chernyavsky, 2007).

After our extensive evaluation and quantification of the influence of seawater Mg:Ca ratio, SO_4 concentration, temperature and atmospheric pCO_2 in abiotic seawater $CaCO_3$ mineralization, our suggested seawater Mg:Ca threshold for calcite predominant seas is 0.65±0.1 (Bots et al., 2011) (Chapter 4), still far lower than the Mg:Ca ratio of ≈2 proposed in literature (Horita et al., 2002; Lowenstein et al., 2003). Because the ocean is such as complex environment, this mismatch between our experimental and the aragonite-calcite seas pattern from the record could also indicate the importance of other variables such as dissolved organics, alkalinity, etc. to changes in carbonate mineralogy.

References

Adams, D. D., Hurtgen, M. T., and Sageman, B. B., 2010, Volcanic triggering of a biogeochemical cascade during Oceanic Anoxic Event 2: Nature Geoscience, v. 3, p. 201.

Andreas J. Andersson, F. T. M. a. N. R. B., 2008, Life on the margin: implications of ocean acidification on Mg-calcite, high latitude and cold-water marine calcifiers: Marine Ecology Progress Series, v. 373, p. 265-274.

Balthasar, U., and Cusack, M., 2015, Aragonite-calcite seas—Quantifying the gray area: Geology, v. 43, no. 2, p. 99-102.

Berner, R. A., 2004, A model for calcium, magnesium and sulfate in seawater over Phanerozoic time: American Journal of Science, v. 304, no. 5, p. 438-453.

Bots, P., Benning, L., Rickaby, R., and Shaw, S., 2011, The role of SO4 in the switch from calcite to aragonite seas: Geology, v. 39, no. 4, p. 331-334.

Burton, E. A., and Walter, L. M., 1991, The effects of PCO2 and temperature on magnesium incorporation in calcite in seawater and MgCl2-CaCl2 solutions: Geochimica et Cosmochimica Acta, v. 55, no. 3, p. 777-785.

Busenberg, E., and Niel Plummer, L., 1985, Kinetic and thermodynamic factors controlling the distribution of SO32− and Na+ in calcites and selected aragonites: Geochimica et Cosmochimica Acta, v. 49, no. 3, p. 713-725.

Caldeira, K., and Wickett, M. E., 2003, Anthropogenic carbon and ocean pH: Nature, v. 425, p. 365.

Davis, K. J., Dove, P. M., and De Yoreo, J. J., 2000, The role of Mg2+ as an impurity in calcite growth: Science, v. 290, no. 5494, p. 1134-1137.

Demicco, R. V., Lowenstein, T. K., Hardie, L. A., and Spencer, R. J., 2005, Model of seawater composition for the Phanerozoic: Geology, v. 33, no. 11, p. 877-880.

Elizabeth A. Burton, a. L. M. W., 1991, The effects of PCO2 and temperature on magnesium incorporation in calcite in seawater and MgCl2-CaCl2 solutions: Geochimica et Cosmochimica Acta, v. 55, no. 3, p. 777-785.

Elizabeth A. Burton, L. M. W., 1987, Relative precipitation rates of aragonite and Mg calcite from seawater: Temperature or carbonate ion control?: Geology, v. 15, no. 2, p. 111-114.

Fred T. Mackenzie, W. D. B., Finley C. Bishop, Michele Loijens, Jane Schoonmaker and Roland Wollast, 1983, Magnesian calcites; low-temperature occurrence, solubility and solid-solution behavior: Reviews in Mineralogy and Geochemistry, v. 11, no. 1, p. 97-144.

Gomes, M. L., Hurtgen, M. T., and Sageman, B. B., 2016, Biogeochemical sulfur cycling during Cretaceous oceanic anoxic events: A comparison of OAE1a and OAE2: Paleoceanography, v. 31, no. 2, p. 233-251.

Hardie, L. A., 1996, Secular variation in seawater chemistry: An explanation for the coupled secular variation in the mineralogies of marine limestones and potash evaporites over the past 600 m.y: Geology, v. 24, no. 3, p. 279-283.

Hartley, G., and Mucci, A., 1996, The influence of PCO2 on the partitioning of magnesium in calcite overgrowths precipitated from artificial seawater at 25° and 1 atm total pressure: Geochimica et Cosmochimica Acta, v. 60, no. 2, p. 315-324.

Holland, H. D., 2005, Sea level, sediments and the composition of seawater: American Journal of Science, v. 305, no. 3, p. 220-239.

Horita, J., Zimmermann, H., and Holland, H. D., 2002, Chemical evolution of seawater during the Phanerozoic: Implications from the record of marine evaporites: Geochimica et Cosmochimica Acta, v. 66, no. 21, p. 3733-3756.

Janie Lee, J. W. M., 2010, Influences of alkalinity and pCO2 on CaCO3 nucleation from estimated Cretaceous composition seawater representative of "calcite seas": Geology v. 38, no. 2, p. 115-118.

Katz, A., 1973, The interaction of magnesium with calcite during crystal growth at 25–90°C and one atmosphere: Geochimica et Cosmochimica Acta, v. 37, no. 6, p. 1563-1586.

Lowenstein, T. K., Hardie, L. A., Timofeeff, M. N., and Demicco, R. V., 2003, Secular variation in seawater chemistry and the origin of calcium chloride basinal brines: Geology, v. 31, no. 10, p. 857-860.

M. C. Nash, S. U., A. P. Negri and N. E. Cantin, 2015, Ocean acidification does not affect magnesium composition or dolomite formation in living crustose coralline algae, Porolithon onkodes in an experimental system: Biogeosciences Discussions, v. 12, p. 1373-1404.

Morse, J. W., Arvidson, R. S., and Lüttge, A., 2007, Calcium Carbonate Formation and Dissolution: Chemical Reviews, v. 107, no. 2, p. 342-381.

Morse, J. W., Wang, Q., and Tsio, M. Y., 1997, Influences of temperature and Mg:Ca ratio on CaCO3 precipitates from seawater: Geology, v. 25, no. 1, p. 85-87.

Mucci, A., and Morse, J. W., 1983, The incorporation of Mg2+ and Sr2+ into calcite overgrowths: influences of growth rate and solution composition: Geochimica et Cosmochimica Acta, v. 47, no. 2, p. 217-233.

Newton, R. J., Reeves, E. P., Kafousia, N., Wignall, P. B., Bottrell, S. H., and Sha, J.-G., 2011, Low marine sulfate concentrations and the isolation of the European epicontinental sea during the Early Jurassic: Geology, v. 39, no. 1, p. 7-10.

Paris, G., Fehrenbacher, J. S., Sessions, A. L., Spero, H. J., and Adkins, J. F., 2014, Experimental determination of carbonate-associated sulfate δ34S in planktonic foraminifera shells: Geochemistry, Geophysics, Geosystems, v. 15, no. 4, p. 1452-1461.

Plummer, L. N., 1979, Critical review of the kinetics of calcite dissolution and precipitation: Chemical Modeling in Aqueous Systems., p. 539-573.

Poulton, S. W., Henkel, S., März, C., Urquhart, H., Flögel, S., Kasten, S., Damsté, J. S. S., and Wagner, T., 2015, A continental-weathering control on orbitally driven redox-nutrient cycling during Cretaceous Oceanic Anoxic Event 2: Geology, v. 43, no. 11, p. 963-966.

Robert V. Demicco, T. K. L., Lawrence A. Hardie, and Ronald J. Spencer, 2005, Model of seawater composition for the Phanerozoic: Geology, v. 33, no. 11, p. 877-880.

Sandberg, P. A., 1983, An oscillating trend in Phanerozoic non-skeletal carbonate mineralogy: Nature, v. 305, p. 19.

Simon W. Poulton, S. H., Christian März, Hannah Urquhart, Sascha Flögle, Sabine Kasten, Jaap S. Sinninghe, Damsté, Thomas Wagner, 2015, A continental-weathering control on orbitally driven redox-nutrient cycling during Cretaceous Oceanic Anoxic Event 2: Geology, v. 43, no. 11, p. 963-966.

Stack, A. G., and Grantham, M. C., 2010, Growth Rate of Calcite Steps As a Function of Aqueous Calcium-to-Carbonate Ratio: Independent Attachment and Detachment of Calcium and Carbonate Ions: Crystal Growth & Design, v. 10, no. 3, p. 1409-1413.

Stanley, S. M., and Hardie, L. A., 1998, Secular oscillations in the carbonate mineralogy of reef-building and sediment-producing organisms driven by tectonically forced shifts in seawater chemistry: Palaeogeography, Palaeoclimatology, Palaeoecology, v. 144, no. 1, p. 3-19.

Takano, B., 1985, Geochemical implications of sulfate in sedimentary carbonates: Chemical Geology, v. 49, no. 4, p. 393-403.

Videtich, P. E., 1985, Electron Microprobe Study of Mg Distribution in Recent Mg Calcites and Recrystallized Equivalents from the Pleistocene and Tertiary: Journal of Sedimentary Research, v. 55, no. 3, p. 421-429.

Wilkinson, B. H., and Given, R. K., 1986, Secular Variation in Abiotic Marine Carbonates: Constraints on Phanerozoic Atmospheric Carbon Dioxide Contents and Oceanic Mg/Ca Ratios: The Journal of Geology, v. 94, no. 3, p. 321-333.

Wortmann, U. G., and Chernyavsky, B. M., 2007, Effect of evaporite deposition on Early Cretaceous carbon and sulphur cycling: Nature, v. 446, no. 7136, p. 654-656.

Chapter 6
Influence of magnesium, sulfate and temperature on calcium carbonate morphogenesis.

M.P. Ramírez-García[1], Robert J. Newton[1] and Liane G. Benning[1,2]

[1]Sc**h**ool of Earth and Environment, University of Leeds

[2] German Research Centre for Geosciences, GFZ, Potsdam, Germany

Abstract

The morphogenesis and phase changes of calcium carbonate ($CaCO_3$) at different solution Mg:Ca ratios (0 – 5.2 molar), SO_4 concentrations (0 – 110 mM) and temperatures (5, 21 and 35°C) were carefully investigated. $CaCO_3$ precipitates were characterized with scanning electron microscopy, X-ray diffraction (XRD) and electron probe microanalysis (EPMA). It was observed that particle size is significantly influenced by temperature, decreasing as temperature increases. Moreover, the morphology of the precipitates also varied with temperature; especially in calcite which showed a wide range of morphologies such us aggregated particles of regular plate-like, elongated along the c-axis rhombohedras, inter-grown triangles, trigonal prisms, etc. Mg and SO_4 in solution led to changes in crystal morphology and favoured particle aggregation.

6.1. Introduction

Calcium carbonate, one of the most widely existing biominerals produced by organisms, has been widely used as a model system for investigating inorganic precipitation reaction or crystallization due to $CaCO_3$ particles polymorphic forms and particle sizes can significantly affect their final application (Manoli and Dalas, 2000). The controllable synthesis of $CaCO_3$ has received much attention owing to its wide application in such industrial fields as paper, rubber, plastics, paint, etc., (Chen et al., 1989). Recently, capture and conversion of CO_2 from fossil fuel power plants

and other industrial sources into carbonates via aqueous precipitation is an emerging application (Lacroix and Larachi, 2008).

A number of strictly defined parameters, such as morphology, size, structure, specific surface area, chemical purity, brightness, etc., determine the application of $CaCO_3$ particles. Particle morphology is one of the most important parameters; therefore, the control of crystal shape and size is fundamental from the viewpoint of technical application (Ajikumar et al., 2004; Küther et al., 1998; Qi et al., 2002). Many approaches have been developed to control the phases and the morphologies of $CaCO_3$ in order to meet the demands in practical applications. Some of methods developed so far are focused on: the study of organic additives on the crystallization of calcium carbonate (Walsh et al., 1999), the crystallization of needle-like vaterite calcium carbonate using the cooperative effect between Mg and the gold nanoparticles (Lee et al., 2001), the influence of inorganic additives (Mg^{2+}, Fe^{2+}, Ni^{2+} and Zn^{2+} etc.) on the formation of calcium carbonate (Loste et al., 2003a; Ota et al., 1995; Wada et al., 1995), the control of the pH, the supersaturation (Tai and Chen, 1998) or the conductivity (García Carmona et al., 2003), etc.

Although various examples of morphology control have been reported, the exploration of facile and mild synthesis of inorganic minerals with controllable morphology and polymorph in aqueous solution remains non-systematic and challenging. In this paper, $CaCO_3$ polymorphs (calcite, aragonite and vaterite) were synthetized at different Mg and SO_4 concentrations in solution and at 5, 21 and 35ºC using a constant addition method. The influence of inorganic additives such as Mg and SO_4 and temperature on $CaCO_3$ morphology, particle size and polymorphs distribution was evaluated by quantitative and qualitative analyses (XRD, EPMA and SEM).

6.2. Methods

6.2.1. $CaCO_3$ synthesis

The constant addition method that was explained in detail in Chapter 4 was used to carry out $CaCO_3$ precipitation experimental at different Mg:Ca ratios (0 – 5.2 molar), SO_4 concentrations (0 – 110 mM) and at 5, 21 and 35°C. Precipitation of

$CaCO_3$ was induced by continuous injection of two separate $CaCl_2$ (250 mM) + $MgCl_2$ (0-110 mM) and Na_2CO_3 (230 mM) + Na_2SO_4 (0 – 220 mM) solutions into a reactor filled with 450 ml of a batch model seawater solution. The solutions were added at a constant rate of 1.0 ml/h for 48 hours. The batch model seawater solutions were prepared by adding 10 mM $CaCl_2 \cdot 2H_2O$ and keeping the $CaCl_2$, Na_2CO_3 and Na_2SO_4 concentration and the molar ratio of $MgCl_2$ to $CaCl_2$ the same as those of the injected solutions. NaCl was added to reach seawater salinity (35‰). Glass spheres (BioSpec Products 2g/l) were used in all the experiments as precipitation substrates and to mimic oöid formation in seawater. Before injection and to ensure homogeneous conditions, each model seawater batch solution was equilibrated with the atmosphere for at least 3 days in an open beaker (porous plug), while shaking at 270 rpm in an orbital shaker. The pH of the model seawater batch solution was adjusted drop wise with 2N NaOH until a pH ≈8.1 and an alkalinity of ≈1.6 mM was reached. The product was filtered through 0.2 μm polycarbonate track etch membrane filters, washed using Milli-Q water equilibrated with $CaCO_3$ and dried at 35°C for ≈12 hours.

6.2.2. Analysis of crystals

The resulting $CaCO_3$ precipitates were characterized by:

6.2.2.1. Scanning electron microscopy

The solid reaction products were mounted on Scanning Electron Microscopy stubs using conducting carbon tape and were sputter-coated with a ≈20 nm layer of carbon prior to viewing. Morphology and size of the precipitated $CaCO_3$ particles were characterized by SEM using a field emission gun scanning electron microscope (FEG SEM, FEI Quanta 650) operating at 10 keV. From each SEM image, size parameters of the precipitated particles were evaluated using ImageJ software.

6.2.2.2. Electron Microprobe Analysis (EMPA)

To analyse the concentration of Ca, Mg and S in each of the polymorphs present in the solid reaction products, powder aliquots were embedded in epoxy, polished, carbon-coated and analysed by electron probe microanalysis (EPMA) using a JEOL

Hyperprobe JXA-8500F with a thermal field-emission cathode. Si analysis were also performed in order to obtain a parameter which allowed us to detect whether we were analysing only $CaCO_3$ crystals or when part of a glass bead was also present in the selected area of interest. For quantitative chemical analysis the electron probe was operated at 15 kV acceleration voltage, 5 nA beam current and 1 µm spot size. Standardization was done with dolomite (for Mg and Ca), ZnS (for S) and tugtupite (for Si). Counting times on peak and background were 30 and 15 seconds respectively for Mg and S and 10 and 5 seconds respectively for Ca and Si.

6.2.2.3. X-ray powder diffraction (XRD)

The mineralogical composition of the solid samples was characterized by X-ray powder diffraction (XRD) with a silicon internal standard using a Bruker D8 X-Ray Diffractometer (Cu $k\alpha_1$). Data was collected from 2 to 85° (2θ). Samples were prepared by grinding ≈1 mg of sample in isopropanol and applying the dilute slurry to the surface of the sample holder, thus ensuring a smooth and uniform covering. The relative proportion of the different $CaCO_3$ phases in each sample and their unit cell parameters were determined performing Rietveld analysis using Topas 4-2®.

6.3. Results and discussion

In this study the role of solution Mg and SO_4 concentrations and the effect of temperature on the resulting solid $CaCO_3$ morphology and particle sizes were investigated. In the control experiment (no Mg or SO_4 added) at 5, 21 and 35ºC, pure calcite precipitated. The addition of seawater ions changed the phase distribution of the precipitates. The presence of low concentrations of Mg and SO_4 (Mg:Ca≤ 0.65 and [SO_4]≤ 10 mM) provoked the precipitation of magnesian calcite and aragonite. Pure aragonite was formed at Mg:Ca≥ 0.65 mM and SO_4 concentration ≤ 10 mM. In the absence of Mg but with SO_4 in solution, vaterite (a metastable phase) precipitated up to SO_4 concentrations of ≈ 60 mM. Higher SO_4 concentration in solution led to aragonite precipitation (see details in Chapter 4).

Temperature did not have a marked effect on polymorph distribution, but SEM images revealed that the morphology and sizes of the formed $CaCO_3$ particles were greatly affected by the reaction temperature. For identical solution chemical

compositions and reaction times, the size of the precipitated $CaCO_3$ particles decreased as temperature increased. This effect of temperature on calcium carbonate crystal size was observed for the three anhydrous polymorphs (calcite, aragonite and vaterite) and at all experimental conditions (Figure 6.1). As an example, Figure 6.1 shows that at low temperature (5°C), aragonite particles were bigger, with a length varying between 5 and 20 µm and a significant proportion of larger particles, up to 30 µm. However, at 21°C and 35°C the predominant size of aragonite particles varied between 0 to 4 µm, and the percentage of larger particles was much lower.

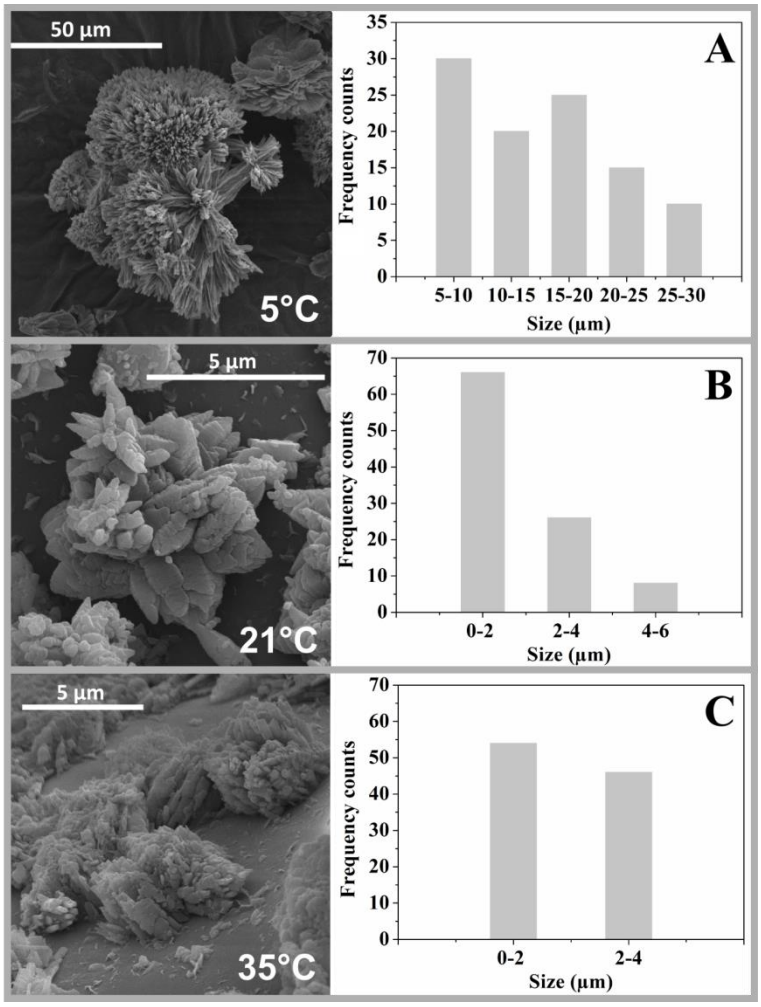

Figure 6. 1: *Influence of temperature on aragonite crystal size: Mg/Ca= 5.2; SO_4= 110 mM; a) 5°C; b) 21°C; b) 35°C.*

In accordance with previous studies (Bots et al., 2011) (Chapter 4), our EPMA analyses show that in experiments with sulphate present in solution, sulfur (S) became incorporated into all three polymorphs. This incorporation is ~ 4 times higher in calcite than in aragonite or vaterite. In addition, the sulfur content in the resulting calcites decreased by about 65% when the reaction temperature increased from 5 to 35°C. As we have shown before the incorporation of S into aragonite and vaterite is independent of temperature (Chapter 4). However, Mg is incorporated only into calcite and the amount of Mg incorporated was positively correlated to the rise of temperature; on average, ≈ 4 times more Mg became incorporated into calcite

at 35°C compared with calcite formed at 5°C, which supports previous findings (Davis et al., 2000b; Lopez et al., 2009). Although a particle size reduction with temperature in the $CaCO_3$ system has so far not been reported prior to his study, previous studies have reported that $CaCO_3$ particles decrease in size with increasing relative sulfate concentration ($[SO_4^{-2}]$:$[CO_3^{2-}]$) in solution (Fernández-Díaz et al., 2010). This event was also correlated with the amount of S detected in the solids, which is linearly dependent with solution $[SO_4^{-2}]$:$[CO_3^{2-}]$ ratio. As mentioned above, our EPMA data showed that S is incorporated into all three studied polymorphs, but it is only in calcite that a linear correlation between the amount of S in the solids and temperature exists. Since the change in morphology is seen in all three polymorphs, but the change in S content is seen only in calcite, this cannot be the overriding control on morphological variation.

The fact that calcium carbonate crystal size increased as temperature decreased could be due to a combination of both a kinetic effect and a variation in the $[CO_3^{2-}]$:$[Ca^{2+}]$ ratio with changing temperature. The kinetic effect is related to the number of nucleation events taking place at the initial stage and also depending on the number of available ions per unit area arriving onto a newly forming crystal. This is naturally also linked to the change in the degree of supersaturation in experimental system with changing temperature, because injection is continual and constant but temperature changed, and it is well-know that supersaturation is inversely proportional to temperature (Babou-Kammoe et al., 2012; Yu et al., 2005). Thus, at low temperature (5°C), there will be fewer nucleation events than at high temperature (21°C and 35°C). The number of available ions in solution to allow the growth of these nuclei will be larger, leading to a lower number of crystals. In addition, due to the lower supersaturation these will grow to bigger sizes. On the other hand, at high temperature, there will be a higher number of nucleation events but these nuclei will once formed will most likely only grow by Ostwald ripening since the number of available ions in solution will be almost negligible.

An increase in temperature also reduces the conversion of CO_2 into CO_3^{2-}, leading to a low concentration of CO_3^{2-} that is surrounded by Ca^{2+}. Hence, an increase in solution temperature results in an increase of Ca^{2+} concentration, which involves an increase in the supersaturation of the reaction medium. Under such conditions, the nucleation phase, which corresponds to the faster generation of a myriad of small

crystal nuclei, prevails, leading to the observed decrease in average $CaCO_3$ particle size (Babou-Kammoe et al., 2012; Sha et al., 2016; Yu et al., 2004).

Our results show that in the presence of Mg and SO_4 in solution, in addition to the above described changes in particle size, significant differences in calcite morphology were also observed with changing temperature. For example, at low Mg concentrations and with no sulfate in solution, calcite crystals formed with elongated, rounded edges and very faceted rhombohedra (Figure 6.2. A). At 21ºC, the most characteristic calcite morphology was elongated along the c-axis rhombohedra with roughened {0 1 1} faces and capped by well-defined {1 0 4} faces. Low magnesian calcite was also quite often observed as trigonal prisms at 21ºC (Figure 6.2. B). At the highest temperature (35ºC), calcite rhombohedra that had smoother edges and surfaces formed. These significant variations in calcite morphology with temperature changing might be related to the positive correlation between temperature and the amount of Mg incorporated into calcite. Thus, an increase in temperature favours the isomorphic substitution of magnesium to calcite in the calcite structure which influences on crystal growth (Falini et al., 1998).

Although aragonite precipitated as rod-like crystals at all three tested temperatures (5, 21 and 35 ºC), needle-like crystal aggregates that formed spherulitic structures were observed primarily in samples precipitated at 35ºC (Figure 6.2. D, E & F).

Vaterite formed as pancake-like plates at all three studied temperatures. However, while at 5ºC vaterite plates were characterized by wider and smoother surfaces; at 21 and 35ºC vaterite precipitated as more faceted and aggregated plates (Figure 6.2. G, H & I).

Because Mg is not incorporated into aragonite and vaterite, and the S content in both polymorphs does not change with temperature, these slight variations in crystal morphology with temperature might be due to a kinetic effect related to variations in growth rate with temperature.

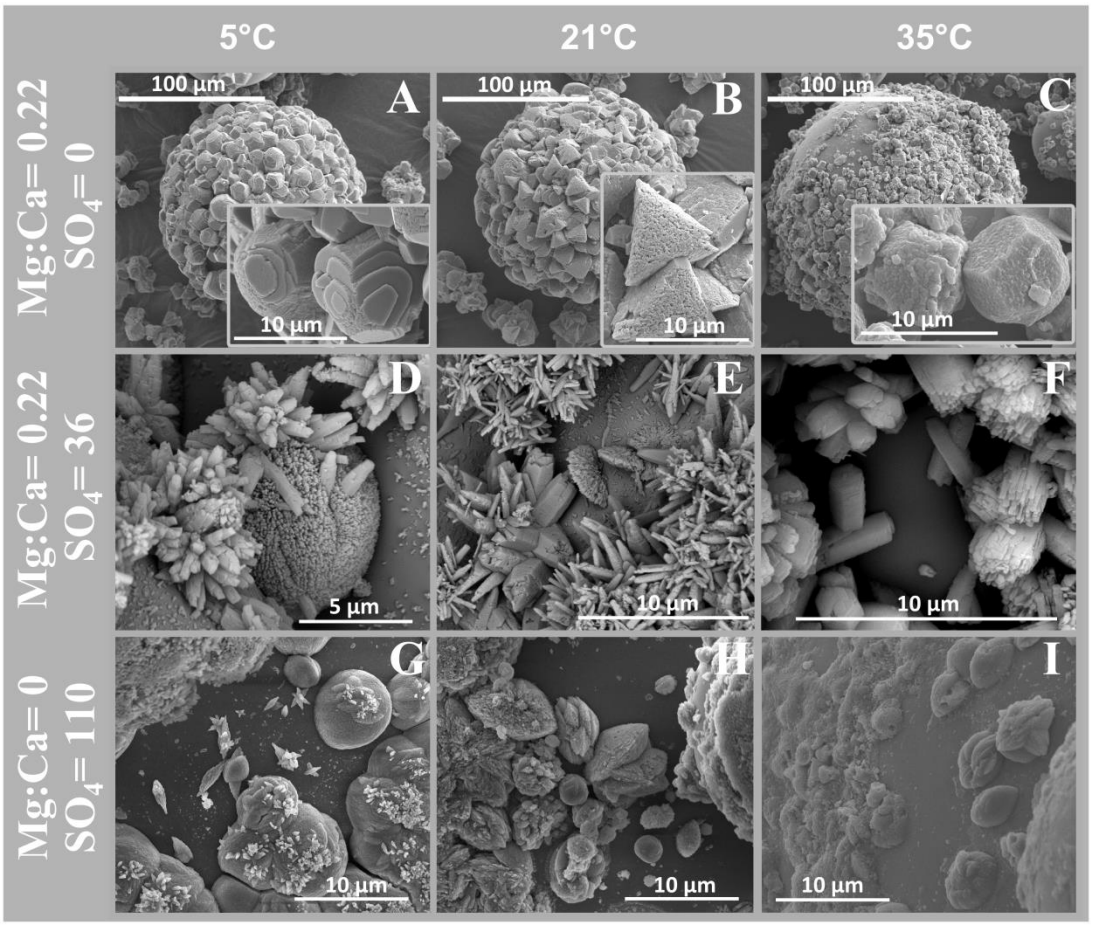

Figure 6. 2: *Influence of temperature on calcite crystal shape.*

We showed above that temperature greatly affected the morphology and shape of the formed calcium carbonate polymorphs. Interestingly, the morphology and shape of the precipitates were also greatly modified by variations in seawater ion contents (Mg and SO_4). While calcite crystals formed aggregated particles of regular plate-like shapes in the Mg and SO_4 free control experiment (Figure 6.3 A), a mixture of calcite particle elongated along the c-axis and capped by well-defined {1 0 4} faces rhombohedra and inter-grown triangles formed when Mg was present in solution (Figure 6.3 B & 3C). Experimental observations have suggested that Mg interacts specifically with the {0 1 1} faces of calcite producing crystals elongated along the c axis (Albeck et al., 1993; Falini et al., 1998). Mg incorporation into calcite also produced modified {1 0 4} rhombohedral morphology in which rugged, faceted and poorly-defined {0 1 1} faces were often observed (inset in Figure 6.3 C) as has been suggested before by (Falini et al., 2009). When both Mg and SO_4 ions were present, calcite particles similar to those observed in the presence of only Mg ions formed, but they had smoother edges (Figure 6.3 D & E).

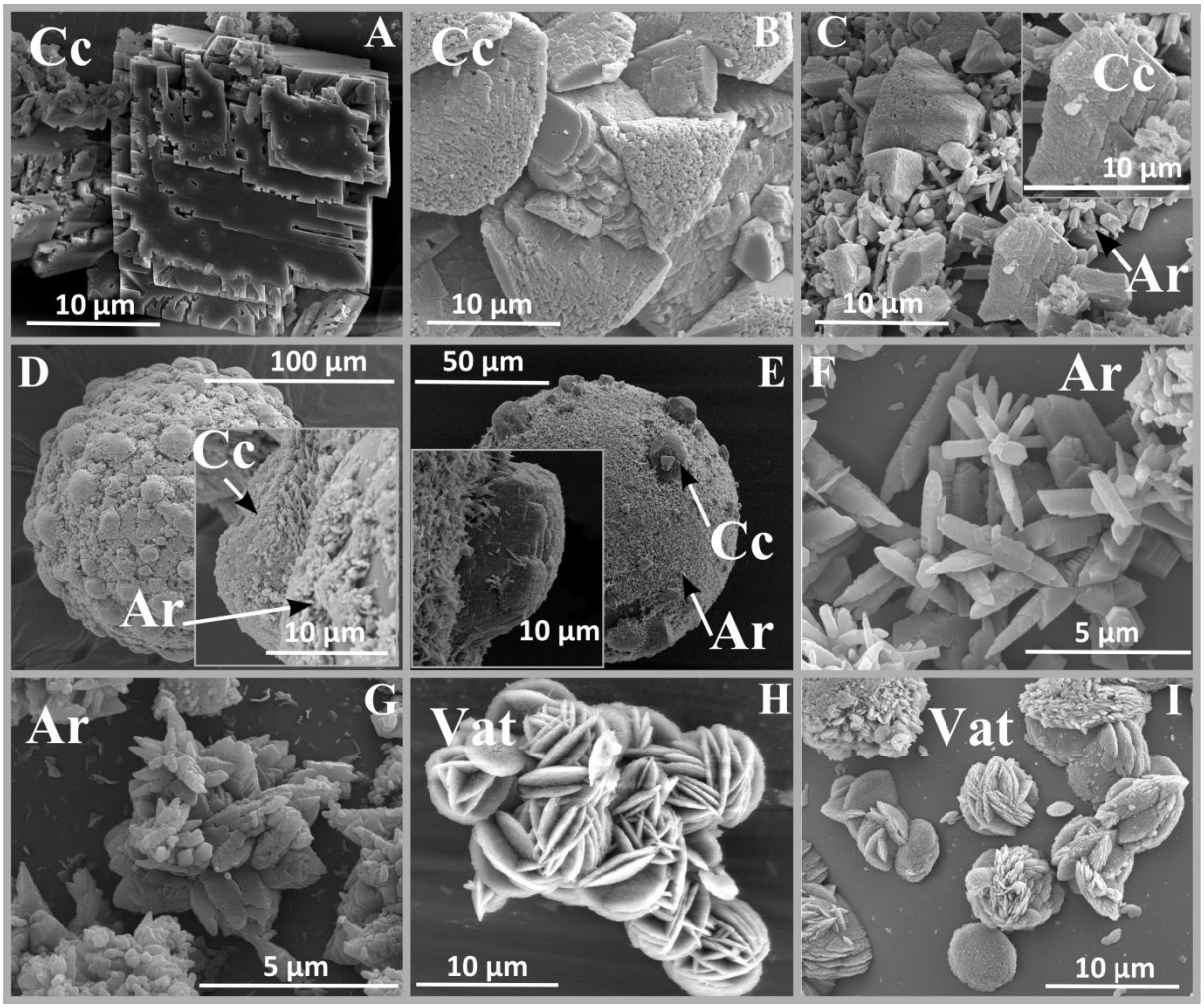

Figure 6. 3: *Influence of Mg and SO_4 on calcium carbonate shape at 21°C: A) Mg:Ca= 0, SO_4= 0 mM; B) Mg:Ca= 0.22, SO_4= 0 mM, C) Mg:Ca= 0.55, SO_4= 0 mM; D) Mg:Ca= 0.22; SO_4= 5 mM; E) Mg:Ca=0.22, SO_4= 10 mM; F) Mg:Ca= 5.2, SO_4= 0 mM; G) Mg:Ca= 5.2, SO_4=110 mM; H) Mg:Ca= 0; SO_4= 10 mM; I) Mg:Ca= 0; SO_4= 15 mM. Cc= calcite; Ar= aragonite; Vat= vaterite.*

Aragonite appeared as single crystals and aggregates of rod- and needle-like crystals of different length and width in all experimental conditions. However in the presence of SO_4 ions, crystal aggregation was more favoured and a decrease in the size of the subunits was observed (Figure 6.3 F & G).

No vaterite formed when Mg was added but even in the presence of variable amounts of SO_4 ions the formed vaterite exhibited the same morphology (pan-cake shaped plates, aggregated to form flaky-floret structures; Figure 6.3 H & I).

6.4. Conclusions

This study shows that Mg, SO_4 and temperature significantly influence calcium carbonate morphology and size. Various crystal morphologies of calcite, such as aggregated particles of regular plate-like, elongated along the c-axis rhombohedras, inter-grown triangles, trigonal prisms, etc. can be obtained by changing the experimental conditions. Magnesium and sulfate in solution favour particle aggregation and specially affect calcite morphology. Slight changes in crystal morphology of aragonite and vaterite were observed in the presence of Mg and SO_4 in solution and at different temperatures. Mg is incorporated only into calcite and it is known that in the presence of this ion there is a isomorphic substitution of magnesium to calcium in calcite structure which is favoured by the presence of sulfate ions, (Falini et al., 1998). Sulfate mainly influences on aragonite and vaterite particles aggregation but not in their morphology. Thus, this would highlight magnesium as the main driver controlling calcite morphology. The fact that calcite precipitated as many random morphologies, tell us that generalized rules and morphology diagrams as a function of Mg, SO_4 and temperature is virtually impossible to construct.

Temperature turned out to be an important parameter for the control of particle size. The observed decrease of crystal size with temperature increasing could be due to a combination of both, a kinetic effect and a variation in the $[CO_3^{2-}]$:$[Ca^{2+}]$ ratio with changing temperature. Moreover, temperature influenced substantially on calcite morphology but slightly on aragonite and vaterite morphology. These changes in calcite morphology with temperature might be related to the correlation between the Mg content in calcite and temperature. Magnesium is only incorporated into calcite and the sulfate content in aragonite and vaterite does not vary with temperature.

Overall, our results address Mg to be the overriding control on calcite morphological variation. However, calcium carbonate crystals showed a wide range of morphologies with different widths and lengths at each temperature that did not allow any clear correlation with particle shape and reaction temperature.

Thus, our results show that $CaCO_3$ particle size can be controlled by working at specific temperature conditions, which is fundamental for certain technical applications (Ajikumar et al., 2004; Küther et al., 1998; Qi et al., 2002).

Nevertheless, specific working conditions of temperature and Mg and SO_4 contents do not allow us to control $CaCO_3$ crystal shape.

References

Ajikumar, P. K., Lakshminarayanan, R., and Valiyaveettil, S., 2004, Controlled deposition of thin films of calcium carbonate on natural and synthetic templates: Crystal Growth & Design, v. 4, no. 2, p. 331-335.

Albeck, S., Aizenberg, J., Addadi, L., and Weiner, S., 1993, Interactions of various skeletal intracrystalline components with calcite crystals: Journal of the American Chemical Society, v. 115, no. 25, p. 11691-11697.

Babou-Kammoe, R., Hamoudi, S., Larachi, F., and Belkacemi, K., 2012, Synthesis of CaCO3 nanoparticles by controlled precipitation of saturated carbonate and calcium nitrate aqueous solutions: The Canadian journal of chemical engineering, v. 90, no. 1, p. 26-33.

Bots, P., Benning, L., Rickaby, R., and Shaw, S., 2011, The role of SO4 in the switch from calcite to aragonite seas: Geology, v. 39, no. 4, p. 331-334.

Chen, L.-S., Mai, Y.-W., and Cotterell, B., 1989, Impact fracture energy of mineral-filled polypropylene: Polymer Engineering & Science, v. 29, no. 8, p. 505-512.

Davis, K. J., Dove, P. M., and De Yoreo, J. J., 2000, The Role of Mg²⁺ as an Impurity in Calcite Growth: Science, v. 290, no. 5494, p. 1134-1137.

Falini, G., Fermani, S., Gazzano, M., and Ripamonti, A., 1998, Structure and morphology of synthetic magnesium calcite: Journal of Materials Chemistry, v. 8, no. 4, p. 1061-1065.

Falini, G., Fermani, S., Tosi, G., and Dinelli, E., 2009, Calcium carbonate morphology and structure in the presence of seawater ions and humic acids: Crystal Growth and Design, v. 9, no. 5, p. 2065-2072.

Fernández-Díaz, L., Fernández-González, Á., and Prieto, M., 2010, The role of sulfate groups in controlling CaCO3 polymorphism: Geochimica et Cosmochimica Acta, v. 74, no. 21, p. 6064-6076.

García Carmona, J., Gómez Morales, J., and Rodríguez Clemente, R., 2003, Rhombohedral-scalenohedral calcite transition produced by adjusting the solution electrical conductivity in the system Ca (OH) 2-CO2-H2O: Journal of colloid and interface science, v. 261, p. 434-440.

Küther, J., Seshadri, R., Knoll, W., and Tremel, W., 1998, Templated growth of calcite, vaterite and aragonite crystals onself-assembled monolayers of substituted alkylthiols on gold: Journal of Materials Chemistry, v. 8, no. 3, p. 641-650.

Lacroix, O., and Larachi, F., 2008, Scrubber Designs for Enzyme-Mediated Capture of CO2: Recent Patents on Chemical Engineering, v. 1, no. 2, p. 93-105.

Lee, I., Han, S. W., Choi, H. J., and Kim, K., 2001, Nanoparticle-Directed Crystallization of Calcium Carbonate: Advanced Materials, v. 13, no. 21, p. 1617-1620.

Lopez, O., Zuddas, P., and Faivre, D., 2009, The influence of temperature and seawater composition on calcite crystal growth mechanisms and kinetics: Implications for Mg incorporation in calcite lattice: Geochimica et Cosmochimica Acta, v. 73, no. 2, p. 337-347.

Loste, E., Wilson, R. M., Seshadri, R., and Meldrum, F. C., 2003, The role of magnesium in stabilising amorphous calcium carbonate and controlling calcite morphologies: Journal of Crystal Growth, v. 254, no. 1-2, p. 206-218.

Manoli, F., and Dalas, E., 2000, Spontaneous precipitation of calcium carbonate in the presence of ethanol, isopropanol and diethylene glycol: Journal of Crystal Growth, v. 218, no. 2-4, p. 359-364.

Ota, Y., Inui, S., Iwashita, T., Kasuga, T., and Abe, Y., 1995, Preparation of aragonite whiskers: Journal of the American Ceramic Society, v. 78, no. 7, p. 1983-1984.

Qi, L., Li, J., and Ma, J., 2002, Biomimetic morphogenesis of calcium carbonate in mixed solutions of surfactants and double-hydrophilic block copolymers: Advanced Materials, v. 14, no. 4, p. 300-303.

Sha, F., Zhu, N., Bai, Y., Li, Q., Guo, B., Zhao, T., Zhang, F., and Zhang, J., 2016, Controllable synthesis of various CaCO3 morphologies based on a CCUS idea: ACS Sustainable Chemistry & Engineering, v. 4, no. 6, p. 3032-3044.

Tai, C. Y., and Chen, F. B., 1998, Polymorphism of CaCO3, precipitated in a constant-composition environment: AIChE Journal, v. 44, no. 8, p. 1790-1798.

Wada, N., Yamashita, K., and Umegaki, T., 1995, Effects of divalent cations upon nucleation, growth and transformation of calcium carbonate polymorphs under conditions of double diffusion: Journal of Crystal Growth, v. 148, no. 3, p. 297-304.

Walsh, D., Lebeau, B., and Mann, S., 1999, Morphosynthesis of calcium carbonate (vaterite) microsponges: Advanced Materials, v. 11, no. 4, p. 324-328.

Yu, J., Lei, M., Cheng, B., and Zhao, X., 2004, Effects of PAA additive and temperature on morphology of calcium carbonate particles: Journal of Solid State Chemistry, v. 177, no. 3, p. 681-689.

Yu, K.-F., Zhao, J.-X., Wei, G.-J., Cheng, X.-R., Chen, T.-G., Felis, T., Wang, P.-X., and Liu, T.-S., 2005, δ18O, Sr/Ca and Mg/Ca records of Porites lutea corals from Leizhou Peninsula, northern South China Sea, and their applicability as paleoclimatic indicators: Palaeogeography, Palaeoclimatology, Palaeoecology, v. 218, no. 1–2, p. 57-73.

Chapter 7

Work in progress: The incorporation of Mg and SO_4 into calcium carbonate and their possible role in regulating past ocean composition.

Besides the results presented above as thesis chapters 4, 5 and 6, I have conducted a further study for which I briefly outline below the current status and preliminary data evaluation. This work is still ongoing.

7.1. Aims and objectives

Over the last 541 million years (the Phanerozoic Eon), oscillations in seawater composition are believed to have controlled the dominant inorganic carbonate mineral polymorph, leading to the concept of "aragonite" and "calcite" seas (Holt et al., 2014; Horita et al., 2002). These variations are important for understanding the evolution of marine calcifiers, the controls on the marine Ca isotope system and the vulnerability of the marine biodiversity to ocean acidification. From analysing marine carbonate containing microorganisms it is well established that the Mg:Ca ratio in $CaCO_3$ minerals is a primary control on polymorph selection (Burton and Walter, 1987). Recently, we have experimentally shown that SO_4 also has a massive effect on polymorph distribution and that an increase in seawater SO_4 dramatically changes the threshold at which calcite switches to aragonite (Bots et al., 2011) (Chapter 4). However, a molecular level understanding of the role and/or effects that SO_4 or Mg incorporation into $CaCO_3$ phases have on polymorphs selection is still lacking. This is despite the fact that this knowledge is fundamental for our ability to monitor/mitigate the vulnerability of today's marine biodiversity to ocean acidification.

A study of natural foraminiferal calcite has shown that Mg is heterogeneously distributed in concentration but homogeneous in terms of the calcite structure where it substitutes for Ca (Branson et al., 2013a). These findings provided a first fundamental step towards a mechanistic understanding of Mg incorporation into one important $CaCO_3$ polymorph, calcite, yet so far these findings have not been explored experimentally. It is important to note that both Mg:Ca ratio in carbonates

and the isotopic composition of carbonate substituted sulfate are considered excellent palaeoenvironmental proxies (recorders of ancient environmental conditions) (Coggon et al., 2010; Cohen et al., 2002; Lear et al., 2002) and , however, the mechanism that drives and controls how the incorporations of these ions actually affects polymorphs selection and how broad changes in solution chemistry, temperature and pCO_2 affect their incorporation at the micro-scale are still unknown. This is because even minute changes in the chemical composition or temperature of the seawater in which $CaCO_3$ precipitate can dramatically change the Mg or SO_4 incorporation and polymorph selection (Bots et al., 2011; Burton, 1993; Burton, 1991) (Chapter 4 and 5).

The aim of this study is therefore to address this gap in our knowledge via spatially resolved scanning transmission X-Ray microscopy (STXM) analyses of $CaCO_3$ polymorphs synthesized at various Mg and SO_4 seawater compositions that are representative of the chemical conditions in ancient and modern oceans.

7.2. Methods

7.2.1. Sample preparation

Calcite, vaterite, aragonite or mixtures were synthesized using a constant addition approach detailed in the methods chapter and in Chapters 4 - 6 of this thesis. Mixed phases were produced at Mg:Ca ratios of 1 to 6, SO_4 concentrations between 0 and 110 mM, temperature from 5 to 35°C and at a partial pressure of CO_2 of 400, 1500 and 3000 ppm using the above described methods. Solution (ICP-MS) and solid characterization (XRD, EPMA, etc., see below) was carried out as described above, except for the additional solid characterization by scanning transmission X-Ray microscopy (STXM) analysis.

In brief, prior to STXM analyses, the bulk mineralogical composition and phase distribution was determined by X-Ray diffraction (XRD) with a silicon internal standard, using a Bruker D8 X-Ray Diffractometer (Cu $k\alpha_1$). Scans were collected from 2 to 85° (2θ) and a quantitative estimate of the relative proportion of the precipitated $CaCO_3$ polymorphs and their unit cell parameters were performed with Topas 4-2®. Samples were dissolved and analysed with inductively coupled optical

emission spectroscopy (ICP-OES) to determine bulk elemental contents, with a focus specifically on Mg and SO_4. For spatially resolved analyses, samples were embedded in epoxy resin and polished to expose the edges of the $CaCO_3$ particles. The polished surfaces were carbon coated and analysed by electron microprobe (EPMA) as described in detail in the Methods chapter and specifically with respect to element analyses in chapters 4 and 5 to determine the spatial distributions of elements. Focused ion beam (FIB) foils were cut from the samples and analysed by transmission electron microscopy (TEM) together with energy dispersive X-Ray spectroscopy (EDS). Several trials with highly-spatially resolved electron energy loss spectroscopy (EELS) analyses were attempted but this was not feasible due to beam damage issues even after short exposures.

For the subsequent STXM analyses, we selected 20 samples (Table 7.1) representing relevant seawater conditions. These samples were pre-imaged with a scanning electron microscope to cross-confirm the mineralogy of the polymorphs in each section and to find adequate STXM analyses areas. Then the selected areas were analysed by EPMA as described above. Following this pre-analyses, the FIB foils were cut from adjacent crystals. Depending on the element to be analysed the FIB foils were cut to different thicknesses. For Mg FIB foils of ≈ 2µm were cut, while for S ≈ 10µm to ≈ 25µm were cut, depending on total concentration as analysed by EMPA. The adequate thickness of the FIB foils depending on their use for either, Mg or S analysis, was determined through a Rapid Access test we did at Diamond Light Source previously to our first STXM beamtime. FIB sections were deposited on 3 mm Si_3N_4 membranes and were imaged and analysed spectrally across the Mg and S edges. In addition to the FIB foils, we also analysed powdered samples (Table 7.1). In such cases for STXM analysis, the powdered sample was mixed with isopropanol and dispersed in an ultrasonic bath. A small quantity of these samples were pipetted onto 3 mm EM Au grids, transferred to a STXM sample holder and mounted on the beamline for analyses.

Table 7. 1: *Samples prepared as thick FIB sections and powder samples for STXM analysis.*

FIB Sections								
Sample	**FIB Thickness (µm)**	**Experimental conditions**		**Solution chemistry**		**Polymorph distribution**		
		T (°C)	**pCO_2 (ppm)**	**Mg:Ca (molar)**	**SO_4 (mol)**	**Calcite (%)**	**Aragonite (%)**	**Vaterite (%)**
1	1.7	21	400	0.22	10	35	65	0
2	9.6	21	400	0.22	10	35	65	0
3	2.6	5	400	0.22	10	11	20	69
4	8.5	5	400	0.22	10	11	20	69
5	2.2	35	400	0.22	10	13	87	0
6	10.3	35	400	0.22	10	13	87	0
7	1.7	21	400	0.22	5	92	8	0
8	9.0	21	400	0.22	5	92	8	0
9	2.1	21	400	0.22	44	0	68	32
10	9.0	21	400	0.22	44	0	68	32
11	3.2	21	400	0.35	5	27	73	0
12	10.5	21	400	0.35	5	27	73	0
13	7.0	21	400	0.00	15	18	0	82
14	10.3	21	400	5.2	28	0	100	0
15	≈ 25.0	21	400	0.00	5	65	0	35
16	≈ 25.0	21	400	0.00	10	90	0	10
17	≈ 25.0	21	400	0.00	15	0	0	100

FIB Sections

Sample	FIB Thickness (µm)	Experimental conditions		Solution chemistry		Polymorph distribution		
		T (°C)	pCO_2 (ppm)	Mg:Ca (molar)	SO_4 (mol)	Calcite (%)	Aragonite (%)	Vaterite (%)
18	≈ 25.0	21	1500	0.00	5	100	0	0
19	≈ 25.0	21	1500	0.00	10	79	0	21
20	≈ 25.0	21	1500	0.00	15	23	21	56

Powder Samples

Sample	Experimental conditions		Solution chemistry		Polymorph distribution		
	T (°C)	pCO_2 (ppm)	Mg:Ca (molar)	SO_4 (mol)	Calcite (%)	Aragonite (%)	Vaterite (%)
21	21	400	0.00	15	0	0	100
22	21	400	5.20	28	0	100	0
23	21	1500	0.00	5	100	0	0
24	21	1500	0.35	15	0	100	0
25	21	3000	0.22	5	100	0	0

7.2.2. STXM data acquisition and pre-analysis

X-Ray absorption near structure spectroscopy (XANES) was used to characterize magnesium and sulphur incorporation in the series of synthetic $CaCO_3$ samples

Data were collected at Canadian Light Source (beamline 10ID-1) and Diamond Light Source (beamline I08). Mg μ-XANES energy stacks were collected over the full Mg K-edge from 1305 to 1360 eV and at a spectral resolution of 0.1 – 0.2 eV. We used a dwell time of 10 ms and a spatial resolution of 400 nm/pixel resolution. We collected S μ-XANES energy stacks over the full S K-edge from 2460 to 2520 eV, at a spatial resolution of 0.2 eV, dwell time of 10 ms and a spatial resolution of 200 – 600 nm/pixel. Data were processed using Mantis and PyMca software.

Mg μ-XANES measurements were carried out first in sample 2 to test whether it would be possible to obtain a good Mg spectrum with one of the thickest samples. However, the signal was very weak because of having very low Mg concentration in the sample and signal attenuation due to sample being very thick. Then, we performed Mg μ-XANES measurements on sample 1, which was the thinnest FIB section that we prepared. Although we obtained a better spectrum than with the thicker sample, the signal still was very weak and it was not possible to perform a quantitative analysis because the number of counts was too low. Building on the experience from these tests, we concluded that it was not the thickness of our FIB sections but the low concentration of Mg in the samples what rendered our Mg μ-XANES analyses to be of rather poor, likely not well quantifiable data. These analyses are still ongoing.

7.3. Preliminary results and interpretation

Results from XRD analyses showed that the incorporation of Mg into calcite caused the unit cell c-axis to decrease by ~0.18%, while S incorporation increases this same c-axis by ~0.23%. For aragonite and vaterite, the incorporation of S changed both their c-axis by up to ~0.11% (Chapter 4). Although, based on literature (Busenberg and Niel Plummer, 1985; Kontrec et al., 2004b) such changes in unit cell parameters are substantial, the reasons for this effect is as of yet not understood and a focus of our on-going research.

The ICP-OES analyses for Mg and S contents in the supernatants and dissolved solids (Table Table A.2 & B.2) revealed that both Mg and S became incorporated into calcite, but that only S is incorporated into aragonite and vaterite. This is a kin to the results presented in Chapter 6 and will not be further discussed here.

The important spatially resolved EPMA results revealed in some cases highly heterogeneous S and Mg distributions. For example, the calcite shown in Figure 7.1 has centres rich in S but Mg rich rims. To better determine this heterogeneous distribution of Mg and S, we aim to perform XRF analysis of these samples at the I08 STXM beamline at Diamond Light Source. Overall the EPMA analyses revealed that at the single crystal-scale, on average between 1000 and 6000 ppm Mg became incorporated into calcite and that at 5 °C ~4 times lower Mg contents were incorporated into the calcite structure than at 35 °C (Table A.2 & Figure 4.2).

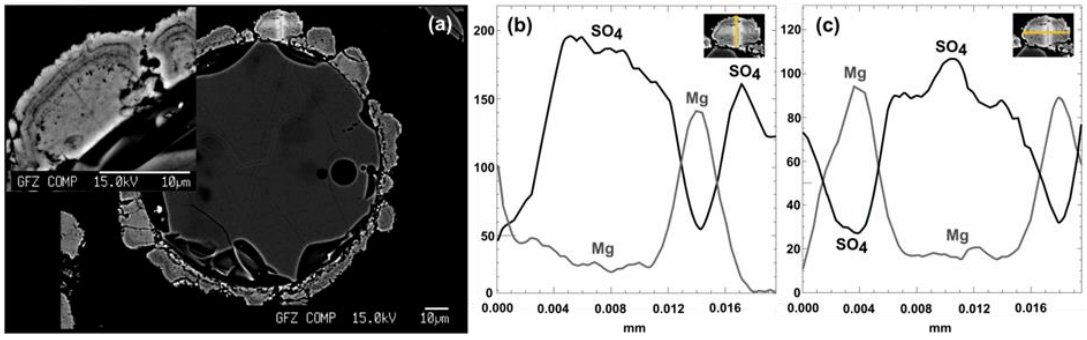

Figure 7. 1: *Calcite grown at 5 mM SO_4, Mg:Ca 0.22 and 21°C a) Photomicrograph of calcite crystals. b) EM vertical and c) horizontal line scans for Mg and S over a calcite crystal.*

As shown with the digested samples and ICP-MS analyses, the EPMA data also confirmed that no Mg was associated with aragonite or vaterite (Table A.2 & B.2). Interestingly however was the fact that aragonite produced at much higher sulfate concentrations contained only ~ 1000 ppm S, while calcite produced at lower concentrations contained locally up to 6000 ppm in its structure.

S μ-XANES analyses worked well and we collected data from 13 samples (samples number: 2, 4, 6, 8, 10, 12, 13, 14, 21 – 25). Preliminary data processing was done using Mantis software and further analysis and data interpretation are on-going. Preliminary results show that sulphur became incorporated as SO_4 into the three $CaCO_3$ polymorphs studied, calcite, aragonite and vaterite. Note however, that compare to literature data they have not been corrected for the observed spectral shifted of 16 eV to the right. Three representative spectra for S edges in calcite, aragonite and vaterite are shown in Figure 7.2. The spectra are almost identical with a white line at 2498.5 eV, a smooth post-edge shoulder at 2501.5 eV and a smooth post-edge hump between 2505 and 2525 eV. The fit of these spectra with standards of known S oxidation states (gypsum, optically clear natural magnesite and synthetic S-Mg-calcite) indicates that the main peak at 2498.5 eV corresponds to sulphate. Small differences among the spectra of the different $CaCO_3$ polymorphs, such as a more pronounced post-edge shoulder and hump in calcite spectrum than in aragonite and vaterite one, are nevertheless visible and such differences could give us information about the incorporation of S into the different polymorphs crystal structures. Furthermore, the

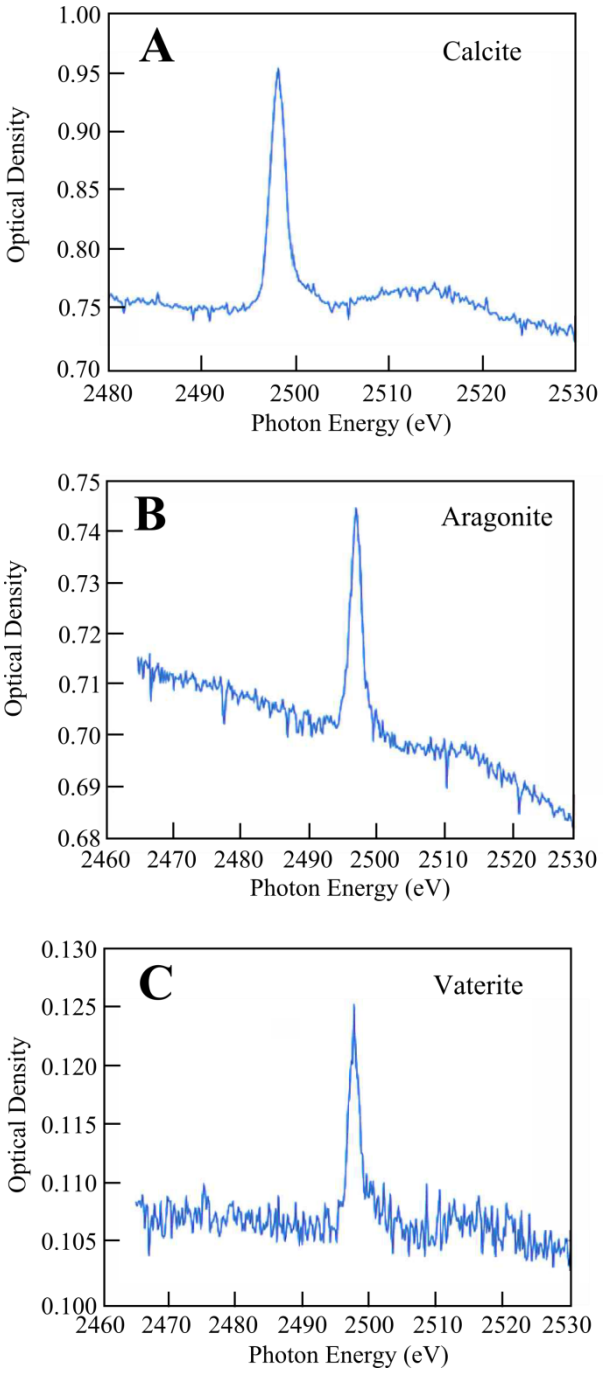

Figure 7. 2: *XANES spectra of synthetic $CaCO_3$. a) Calcite – sample 2; b) Aragonite – sample 14; c) Vaterite – sample 13.*

higher intensity of the main peak of the three polymorphs confirms that more SO_4 was incorporated into calcite than in both, aragonite and vaterite (Figure 7.2). Finally, our data also shows that the incorporation of SO_4 into calcite increased with increasing partial pressure of carbon dioxide (Figure 7.3). Nevertheless, as mentioned above, further data processing is needed to be able to interpret properly our results.

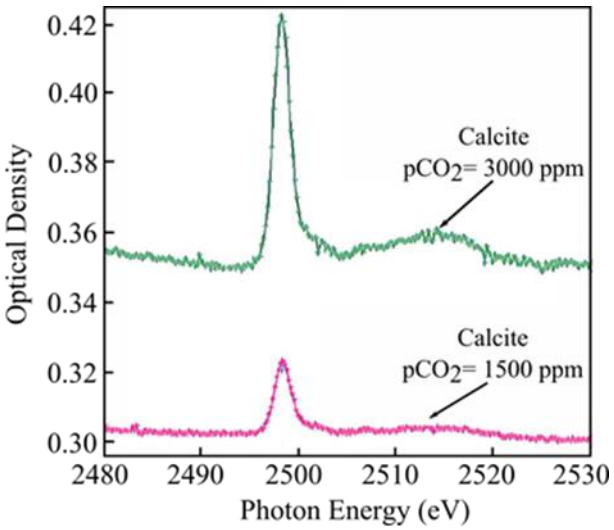

Figure 7. 3: *S XANES spectra of synthetic calcite grown at 3000 ppm of partial pressure of carbon dioxide (green spectrum) and at 1500 ppm of partial pressure of carbon dioxide (pink spectrum).*

7.4. Future work

This work will allow us to analyse and evaluate the variations in the coordination and incorporation of S in the different crystal structures of calcite, aragonite and vaterite which is still unknown. Preliminary data show that sulphur is incorporated as SO_4 into the three studied polymorphs, calcite, aragonite and vaterite and differences in their spectra could give us information about how this anion is integrated into each $CaCO_3$ polymorph. Data evaluation is still on-going and this unique data set together with our Mg-XANES data from analyses at the Canadian Light Source and other geochemical data will help us to validate for the first time the hypothesis that Mg:Ca and SO_4 contents in abiogenic precipitates can be used as a paleo-proxy for past, present and future ocean chemistry. This study will also help us understand how Mg:Ca application may vary in the past where seawater chemistry was different, although it would be needed to face the massive problem of how this is translated into biogenic rather than abiological carbonate precipitation mechanisms.

References

Adabi, M. H., 2004, A re-evaluation of aragonite versus calcite seas: Carbonates and Evaporites, v. 19, no. 2, p. 133.

Adams, D. D., Hurtgen, M. T., and Sageman, B. B., 2010, Volcanic triggering of a biogeochemical cascade during Oceanic Anoxic Event 2: Nature Geoscience, v. 3, p. 201.

Addadi, L., Raz, S., and Weiner, S., 2003, Taking Advantage of Disorder: Amorphous Calcium Carbonate and Its Roles in Biomineralization: Advanced Materials, v. 15, no. 12, p. 959-970.

Ajikumar, P. K., Lakshminarayanan, R., and Valiyaveettil, S., 2004, Controlled deposition of thin films of calcium carbonate on natural and synthetic templates: Crystal Growth & Design, v. 4, no. 2, p. 331-335.

Albeck, S., Aizenberg, J., Addadi, L., and Weiner, S., 1993, Interactions of various skeletal intracrystalline components with calcite crystals: Journal of the American Chemical Society, v. 115, no. 25, p. 11691-11697.

Albright, J. N., 1971, Mineralogical notes vaterite stability: American Mineralogist: Journal of Earth and Planetary Materials, v. 56, no. 3-4_Part_1, p. 620-624.

Alruopn, P. L., 1977, Structural refinements of dolomite and a magnesian calcite and implications for dolomite formation in the marine environment: American Mineralogist, v. 62, p. 772-783.

Andreas J. Andersson, F. T. M. a. N. R. B., 2008, Life on the margin: implications of ocean acidification on Mg-calcite, high latitude and cold-water marine calcifiers: Marine Ecology Progress Series, v. 373, p. 265-274.

Appelo, C., and Postma, D., 2005, Geochemistry, groundwater and pollution, CRC: Balkema, Roterdam.

Appelo, C., Postma, D., Appelo, C., 2005, Geochemistry, Groundwater and Pollution: London: CRC Press.

Archer, D., Kheshgi, H., and Maier-Reimer, E., 1997, Multiple timescales for neutralization of fossil fuel CO2: Geophysical Research Letters, v. 24, no. 4, p. 405-408.

Babou-Kammoe, R., Hamoudi, S., Larachi, F., and Belkacemi, K., 2012, Synthesis of CaCO3 nanoparticles by controlled precipitation of saturated carbonate and calcium nitrate aqueous solutions: The Canadian journal of chemical engineering, v. 90, no. 1, p. 26-33.

Balthasar, U., and Cusack, M., 2015, Aragonite-calcite seas—Quantifying the gray area: Geology, v. 43, no. 2, p. 99-102.

Berner, R. A., 1975, The role of magnesium in the crystal growth of calcite and aragonite from sea water: Geochimica et Cosmochimica Acta, v. 39, no. 4, p. 489-504.

Berner, R. A., 1994, GEOCARB II: A revised model of atmospheric CO[sub 2] over phanerozoic time: American Journal of Science; (United States), p. Medium: X; Size: Pages: 56-91.

Berner, R. A., 2004, A model for calcium, magnesium and sulfate in seawater over Phanerozoic time: American Journal of Science, v. 304, no. 5, p. 438-453.

Bischoff, J. L., 1968, Catalysis, inhibition, and the calcite-aragonite problem; [Part] 2, The vaterite-aragonite transformation: American Journal of Science, v. 266, no. 2, p. 80-90.

Bischoff, J. L., and Fyfe, W., 1968, Catalysis, inhibition, and the calcite-aragonite problem;[Part] 1, The aragonite-calcite transformation: American Journal of Science, v. 266, no. 2, p. 65-79.

Böhm, F., Gussone, N., Eisenhauer, A., Dullo, W.-C., Reynaud, S., and Paytan, A., 2006, Calcium isotope fractionation in modern scleractinian corals: Geochimica et Cosmochimica Acta, v. 70, no. 17, p. 4452-4462.

Bots, P., Benning, L., Rickaby, R., and Shaw, S., 2011, The role of SO4 in the switch from calcite to aragonite seas: Geology, v. 39, no. 4, p. 331-334.

Bots, P., Benning, L. G., Rodriguez-Blanco, J.-D., Roncal-Herrero, T., and Shaw, S., 2012, Mechanistic insights into the crystallization of amorphous calcium carbonate (ACC): Crystal Growth & Design, v. 12, no. 7, p. 3806-3814.

Bots P. , B. L. G., Rickaby R. E. M., and Shaw S., 2011, The role of SO4 in the switch from calcite to aragonite seas: Geology, v. 39, no. 4, p. 331-334.

Brand, U., Posenato, R., Came, R., Affek, H., Angiolini, L., Azmy, K., and Farabegoli, E., 2012, The end-Permian mass extinction: A rapid volcanic CO2 and CH4-climatic catastrophe: Chemical Geology, v. 322–323, p. 121-144.

Branson, O., Redfern, S. A., Tyliszczak, T., Sadekov, A., Langer, G., Kimoto, K., and Elderfield, H., 2013a, The coordination of Mg in foraminiferal calcite: Earth and Planetary Science Letters, v. 383, p. 134-141.

Branson, O., Redfern, S. A. T., Tyliszczak, T., Sadekov, A., Langer, G., Kimoto, K., and Elderfield, H., 2013b, The coordination of Mg in foraminiferal calcite: Earth and Planetary Science Letters, v. 383, p. 134-141.

Burton, E. A., 1993, Controls on marine carbonate cement mineralogy: review and reassessment: Chemical Geology, v. 105, no. 1, p. 163-179.

Burton, E. A., and Walter, L. M., 1987, Relative precipitation rates of aragonite and Mg calcite from seawater: Temperature or carbonate ion control?: Geology, v. 15, no. 2, p. 111-114.

Burton, E. A., and Walter, L. M., 1991, The effects of PCO2 and temperature on magnesium incorporation in calcite in seawater and MgCl2-CaCl2 solutions: Geochimica et Cosmochimica Acta, v. 55, no. 3, p. 777-785.

Busenberg, E., and Niel Plummer, L., 1985, Kinetic and thermodynamic factors controlling the distribution of SO32− and Na+ in calcites and selected aragonites: Geochimica et Cosmochimica Acta, v. 49, no. 3, p. 713-725.

-, 1989, Thermodynamics of magnesian calcite solid-solutions at 25°C and 1 atm total pressure: Geochimica et Cosmochimica Acta, v. 53, no. 6, p. 1189-1208.

Busenberg, E., and Plummer, L. N., 1989, Thermodynamics of magnesian calcite solid-solutions at 25 C and 1 atm total pressure: Geochimica et Cosmochimica Acta, v. 53, no. 6, p. 1189-1208.

Caldeira, K., and Wickett, M. E., 2003, Anthropogenic carbon and ocean pH: Nature, v. 425, p. 365.

Cantaert, B., Kim, Y. Y., Ludwig, H., Nudelman, F., Sommerdijk, N. A., and Meldrum, F. C., 2012, Think positive: phase separation enables a positively charged additive to induce dramatic changes in calcium carbonate morphology: Advanced Functional Materials, v. 22, no. 5, p. 907-915.

Chang, V. T. C., Williams, R. J. P., Makishima, A., Belshawl, N. S., and O'Nions, R. K., 2004, Mg and Ca isotope fractionation during CaCO3 biomineralisation: Biochemical and Biophysical Research Communications, v. 323, no. 1, p. 79-85.

Chen, L.-S., Mai, Y.-W., and Cotterell, B., 1989, Impact fracture energy of mineral-filled polypropylene: Polymer Engineering & Science, v. 29, no. 8, p. 505-512.

Coggon, R. M., Teagle, D. A. H., Smith-Duque, C. E., Alt, J. C., and Cooper, M. J., 2010, Reconstructing Past Seawater Mg/Ca and Sr/Ca from Mid-Ocean Ridge Flank Calcium Carbonate Veins: Science, v. 327, no. 5969, p. 1114-1117.

Cohen, A. L., Owens, K. E., Layne, G. D., and Shimizu, N., 2002, The Effect of Algal Symbionts on the Accuracy of Sr/Ca Paleotemperatures from Coral: Science, v. 296, no. 5566, p. 331-333.

Crowley, T. J., and Berner, R. A., 2001, CO₂ and Climate Change: Science, v. 292, no. 5518, p. 870-872.

Cusack, M., and Freer, A., 2008, Biomineralization: Elemental and Organic Influence in Carbonate Systems: Chemical Reviews, v. 108, no. 11, p. 4433-4454.

Davis, K. J., Dove, P. M., and De Yoreo, J. J., 2000a, The role of Mg2+ as an impurity in calcite growth: Science, v. 290, no. 5494, p. 1134-1137.

Davis, K. J., Dove, P. M., and De Yoreo, J. J., 2000b, The Role of Mg²⁺ as an Impurity in Calcite Growth: Science, v. 290, no. 5494, p. 1134-1137.

Davis, K. J., Dove, P. M., Wasylenki, L. E., and De Yoreo, J. J., 2004, Morphological consequences of differential Mg2+ incorporation at structurally distinct steps on calcite: American Mineralogist, v. 89, no. 5-6, p. 714-720.

De Choudens-Sánchez, V., and González, L. A., 2009, Calcite and Aragonite Precipitation Under Controlled Instantaneous Supersaturation: Elucidating the Role of CaCO3 Saturation State and Mg/Ca Ratio on Calcium Carbonate Polymorphism: Journal of Sedimentary Research, v. 79, no. 6, p. 363-376.

de Villiers, S., Dickson, J. A. D., and Ellam, R. M., 2005, The composition of the continental river weathering flux deduced from seawater Mg isotopes: Chemical Geology, v. 216, no. 1, p. 133-142.

Demicco, R. V., Lowenstein, T. K., Hardie, L. A., and Spencer, R. J., 2005, Model of seawater composition for the Phanerozoic: Geology, v. 33, no. 11, p. 877-880.

Dickson, J. A. D., 2002, Fossil Echinoderms As Monitor of the Mg/Ca Ratio of Phanerozoic Oceans: Science, v. 298, no. 5596, p. 1222-1224.

-, 2004, Echinoderm Skeletal Preservation: Calcite-Aragonite Seas and the Mg/Ca Ratio of Phanerozoic Oceans: Journal of Sedimentary Research, v. 74, no. 3, p. 355-365.

Doner, H. E., and Pratt, P. F., 1969, Solubility of Calcium Carbonate Precipitated in Aqueous Solutions of Magnesium and Sulfate Salts1: Soil Science Society of America Journal, v. 33, no. 5, p. 690-693.

Dwyer, G. S., Cronin, T. M., Baker, P. A., Raymo, M. E., Buzas, J. S., Corrège. T., 1995, North atlantic deepwater temperature change during late pliocene and late quaternary climatic cycles, Science, Volume 270, p. 1347 - 1351.

Elderfield, H., Bertram, C. J., and Erez, J., 1996, A biomineralization model for the incorporation of trace elements into foraminiferal calcium carbonate: Earth and Planetary Science Letters, v. 142, no. 3, p. 409-423.

Elizabeth A. Burton, a. L. M. W., 1991, The effects of PCO2 and temperature on magnesium incorporation in calcite in seawater and MgCl2-CaCl2 solutions: Geochimica et Cosmochimica Acta, v. 55, no. 3, p. 777-785.

Elizabeth A. Burton, L. M. W., 1987, Relative precipitation rates of aragonite and Mg calcite from seawater: Temperature or carbonate ion control?: Geology, v. 15, no. 2, p. 111-114.

Falini, G., Fermani, S., Gazzano, M., and Ripamonti, A., 1998, Structure and morphology of synthetic magnesium calcite: Journal of Materials Chemistry, v. 8, no. 4, p. 1061-1065.

Falini, G., Fermani, S., Tosi, G., and Dinelli, E., 2009, Calcium carbonate morphology and structure in the presence of seawater ions and humic acids: Crystal Growth and Design, v. 9, no. 5, p. 2065-2072.

Fantle, M. S., and DePaolo, D. J., 2007, Ca isotopes in carbonate sediment and pore fluid from ODP Site 807A: The Ca2+(aq)–calcite equilibrium fractionation factor and calcite recrystallization rates in Pleistocene sediments: Geochimica et Cosmochimica Acta, v. 71, no. 10, p. 2524-2546.

Feely, R. A., Sabine, C. L., Hernandez-Ayon, J. M., Ianson, D., and Hales, B., 2008, Evidence for Upwelling of Corrosive "Acidified" Water onto the Continental Shelf: Science, v. 320, no. 5882, p. 1490-1492.

Fernández-Díaz, L., Fernández-González, Á., and Prieto, M., 2010, The role of sulfate groups in controlling CaCO3 polymorphism: Geochimica et Cosmochimica Acta, v. 74, no. 21, p. 6064-6076.

Finch, A. A., and Allison, N., 2008, Mg structural state in coral aragonite and implications for the paleoenvironmental proxy: Geophysical Research Letters, v. 35, no. 8.

Folk, R. L., 1974, The natural history of crystalline calcium carbonate; effect of magnesium content and salinity: Journal of Sedimentary Research, v. 44, no. 1, p. 40-53.

Fred T. Mackenzie, W. D. B., Finley C. Bishop, Michele Loijens, Jane Schoonmaker and Roland Wollast, 1983, Magnesian calcites; low-

temperature occurrence, solubility and solid-solution behavior: Reviews in Mineralogy and Geochemistry, v. 11, no. 1, p. 97-144.

Galy, A., Bar-Matthews, M., Halicz, L., and O'Nions, R. K., 2002, Mg isotopic composition of carbonate: insight from speleothem formation: Earth and Planetary Science Letters, v. 201, no. 1, p. 105-115.

García Carmona, J., Gómez Morales, J., and Rodríguez Clemente, R., 2003, Rhombohedral-scalenohedral calcite transition produced by adjusting the solution electrical conductivity in the system Ca (OH) 2-CO2-H2O: Journal of colloid and interface science, v. 261, p. 434-440.

Gebauer, D., Gunawidjaja, P. N., Ko, J. Y. P., Bacsik, Z., Aziz, B., Liu, L., Hu, Y., Bergström, L., Tai, C.-W., Sham, T.-K., Edén, M., and Hedin, N., 2010, Proto-Calcite and Proto-Vaterite in Amorphous Calcium Carbonates: Angewandte Chemie International Edition, v. 49, no. 47, p. 8889-8891.

Gleeson, D. F., WILLIAMSON, C., GRASBY, S. E., PAPPALARDO, R. T., SPEAR, J. R., and TEMPLETON, A. S., 2011, Low temperature S0 biomineralization at a supraglacial spring system in the Canadian High Arctic: Geobiology, v. 9, no. 4, p. 360-375.

Gomes, M. L., Hurtgen, M. T., and Sageman, B. B., 2016, Biogeochemical sulfur cycling during Cretaceous oceanic anoxic events: A comparison of OAE1a and OAE2: Paleoceanography, v. 31, no. 2, p. 233-251.

Goodwin, A. L., Michel, F. M., Phillips, B. L., Keen, D. A., Dove, M. T., and Reeder, R. J., 2010, Nanoporous Structure and Medium-Range Order in Synthetic Amorphous Calcium Carbonate: Chemistry of Materials, v. 22, no. 10, p. 3197-3205.

Graf, D. L., 1961, Crystallographic tables for the rhombohedral carbonates: American Mineralogist: Journal of Earth and Planetary Materials, v. 46, no. 11-12, p. 1283-1316.

Hardie, L. A., 1990, The roles of rifting and hydrothermal CaCl 2 brines in the origin of potash evaporites; an hypothesis: American Journal of Science, v. 290, no. 1, p. 43-106.

Hardie, L. A., 1991, On the Significance of Evaporites: Annual Review of Earth and Planetary Sciences, v. 19, no. 1, p. 131-168.

Hardie, L. A., 1996, Secular variation in seawater chemistry: An explanation for the coupled secular variation in the mineralogies of marine limestones and potash evaporites over the past 600 m.y: Geology, v. 24, no. 3, p. 279-283.

Hartley, G., and Mucci, A., 1996, The influence of PCO2 on the partitioning of magnesium in calcite overgrowths precipitated from artificial seawater at 25° and 1 atm total pressure: Geochimica et Cosmochimica Acta, v. 60, no. 2, p. 315-324.

Hasiuk, F. J., and Lohmann, K. C., 2008, Mississippian Paleocean Chemistry from Biotic and Abiotic Carbonate, Muleshoe Mound, Lake Valley Formation, New Mexico, U.S.A: Journal of Sedimentary Research, v. 78, no. 2, p. 147-164.

Holland, H. D., 2005, Sea level, sediments and the composition of seawater: American Journal of Science, v. 305, no. 3, p. 220-239.

Holland, H. D., Horita, J., and Seyfried, J. W. E., 1996, On the secular variations in the composition of Phanerozoic marine potash evaporites: Geology, v. 24, no. 11, p. 993-996.

Holt, N. M., García-Veigas, J., Lowenstein, T. K., Giles, P. S., and Williams-Stroud, S., 2014, The major-ion composition of Carboniferous seawater: Geochimica et Cosmochimica Acta, v. 134, p. 317-334.

Hönisch, B., Ridgwell, A., Schmidt, D. N., Thomas, E., Gibbs, S. J., Sluijs, A., Zeebe, R., Kump, L., Martindale, R. C., Greene, S. E., Kiessling, W., Ries, J., Zachos, J. C., Royer, D. L., Barker, S., Marchitto, T. M., Moyer, R., Pelejero, C., Ziveri, P., Foster, G. L., and Williams, B., 2012, The Geological Record of Ocean Acidification: Science, v. 335, no. 6072, p. 1058-1063.

Horita, J., Zimmermann, H., and Holland, H. D., 2002, Chemical evolution of seawater during the Phanerozoic: Implications from the record of marine evaporites: Geochimica et Cosmochimica Acta, v. 66, no. 21, p. 3733-3756.

Huber, B. T., Norris, R. D., and MacLeod, K. G., 2002, Deep-sea paleotemperature record of extreme warmth during the Cretaceous: Geology, v. 30, no. 2, p. 123-126.

Immenhauser, A., Buhl, D., Richter, D., Niedermayr, A., Riechelmann, D., Dietzel, M., and Schulte, U., 2010, Magnesium-isotope fractionation during low-Mg calcite precipitation in a limestone cave–Field study and experiments: Geochimica et Cosmochimica Acta, v. 74, no. 15, p. 4346-4364.

Janie Lee, J. W. M., 2010, Influences of alkalinity and pCO2 on CaCO3 nucleation from estimated Cretaceous composition seawater representative of "calcite seas": Geology v. 38, no. 2, p. 115-118.

Kamhi, S. R., 1963, On the structure of vaterite CaCO3: Acta Crystallographica, v. 16, no. 8, p. 770-772.

Katz, A., 1973, The interaction of magnesium with calcite during crystal growth at 25–90°C and one atmosphere: Geochimica et Cosmochimica Acta, v. 37, no. 6, p. 1563-1586.

Kester, D. R., Duedall, I. W., Connors, D. N., and Pytkowicz, R. M., 1967, PREPARATION OF ARTIFICIAL SEAWATER1: Limnology and Oceanography, v. 12, no. 1, p. 176-179.

Kitano, Y., Kanamori, N., and Oomori, T., 1971, Measurements of distribution coefficients and barium between carbonate precipitate —Abnormally high values of distribution measured at early stages of carbonate of strontium and solution coefficients formation: GEOCHEMICAL JOURNAL, v. 4, no. 4, p. 183-206.

Kontrec, J., Kralj, D., Brečević, L., Falini, G., Fermani, S., Noethig-Laslo, V., and Mirosavljević, K., 2004a, Incorporation of Inorganic Anions in Calcite: European Journal of Inorganic Chemistry, v. 2004, no. 23, p. 4579-4585.

Kontrec, J., Kralj, D., Brečević, L., Falini, G., Fermani, S., Noethig-Laslo, V., and Mirosavljević, K., 2004b, Incorporation of inorganic anions in calcite: European Journal of Inorganic Chemistry, v. 2004, no. 23, p. 4579-4585.

Küther, J., Seshadri, R., Knoll, W., and Tremel, W., 1998, Templated growth of calcite, vaterite and aragonite crystals onself-assembled monolayers of

substituted alkylthiols on gold: Journal of Materials Chemistry, v. 8, no. 3, p. 641-650.

Lacroix, O., and Larachi, F., 2008, Scrubber Designs for Enzyme-Mediated Capture of CO2: Recent Patents on Chemical Engineering, v. 1, no. 2, p. 93-105.

Lam, R. S. K., Charnock, J. M., Lennie, A., and Meldrum, F. C., 2007, Synthesis-dependant structural variations in amorphous calcium carbonate: CrystEngComm, v. 9, no. 12, p. 1226-1236.

Land, L. S., and Hoops, G. K., 1973, Sodium in carbonate sediments and rocks; a possible index to the salinity of diagenetic solutions: Journal of Sedimentary Research, v. 43, no. 3, p. 614-617.

Le Bail, A., Ouhenia, S., and Chateigner, D., 2011, Microtwinning hypothesis for a more ordered vaterite model: Powder Diffraction, v. 26, no. 1, p. 16-21.

Lear, C. H., Elderfield, H., and Wilson, P. A., 2000, Cenozoic Deep-Sea Temperatures and Global Ice Volumes from Mg/Ca in Benthic Foraminiferal Calcite: Science, v. 287, no. 5451, p. 269-272.

Lear, C. H., Rosenthal, Y., and Slowey, N., 2002, Benthic foraminiferal Mg/Ca-paleothermometry: a revised core-top calibration: Geochimica et Cosmochimica Acta, v. 66, no. 19, p. 3375-3387.

Lee, I., Han, S. W., Choi, H. J., and Kim, K., 2001, Nanoparticle-Directed Crystallization of Calcium Carbonate: Advanced Materials, v. 13, no. 21, p. 1617-1620.

Lee, J., and Morse, J. W., 2010, Influences of alkalinity and pCO2 on CaCO3 nucleation from estimated Cretaceous composition seawater representative of "calcite seas": Geology, v. 38, no. 2, p. 115-118.

Li, W., Chakraborty, S., Beard, B. L., Romanek, C. S., and Johnson, C. M., 2012, Magnesium isotope fractionation during precipitation of inorganic calcite under laboratory conditions: Earth and Planetary Science Letters, v. 333-334, p. 304-316.

Lippmann, F., 1973, Sedimentary Carbonate Minerals: Springer.

-, 2012, Sedimentary Carbonate Minerals: Science & Business Media.

Lopez, O., Zuddas, P., and Faivre, D., 2009, The influence of temperature and seawater composition on calcite crystal growth mechanisms and kinetics: Implications for Mg incorporation in calcite lattice: Geochimica et Cosmochimica Acta, v. 73, no. 2, p. 337-347.

Lorens, R. B., and Bender, M. L., 1980, The impact of solution chemistry on Mytilus edulis calcite and aragonite: Geochimica et Cosmochimica Acta, v. 44, no. 9, p. 1265-1278.

Loste, E., Park, R. J., Warren, J., and Meldrum, F. C., 2004, Precipitation of calcium carbonate in confinement: Advanced Functional Materials, v. 14, no. 12, p. 1211-1220.

Loste, E., Wilson, R. M., Seshadri, R., and Meldrum, F. C., 2003a, The role of magnesium in stabilising amorphous calcium carbonate and controlling calcite morphologies: Journal of Crystal Growth, v. 254, no. 1, p. 206-218.

Loste, E., Wilson, R. M., Seshadri, R., and Meldrum, F. C., 2003b, The role of magnesium in stabilising amorphous calcium carbonate and controlling calcite morphologies: Journal of Crystal Growth, v. 254, no. 1-2, p. 206-218.

Lowenstein, T. K., Hardie, L. A., Timofeeff, M. N., and Demicco, R. V., 2003, Secular variation in seawater chemistry and the origin of calcium chloride basinal brines: Geology, v. 31, no. 10, p. 857-860.

Lowenstein, T. K., Timofeeff, M. N., Brennan, S. T., Hardie, L. A., and Demicco, R. V., 2001, Oscillations in Phanerozoic Seawater Chemistry: Evidence from Fluid Inclusions: Science, v. 294, no. 5544, p. 1086-1088.

M. C. Nash, S. U., A. P. Negri and N. E. Cantin, 2015, Ocean acidification does not affect magnesium composition or dolomite formation in living crustose coralline algae, Porolithon onkodes in an experimental system: Biogeosciences Discussions, v. 12, p. 1373-1404.

Mackenzie, F. T., and Morse, J. W., 1992, Sedimentary carbonates through Phanerozoic time: Geochimica et Cosmochimica Acta, v. 56, no. 8, p. 3281-3295.

Mackenzie, F. T., and Pigott, J. D., 1981, Tectonic controls of Phanerozoic sedimentary rock cycling: Journal of the Geological Society, v. 138, no. 2, p. 183-196.

Mahamid, J., Aichmayer, B., Shimoni, E., Ziblat, R., Li, C., Siegel, S., Paris, O., Fratzl, P., Weiner, S., and Addadi, L., 2010, Mapping amorphous calcium phosphate transformation into crystalline mineral from the cell to the bone in zebrafish fin rays: Proceedings of the National Academy of Sciences, v. 107, no. 14, p. 6316-6321.

Manoli, F., and Dalas, E., 2000, Spontaneous precipitation of calcium carbonate in the presence of ethanol, isopropanol and diethylene glycol: Journal of Crystal Growth, v. 218, no. 2-4, p. 359-364.

Martin, R. E., 1995, Cyclic and secular variation in microfossil biomineralization: clues to the biogeochemical evolution of Phanerozoic oceans: Global and Planetary Change, v. 11, no. 1, p. 1-23.

Mavromatis, V., Gautier, Q., Bosc, O., and Schott, J., 2013, Kinetics of Mg partition and Mg stable isotope fractionation during its incorporation in calcite: Geochimica et Cosmochimica Acta, v. 114, p. 188-203.

Medeiros, S., Albuquerque, E., Maia Jr, F., Caetano, E., and Freire, V., 2007, First-principles calculations of structural, electronic, and optical absorption properties of CaCO3 Vaterite: Chemical Physics Letters, v. 435, no. 1-3, p. 59-64.

Meldrum, F. C., and Cölfen, H., 2008, Controlling Mineral Morphologies and Structures in Biological and Synthetic Systems: Chemical Reviews, v. 108, no. 11, p. 4332-4432.

Meyer, H., 1969, Struktur und fehlordnung des vaterits: Zeitschrift für Kristallographie-Crystalline Materials, v. 128, no. 1-6, p. 183-212.

Michel, F. M., MacDonald, J., Feng, J., Phillips, B. L., Ehm, L., Tarabrella, C., Parise, J. B., and Reeder, R. J., 2008, Structural Characteristics of Synthetic

Amorphous Calcium Carbonate: Chemistry of Materials, v. 20, no. 14, p. 4720-4728.

MmxcRAF, S., and Rrnnrn, R., 1985, High-temperature structure refinements of calcite and magnesite: American Mineralogist, v. 70, p. 590400.

Morse, J. W., & Mackenzie, F. T., 1990, Geochemistry of sedimentary carbonates: Elsevier, v. 48.

Morse, J. W., Arvidson, R. S., and Lüttge, A., 2007, Calcium Carbonate Formation and Dissolution: Chemical Reviews, v. 107, no. 2, p. 342-381.

Morse, J. W., and Bender, M. L., 1990, Partition coefficients in calcite: Examination of factors influencing the validity of experimental results and their application to natural systems: Chemical Geology, v. 82, p. 265-277.

Morse, J. W., and Casey, W. H., 1988, Ostwald processes and mineral paragenesis in sediments: American Journal of Science, v. 288, no. 6, p. 537-560.

Morse, J. W., and Mackenzie, F. T., 1990, Geochemistry of sedimentary carbonates, Elsevier.

Morse, J. W., Wang, Q., and Tsio, M. Y., 1997a, Influences of temperature and Mg: Ca ratio on CaCO3 precipitates from seawater: Geology, v. 25, no. 1, p. 85-87.

Morse, J. W., Wang, Q., and Tsio, M. Y., 1997b, Influences of temperature and Mg:Ca ratio on CaCO3 precipitates from seawater: Geology, v. 25, no. 1, p. 85-87.

Mucci, A., 1987, Influence of temperature on the composition of magnesian calcite overgrowths precipitated from seawater: Geochimica et Cosmochimica Acta, v. 51, no. 7, p. 1977-1984.

Mucci, A., and Morse, J. W., 1983, The incorporation of Mg2+ and Sr2+ into calcite overgrowths: influences of growth rate and solution composition: Geochimica et Cosmochimica Acta, v. 47, no. 2, p. 217-233.

Mucci, A., Morse, J. W., and Kaminsky, M. S., 1985, Auger spectroscopy analysis of magnesian calcite overgrowths precipitated from seawater and solutions of similar composition: Am. J. Sci.; (United States), p. Medium: X; Size: Pages: 289-305.

Newton, R. J., Reeves, E. P., Kafousia, N., Wignall, P. B., Bottrell, S. H., and Sha, J.-G., 2011, Low marine sulfate concentrations and the isolation of the European epicontinental sea during the Early Jurassic: Geology, v. 39, no. 1, p. 7-10.

Nürnberg, D., Bijma, J., and Hemleben, C., 1996, Assessing the reliability of magnesium in foraminiferal calcite as a proxy for water mass temperatures: Geochimica et Cosmochimica Acta, v. 60, no. 5, p. 803-814.

O'Neil, J. R., Clayton, R. N., and Mayeda, T. K., 1969, Oxygen isotope fractionation in divalent metal carbonates: The Journal of Chemical Physics, v. 51, no. 12, p. 5547-5558.

Ota, Y., Inui, S., Iwashita, T., Kasuga, T., and Abe, Y., 1995, Preparation of aragonite whiskers: Journal of the American Ceramic Society, v. 78, no. 7, p. 1983-1984.

Paris, G., Fehrenbacher, J. S., Sessions, A. L., Spero, H. J., and Adkins, J. F., 2014, Experimental determination of carbonate-associated sulfate δ34S in planktonic foraminifera shells: Geochemistry, Geophysics, Geosystems, v. 15, no. 4, p. 1452-1461.

Pascual-Cebrian, E., Götz, S., Bover-Arnal, T., Skelton, P. W., Gili, E., Salas, R., and Stinnesbeck, W., 2016, Calcite/aragonite ratio fluctuations in Aptian rudist bivalves: Correlation with changing temperatures: Geology, v. 44, no. 2, p. 135-138.

Pearce, C. R., Saldi, G. D., Schott, J., and Oelkers, E. H., 2012, Isotopic fractionation during congruent dissolution, precipitation and at equilibrium: Evidence from Mg isotopes: Geochimica et Cosmochimica Acta, v. 92, p. 170-183.

Pingitore, N. E., Meitzner, G., and Love, K. M., 1995, Identification of sulfate in natural carbonates by x-ray absorption spectroscopy: Geochimica et Cosmochimica Acta, v. 59, no. 12, p. 2477-2483.

Plummer, L. N., 1979, Critical review of the kinetics of calcite dissolution and precipitation: Chemical Modeling in Aqueous Systems., p. 539-573.

Plummer, L. N., and Busenberg, E., 1982, The solubilities of calcite, aragonite and vaterite in CO2-H2O solutions between 0 and 90 C, and an evaluation of the aqueous model for the system CaCO3-CO2-H2O: Geochimica et Cosmochimica Acta, v. 46, no. 6, p. 1011-1040.

Pogge von Strandmann, P. A., Forshaw, J., and Schmidt, D., 2014, Modern and Cenozoic records of seawater magnesium from foraminiferal Mg isotopes: Biogeosciences, v. 11, no. 18, p. 5155-5168.

Poulton, S. W., Henkel, S., März, C., Urquhart, H., Flögel, S., Kasten, S., Damsté, J. S. S., and Wagner, T., 2015, A continental-weathering control on orbitally driven redox-nutrient cycling during Cretaceous Oceanic Anoxic Event 2: Geology, v. 43, no. 11, p. 963-966.

Qi, L., Li, J., and Ma, J., 2002, Biomimetic morphogenesis of calcium carbonate in mixed solutions of surfactants and double-hydrophilic block copolymers: Advanced Materials, v. 14, no. 4, p. 300-303.

Quigley, D., and Rodger, P. M., 2008, Free energy and structure of calcium carbonate nanoparticles during early stages of crystallization: The Journal of Chemical Physics, v. 128, no. 22, p. 221101.

Railsback, L. B., and Anderson, T. F., 1987, Control of Triassic seawater chemistry and temperature on the evolution of post-Paleozoic aragonite-secreting faunas: Geology, v. 15, no. 11, p. 1002-1005.

Raiteri, P., and Gale, J. D., 2010, Water is the key to nonclassical nucleation of amorphous calcium carbonate: Journal of the American Chemical Society, v. 132, no. 49, p. 17623-17634.

Reynaud, S., Ferrier-Pagès, C., Meibom, A., Mostefaoui, S., Mortlock, R., Fairbanks, R., and Allemand, D., 2007, Light and temperature effects on Sr/Ca and Mg/Ca ratios in the scleractinian coral Acropora sp: Geochimica et Cosmochimica Acta, v. 71, no. 2, p. 354-362.

Ridgwell, A., and Zeebe, R. E., 2005, The role of the global carbonate cycle in the regulation and evolution of the Earth system: Earth and Planetary Science Letters, v. 234, no. 3, p. 299-315.

Ries, J. B., Cohen, A. L., and McCorkle, D. C., 2009, Marine calcifiers exhibit mixed responses to CO2-induced ocean acidification: Geology, v. 37, no. 12, p. 1131-1134.

Robert V. Demicco, T. K. L., Lawrence A. Hardie, and Ronald J. Spencer, 2005, Model of seawater composition for the Phanerozoic: Geology, v. 33, no. 11, p. 877-880.

Rodriguez-Blanco, J., Shaw, S., and Benning, L., 2008, How to make 'stable'ACC: protocol and preliminary structural characterization: Mineralogical Magazine, v. 72, no. 1, p. 283-286.

Rodriguez-Blanco, J. D., Shaw, S., and Benning, L. G., 2011, The kinetics and mechanisms of amorphous calcium carbonate (ACC) crystallization to calcite, via vaterite: Nanoscale, v. 3, no. 1, p. 265-271.

Rodriguez-Blanco, J. D., Shaw, S., Bots, P., Roncal-Herrero, T., and Benning, L. G., 2012, The role of pH and Mg on the stability and crystallization of amorphous calcium carbonate: Journal of Alloys and Compounds, v. 536, p. S477-S479.

Rosenthal, Y., Boyle, E. A., and Slowey, N., 1997, Temperature control on the incorporation of magnesium, strontium, fluorine, and cadmium into benthic foraminiferal shells from Little Bahama Bank: Prospects for thermocline paleoceanography: Geochimica et Cosmochimica Acta, v. 61, no. 17, p. 3633-3643.

Saenger, C., and Wang, Z., 2014, Magnesium isotope fractionation in biogenic and abiogenic carbonates: implications for paleoenvironmental proxies: Quaternary Science Reviews, v. 90, p. 1-21.

Sandberg, P. A., 1983a, An oscillating trend in Phanerozoic non-skeletal carbonate mineralogy: Nature, v. 305, p. 19.

-, 1983b, An oscillating trend in Phanerozoic non-skeletal carbonate mineralogy: Nature, v. 305, no. 5929, p. 19-22.

Sandberg, P. A., 1985, Nonskeletal Aragonite and pCO2 in the Phanerozoic and Proterozoic, The Carbon Cycle and Atmospheric CO2: Natural Variations Archean to Present, p. 585-594.

Sha, F., Zhu, N., Bai, Y., Li, Q., Guo, B., Zhao, T., Zhang, F., and Zhang, J., 2016, Controllable synthesis of various CaCO3 morphologies based on a CCUS idea: ACS Sustainable Chemistry & Engineering, v. 4, no. 6, p. 3032-3044.

Simon W. Poulton, S. H., Christian März, Hannah Urquhart, Sascha Flögle, Sabine Kasten, Jaap S. Sinninghe, Damsté, Thomas Wagner, 2015, A continental-weathering control on orbitally driven redox-nutrient cycling during Cretaceous Oceanic Anoxic Event 2: Geology, v. 43, no. 11, p. 963-966.

Smeets, P. J., Cho, K. R., Kempen, R. G., Sommerdijk, N. A., and De Yoreo, J. J., 2015, Calcium carbonate nucleation driven by ion binding in a biomimetic matrix revealed by in situ electron microscopy: Nature materials, v. 14, no. 4, p. 394.

Spencer, R., and Hardie, L., 1990, Control of seawater composition by mixing of river waters and mid-ocean ridge hydrothermal brines: Fluid-mineral interactions: A tribute to HP Eugster: Geochemical Society Special Publication, v. 19, p. 409-419.

Stack, A. G., and Grantham, M. C., 2010, Growth Rate of Calcite Steps As a Function of Aqueous Calcium-to-Carbonate Ratio: Independent Attachment and Detachment of Calcium and Carbonate Ions: Crystal Growth & Design, v. 10, no. 3, p. 1409-1413.

Stanley, S. M., 2006, Influence of seawater chemistry on biomineralization throughout phanerozoic time: Paleontological and experimental evidence: Palaeogeography, Palaeoclimatology, Palaeoecology, v. 232, no. 2, p. 214-236.

Stanley, S. M., and Hardie, L. A., 1998, Secular oscillations in the carbonate mineralogy of reef-building and sediment-producing organisms driven by tectonically forced shifts in seawater chemistry: Palaeogeography, Palaeoclimatology, Palaeoecology, v. 144, no. 1, p. 3-19.

Stephens, C. J., Ladden, S. F., Meldrum, F. C., and Christenson, H. K., 2010, Amorphous calcium carbonate is stabilized in confinement: Advanced Functional Materials, v. 20, no. 13, p. 2108-2115.

Tai, C. Y., and Chen, F. B., 1998, Polymorphism of CaCO3, precipitated in a constant-composition environment: AIChE Journal, v. 44, no. 8, p. 1790-1798.

Takano, B., 1985, Geochemical implications of sulfate in sedimentary carbonates: Chemical Geology, v. 49, no. 4, p. 393-403.

Tester, C. C., Brock, R. E., Wu, C.-H., Krejci, M. R., Weigand, S., and Joester, D., 2011, In vitro synthesis and stabilization of amorphous calcium carbonate (ACC) nanoparticles within liposomes: CrystEngComm, v. 13, no. 12, p. 3975-3978.

Tester, C. C., and Joester, D., 2013, Precipitation in liposomes as a model for intracellular biomineralization, Methods in enzymology, Volume 532, Elsevier, p. 257-276.

Tester, C. C., Whittaker, M. L., and Joester, D., 2014, Controlling nucleation in giant liposomes: Chemical Communications, v. 50, no. 42, p. 5619-5622.

Tester, C. C., Wu, C.-H., Weigand, S., and Joester, D., 2012, Precipitation of ACC in liposomes—a model for biomineralization in confined volumes: Faraday Discussions, v. 159, p. 345-356.

Tribello, G. A., Bruneval, F., Liew, C., and Parrinello, M., 2009, A Molecular Dynamics Study of the Early Stages of Calcium Carbonate Growth: The Journal of Physical Chemistry B, v. 113, no. 34, p. 11680-11687.

Videtich, P. E., 1985, Electron Microprobe Study of Mg Distribution in Recent Mg Calcites and Recrystallized Equivalents from the Pleistocene and Tertiary: Journal of Sedimentary Research, v. 55, no. 3, p. 421-429.

Volodymyr M. Kovalevich, Tadeusz Marek Peryt, and Oleg I. Petrichenko, 1998, Secular Variation in Seawater Chemistry during the Phanerozoic as Indicated

by Brine Inclusions in Halite: The Journal of Geology, v. 106, no. 6, p. 695-712.

Wada, N., Yamashita, K., and Umegaki, T., 1995, Effects of divalent cations upon nucleation, growth and transformation of calcium carbonate polymorphs under conditions of double diffusion: Journal of Crystal Growth, v. 148, no. 3, p. 297-304.

Wallmann, K., 2001, Controls on the cretaceous and cenozoic evolution of seawater composition, atmospheric CO2 and climate: Geochimica et Cosmochimica Acta, v. 65, no. 18, p. 3005-3025.

Walsh, D., Lebeau, B., and Mann, S., 1999, Morphosynthesis of calcium carbonate (vaterite) microsponges: Advanced Materials, v. 11, no. 4, p. 324-328.

Walter, L. M., 1983, An oscillating trend in Phanerozoic non-skeletal carbonate mineralogy: Nature, v. 305, p. 19.

-, 1986, Relative efficiency of carbonate dissolution and precipitation during diagenesis: a progress report on the role of solution chemistry.

Wang, J., and Becker, U., 2009, Structure and carbonate orientation of vaterite (CaCO3): American Mineralogist, v. 94, no. 2-3, p. 380-386.

Wang, Z., Hu, P., Gaetani, G., Liu, C., Saenger, C., Cohen, A., and Hart, S., 2013, Experimental calibration of Mg isotope fractionation between aragonite and seawater: Geochimica et Cosmochimica Acta, v. 102, p. 113-123.

Wei, G., Sun, M., Li, X., and Nie, B., 2000, Mg/Ca, Sr/Ca and U/Ca ratios of a porites coral from Sanya Bay, Hainan Island, South China Sea and their relationships to sea surface temperature: Palaeogeography, Palaeoclimatology, Palaeoecology, v. 162, no. 1–2, p. 59-74.

Weiner, S., and Dove, P. M., 2003, An Overview of Biomineralization Processes and the Problem of the Vital Effect: Reviews in Mineralogy and Geochemistry, v. 54, no. 1, p. 1-29.

Wilkinson, B. H., and Algeo, T. J., 1989, Sedimentary carbonate record of calcium-magnesium cycling: American Journal of Science, v. 289, no. 10, p. 1158-1194.

Wilkinson, B. H., Buczynski, C., and Owen, R. M., 1984, Chemical control of carbonate phases; implications from Upper Pennsylvanian calcite-aragonite ooids of southeastern Kansas: Journal of Sedimentary Research, v. 54, no. 3, p. 932-947.

Wilkinson, B. H., and Given, R. K., 1986, Secular Variation in Abiotic Marine Carbonates: Constraints on Phanerozoic Atmospheric Carbon Dioxide Contents and Oceanic Mg/Ca Ratios: The Journal of Geology, v. 94, no. 3, p. 321-333.

Wilkinson, B. H., Owen, R. M., and Carroll, A. R., 1985, Submarine hydrothermal weathering, global eustasy, and carbonate polymorphism in Phanerozoic marine oolites: Journal of Sedimentary Research, v. 55, no. 2, p. 171-183.

Wortmann, U. G., and Chernyavsky, B. M., 2007, Effect of evaporite deposition on Early Cretaceous carbon and sulphur cycling: Nature, v. 446, no. 7136, p. 654-656.

Yasushi, K., 1962, The Behavior of Various Inorganic Ions in the Separation of Calcium Carbonate from a Bicarbonate Solution: Bulletin of the Chemical Society of Japan, v. 35, no. 12, p. 1973-1980.

Young, E. D., and Galy, A., 2004, The Isotope Geochemistry and Cosmochemistry of Magnesium: Reviews in Mineralogy and Geochemistry, v. 55, no. 1, p. 197-230.

Yu, J., Lei, M., Cheng, B., and Zhao, X., 2004, Effects of PAA additive and temperature on morphology of calcium carbonate particles: Journal of Solid State Chemistry, v. 177, no. 3, p. 681-689.

Yu, K.-F., Zhao, J.-X., Wei, G.-J., Cheng, X.-R., Chen, T.-G., Felis, T., Wang, P.-X., and Liu, T.-S., 2005, δ18O, Sr/Ca and Mg/Ca records of Porites lutea corals from Leizhou Peninsula, northern South China Sea, and their applicability as paleoclimatic indicators: Palaeogeography, Palaeoclimatology, Palaeoecology, v. 218, no. 1–2, p. 57-73.

Zhuravlev, A. Y., and Wood, R. A., 2009, Controls on carbonate skeletal mineralogy: Global CO2 evolution and mass extinctions: Geology, v. 37, no. 12, p. 1123-1126.

Zimmermann, H., 2000, Tertiary seawater chemistry; implications from primary fluid inclusions in marine halite: American Journal of Science, v. 300, no. 10, p. 723-767.

Chapter 8
Conclusions and Future Work

8.1. Conclusions

The overall aim of this PhD was to evaluate the key effects as well as the relative effects of changes in solution chemistry (Mg:Ca ratio and SO_4 concentration) and changes in physical parameters such as temperature and pCO_2 have on the formation, transformation and structure of calcium carbonate phases.

8.1.1. Influence of solution chemistry and temperature on $CaCO_3$ mineralogy

In Chapter 4, an evaluation and quantification of the influence of seawater Mg:Ca ratio, SO_4 concentration and temperature in abiotic seawater $CaCO_3$ mineralization is carried out. Constant addition experiments were used to simulate calcium carbonate precipitation in seawater, ranging the sulfate and magnesium concentrations suggested for Phanerozoic seawater (Horita et al., 2002) and at three different temperatures (5, 21 and 35°C).

Our results confirm seawater Mg:Ca ratio and SO_4 concentration as dominant drivers since small differences in their values can be invoked as controlling the variation in abiotic $CaCO_3$ polymorphs. We propose lower Mg:Ca and SO_4 thresholds on seawater chemistry for calcite predominance seas (Mg:Ca$\leq$ 0.65, SO4$\leq$ 10 mM) (Bots et al., 2011) than those suggested by the geological records (Mg:Ca$\approx$ 2) (Horita et al., 2002; Lowenstein et al., 2003).

Outlining the role of temperature on aragonite-calcite seas, our experimental data elucidate that changes in seawater temperature (5 - 35°C) did not lead to variations in the secular oscillations between predominant aragonite and calcite precipitation. Temperature changes from 5 to 35°C, only caused a variation of 0.2 units in the value of the Mg:Ca threshold (Mg:Ca $\approx$0.65$\pm$0.1) and did not affect the SO_4 threshold which was $\approx$10 mM at the three studied temperatures (when Mg:Ca$\leq$ 0.22). Thus, the synchronized oscillations between calcite and aragonite sea states seen in the geological record are separated by distinct seawater Mg:Ca ratio and SO_4

boundaries which are independent of temperature. Hence, the view of Phanerozoic aragonite-calcite seas should not be temperature corrected.

Our study confirms a strong correlation of the partition coefficient of Mg into abiogenic calcite with temperature and also reveals that this relationship is also controlled by the Mg:Ca ratio in seawater but is independent on SO_4 concentration in seawater. EPMA data showed that the Mg incorporation into calcite was directly proportional to seawater temperature over the seawater Mg:Ca range where calcite precipitation was possible (Mg:Ca= 0.00 – 1.00) but that the nature of this relationship is also dependent on seawater Mg:Ca ratio. Our results indicated that the proportion of Mg incorporated into calcite increases with temperature ≈3 times more rapidly when seawater Mg:Ca ratio was ≥ 0.55 than when seawater Mg:Ca ratio was ≤0.55. Here, we validate abiogenic calcite Mg:Ca as a reliable and quantitative proxy for past global seawater temperature change if its dependence on both the temperature and the Mg:Ca ratio of the seawater is considered. We propose the use of seawater Mg:Ca-specific equations to provide more accurate temperature estimates instead of a single calibration equation since the relationship between Mg:Ca in calcite and temperature varies with only small variations in the seawater Mg:Ca ratio.

8.1.2. Implications of ocean acidification on abiogenic marine $CaCO_3$ mineralogy and on Phanerozoic aragonite-calcite seas.

In Chapter 5, experiments were designed to study how changes in pCO_2 (400, 1500 and 3000 ppm) together with changes in seawater Mg:Ca ratio and SO_4 concentration affect the mineralogy of abiotic $CaCO_3$.

The results of this study indicate that calcium carbonate precipitation in the ocean occurs even at extreme atmospheric partial pressures of carbon dioxide (up to pCO_2 of 3000 ppm) (Janie Lee, 2010). Therefore, an increase in ocean acidification due to an increase in the atmospheric pCO_2 resulting from anthropogenic emissions of CO_2 may not have severe consequences for inorganic marine carbonates as the current projections related to increased rates of dissolution as pH declines.

An increase of atmospheric pCO_2 from 400 ppm to 3000 ppm and its consequent decrease of seawater pH from 8.2 to 7.6 would cause a decrease of the seawater Mg:Ca ratio and SO_4 concentration ranges that limit the current aragonite-calcite co-

precipitation field. Lower seawater pH scenarios would be characterized by having a wider pure calcite precipitation field and higher proportion of calcite with respect to aragonite in the aragonite-calcite co-precipitation field, but these variations in abiotic marine $CaCO_3$ mineralogy with pH would be only manifested in the seawater Mg:Ca ratio range from 0 to 1. The stability field for pure aragonite would remain constant. Thus, under future increasingly acidic seawater conditions, abiotic carbonate minerals such as calcite and low Mg-calcite could become increasingly dominant but only in ocean environments of very low seawater Mg:Ca ratios (Mg:Ca$\leq$ 1), which according to the records, hardly ever has occurred in oceans. For the same reasons, pCO_2 and seawater pH do not need to be considered as major controls on the Phanerozoic oscillations between aragonite and calcite seas and the dominant controls can be considered to be Mg:Ca and SO_4 concentration alone.

Our work also shows that changes in atmospheric pCO_2 and consequently changes in seawater pH affect significantly the incorporation of SO_4 into calcite. We show evidences that lower SO_4 contents in marine calcitic carbonates can be attributed to the relative contribution of high atmospheric carbon dioxide concentrations (>400 ppm), low seawater SO_4 concentrations and high temperatures ($\geq$35°C) (Chapter 4), which are environmental conditions characteristic of oceanic anoxic events. Here, we prove a clear relationship among abiogenic calcite SO_4 content, seawater SO_4 concentration and seawater pH. Therefore, we propose abiogenic calcite SO_4 content as a reliable quantitative proxy for past global seawater pH if its dependence on both pH and seawater SO_4 concentration is considered. The use of SO_4 content in abiogenic calcite as a paleo-pH proxy would help to constrain ancient marine pH and therefore ancient atmospheric carbon dioxide concentrations.

Now, from our extensive experimental data set of characterized $CaCO_3$ samples precipitated at a wide range of seawater Mg:Ca ratios, SO_4 concentrations, temperature and atmospheric pCO_2 values, it can be concluded that neither temperature nor atmospheric pCO_2 lead to large variations in the predominant $CaCO_3$ polymorph distribution. Note that it has been considered as predominant polymorph which its presence in the sample is $\geq$ 50%. The main driving forces controlling the precipitation of $CaCO_3$ polymorphs are seawater Mg:Ca ratio and SO_4 concentration (Bots et al., 2011) (Chapter 4).

It can also be concluded that switches between aragonite and calcite seas calculated from the stability fields from our experimental results would only match the proxy data for seawater chemistry in the geological record if the lowest suggested seawater SO_4 concentrations are considered ($[SO_4] \leq 10$ mM) (Adams et al., 2010; Newton et al., 2011; Poulton et al., 2015; Wortmann and Chernyavsky, 2007).

After our extensive evaluation and quantification of the influence of seawater Mg:Ca ratio, SO_4 concentration, temperature and atmospheric pCO_2 in abiotic seawater $CaCO_3$ mineralization, our suggested seawater Mg:Ca threshold for calcite predominant seas is 0.65±0.1 (Bots et al., 2011) (Chapter 4), still far lower than the Mg:Ca ratio of ≈2 proposed in literature (Horita et al., 2002; Lowenstein et al., 2003). Because the ocean is such as complex environment, this mismatch between our experimental and the aragonite-calcite seas pattern from the record could also indicate the importance of other variables such as dissolved organics, alkalinity, etc. to changes in carbonate mineralogy.

8.1.3. Influence of solution chemistry and temperature on $CaCO_3$ morphogenesis.

In Chapter 6, the role of solution Mg and SO_4 concentrations and the effect of temperature on the resulting solid $CaCO_3$ morphology and particle sizes were investigated.

From SEM analyses, we show that the morphology and sizes of the formed $CaCO_3$ particles were greatly affected by the reaction temperature. For identical solution chemical compositions and reaction times, the size of the precipitated $CaCO_3$ particles decreased as temperature increased. The fact that calcium carbonate crystal size increased as temperature decreased could be due to a combination of both a kinetic effect and a variation in the $[CO_3^{2-}]$:$[Ca^{2+}]$ ratio with changing temperature. The kinetic effect is related to the number of nucleation events taking place at the initial stage and also depending on the number of available ions per unit area arriving onto a newly forming crystal. An increase in temperature also reduces the conversion of CO_2 into CO_3^{2-}, leading to a low concentration of CO_3^{2-} that is surrounded by Ca^{2+}. Hence, an increase in solution temperature results in an increase of Ca^{2+} concentration, which involves an increase in the supersaturation of the reaction medium. Under such conditions, the nucleation phase, which corresponds to

the faster generation of a myriad of small crystal nuclei, prevails, leading to the observed decrease in average $CaCO_3$ particle size (Babou-Kammoe et al., 2012; Sha et al., 2016; Yu et al., 2004).

Moreover, temperature influenced substantially on calcite morphology but slightly on aragonite and vaterite morphology. These changes in calcite morphology with temperature might be related to the positive correlation between the Mg content in calcite and temperature; on average, ≈ 4 times more Mg became incorporated into calcite at 35°C compared with calcite formed at 5°C. Magnesium is only incorporated into calcite and the sulfate content in aragonite and vaterite does not vary with temperature. Thus, an increase in temperature favours the isomorphic substitution of magnesium to calcite in the calcite structure which influences on crystal growth (Falini et al., 1998). Overall, our results address Mg to be the overriding control on calcite morphological variation. However, calcium carbonate crystals showed a wide range of morphologies with different widths and lengths at each temperature that did not allow any clear correlation with particle size and reaction temperature.

The morphology and shape of the precipitates were also greatly modified by variations in seawater ion contents (Mg and SO_4). Magnesium and sulfate in solution favour particle aggregation and specially affect calcite morphology. Various crystal morphologies of calcite, such as aggregated particles of regular plate-like, elongated along the c-axis rhombohedras, inter-grown triangles, trigonal prisms, etc. can be obtained by changing the experimental conditions. As mentioned above, Mg is incorporated only into calcite and it is known that in the presence of this ion there is a isomorphic substitution of magnesium to calcium in calcite structure which is favoured by the presence of sulfate ions, (Falini et al., 1998). Sulfate mainly influences on aragonite and vaterite particles aggregation but not in their morphology. Thus, this would highlight again magnesium as the main driver controlling calcite morphology. The fact that calcite precipitated as many random morphologies, tell us that generalized rules and morphology diagrams as a function of Mg, SO_4 and temperature is virtually impossible to construct.

8.2. Future work

There are still many open questions in the field of calcium carbonate mineralogy that need addressing in order to further our understanding of the mechanisms and rates of calcium carbonate precipitation. Here we discuss several approaches and suggestions for further theoretical and laboratory studies that we assert are still needed to help progress this field in the future:

a) Mg isotope variability in carbonates has been recently explored as a potential paleoenvironmental proxy (Pearce et al., 2012; Pogge von Strandmann et al., 2014; Saenger and Wang, 2014). The variations observed in natural carbonates clearly show that Mg isotopes are fractionated during their incorporation into the carbonate lattice, with a strong mineralogical control on the degree to which ^{26}Mg is excluded from the mineral. However, the Mg isotope composition of carbonates could also be affected by other processes including temperature, growth rate, kinetic isotope fractionation and biologically-mediated vitals effects (Saenger and Wang, 2014). Evaluating if the Mg isotope composition of biogenic and abiogenic carbonates may be a useful paleoenvironmental proxy requires an understanding of how the processes mentioned above affect Mg isotope fractionation. Furthermore, a thorough understanding of Mg isotope fractionation in carbonates may help elucidate the isotope fractionation mechanism of other elements (e.g. oxygen, strontium, calcium) and the partitioning of cations (e.g. magnesium, strontium) between carbonate and solution, many of which have been applied as paleotemperature proxies (e.g., (Böhm et al., 2006; Lear et al., 2002; O'Neil et al., 1969)).

Mg isotopes analyses are clearly an active research field with lots going on at the moment and will allow us to:

- Evaluate how variations in some factors such as solution chemistry (e.g. magnesium and sulfate concentration) and temperature affect the Mg isotope fractionation between carbonates and solution ($\Delta^{26} Mg_{carb\text{-}sol}$) in abiogenic carbonate minerals.

- Get a better sense of Mg fractionation under marine conditions and how this may have changed over the Phanerozoic. It would be worth validating if the assumptions made by isotope geochemists when studying paleoenvironmental proxies using magnesium isotopes are consistent.

- Combine Mg, Ca and stable Sr analyses of experimental samples to get a sense of how carbonate precipitation may have affected all three cation fluxes over the Phanerozoic and how this relates to the Mg:Ca and Sr:Ca stories.

b) Many marine organisms (e.g., sponges, molluscs, bivalves, etc.) crystallize calcite or aragonite via amorphous calcium carbonate (ACC) by increasing the supersaturation levels locally. In these marine organisms the stabilization and controlled transformation of metastable amorphous precursor phases is critical. The nucleation and growth of a crystalline phase is only observed after the ACC particle grows past a critical size and may be modulated and template by macromolecules and interfaces (Adabi, 2004; Loste et al., 2004; Mahamid et al., 2010). Soluble additives, for example Mg, proteins or polymers, may affect precipitation both by direct binding and by controlling aggregation (Gebauer et al., 2010). Recent studies have demonstrated ACCs stabilization by confinement between carboxy-terminated self-assembled monolayers (Stephens et al., 2010). Recent work (Cantaert et al., 2012; Smeets et al., 2015) also indicates that by coating with stabilizing agent, poly-aspartic acid, to arrest growth and aggregation, ACC crystallization is inhibited below a particle size of 100 nm. In either case it is not entirely clear what role the organic plays. Giant liposomes have been shown as a "privileged environment" where ACC nanoparticles can remain stable against aggregation, they seemingly do not crystallize for at least 20 hours, and are ideally suited to investigate the influence of lipid chemistry, particle size and soluble additives on ACC *in situ* (Tester et al., 2011; Tester and Joester, 2013; Tester et al., 2014; Tester et al., 2012). However, at this time, there is a fascinating disconnect between experimental observations, theoretical considerations, and simulations regarding the stability of ACC in confinement.

Thus, studying calcium carbonate precipitation in confinement and in the presence of organics (e.g., microemulsions, lipids) to mimic the far from equilibrium conditions that occur in some marine organisms and to figure out the effects of Mg, SO_4, temperature and pH on the crystallization pathways would allow us to:

- Evaluate possible confinement molecules to perform controlled calcium carbonate nucleation and growth experiments, and to select the most suitable one where the stabilization and controlled transformation of ACC are possible.

- Characterize any phase formation and transformations as well as how polymorph selection in the nucleation and growth of calcium carbonate in confinement occurs; this will allow us to better understand the biological control over mineral nucleation and growth.

- Study how the parameters studied in our work (Mg, SO_4, temperature and changes in pH correlated with changes in pCO_2) influence or control calcium carbonate precipitation by biomineralizing organisms.

References

Adabi, M. H., 2004, A re-evaluation of aragonite versus calcite seas: Carbonates and Evaporites, v. 19, no. 2, p. 133.

Adams, D. D., Hurtgen, M. T., and Sageman, B. B., 2010, Volcanic triggering of a biogeochemical cascade during Oceanic Anoxic Event 2: Nature Geoscience, v. 3, p. 201.

Addadi, L., Raz, S., and Weiner, S., 2003, Taking Advantage of Disorder: Amorphous Calcium Carbonate and Its Roles in Biomineralization: Advanced Materials, v. 15, no. 12, p. 959-970.

Ajikumar, P. K., Lakshminarayanan, R., and Valiyaveettil, S., 2004, Controlled deposition of thin films of calcium carbonate on natural and synthetic templates: Crystal Growth & Design, v. 4, no. 2, p. 331-335.

Albeck, S., Aizenberg, J., Addadi, L., and Weiner, S., 1993, Interactions of various skeletal intracrystalline components with calcite crystals: Journal of the American Chemical Society, v. 115, no. 25, p. 11691-11697.

Albright, J. N., 1971, Mineralogical notes vaterite stability: American Mineralogist: Journal of Earth and Planetary Materials, v. 56, no. 3-4_Part_1, p. 620-624.

Alruopn, P. L., 1977, Structural refinements of dolomite and a magnesian calcite and implications for dolomite formation in the marine environment: American Mineralogist, v. 62, p. 772-783.

Andreas J. Andersson, F. T. M. a. N. R. B., 2008, Life on the margin: implications of ocean acidification on Mg-calcite, high latitude and cold-water marine calcifiers: Marine Ecology Progress Series, v. 373, p. 265-274.

Appelo, C., and Postma, D., 2005, Geochemistry, groundwater and pollution, CRC: Balkema, Roterdam.

Appelo, C., Postma, D., Appelo, C., 2005, Geochemistry, Groundwater and Pollution: London: CRC Press.

Archer, D., Kheshgi, H., and Maier-Reimer, E., 1997, Multiple timescales for neutralization of fossil fuel CO2: Geophysical Research Letters, v. 24, no. 4, p. 405-408.

Babou-Kammoe, R., Hamoudi, S., Larachi, F., and Belkacemi, K., 2012, Synthesis of CaCO3 nanoparticles by controlled precipitation of saturated carbonate and calcium nitrate aqueous solutions: The Canadian journal of chemical engineering, v. 90, no. 1, p. 26-33.

Bach, L. T., 2015, Reconsidering the role of carbonate ion concentration in calcification by marine organisms: Biogeosciences (BG), v. 12, p. 4939-4951.

Balthasar, U., and Cusack, M., 2015, Aragonite-calcite seas—Quantifying the gray area: Geology, v. 43, no. 2, p. 99-102.

Berner, R. A., 1975, The role of magnesium in the crystal growth of calcite and aragonite from sea water: Geochimica et Cosmochimica Acta, v. 39, no. 4, p. 489-504.

Berner, R. A., 1994, GEOCARB II: A revised model of atmospheric CO[sub 2] over phanerozoic time: American Journal of Science; (United States), p. Medium: X; Size: Pages: 56-91.

Berner, R. A., 2004, A model for calcium, magnesium and sulfate in seawater over Phanerozoic time: American Journal of Science, v. 304, no. 5, p. 438-453.

Bischoff, J. L., 1968, Catalysis, inhibition, and the calcite-aragonite problem; [Part] 2, The vaterite-aragonite transformation: American Journal of Science, v. 266, no. 2, p. 80-90.

Bischoff, J. L., and Fyfe, W., 1968, Catalysis, inhibition, and the calcite-aragonite problem;[Part] 1, The aragonite-calcite transformation: American Journal of Science, v. 266, no. 2, p. 65-79.

Böhm, F., Gussone, N., Eisenhauer, A., Dullo, W.-C., Reynaud, S., and Paytan, A., 2006, Calcium isotope fractionation in modern scleractinian corals: Geochimica et Cosmochimica Acta, v. 70, no. 17, p. 4452-4462.

Bots, P., Benning, L., Rickaby, R., and Shaw, S., 2011, The role of SO4 in the switch from calcite to aragonite seas: Geology, v. 39, no. 4, p. 331-334.

Bots, P., Benning, L. G., Rodriguez-Blanco, J.-D., Roncal-Herrero, T., and Shaw, S., 2012, Mechanistic insights into the crystallization of amorphous calcium carbonate (ACC): Crystal Growth & Design, v. 12, no. 7, p. 3806-3814.

Bots P. , B. L. G., Rickaby R. E. M., and Shaw S., 2011, The role of SO4 in the switch from calcite to aragonite seas: Geology, v. 39, no. 4, p. 331-334.

Brand, U., Posenato, R., Came, R., Affek, H., Angiolini, L., Azmy, K., and Farabegoli, E., 2012, The end-Permian mass extinction: A rapid volcanic CO2 and CH4-climatic catastrophe: Chemical Geology, v. 322–323, p. 121-144.

Branson, O., Redfern, S. A., Tyliszczak, T., Sadekov, A., Langer, G., Kimoto, K., and Elderfield, H., 2013a, The coordination of Mg in foraminiferal calcite: Earth and Planetary Science Letters, v. 383, p. 134-141.

Branson, O., Redfern, S. A. T., Tyliszczak, T., Sadekov, A., Langer, G., Kimoto, K., and Elderfield, H., 2013b, The coordination of Mg in foraminiferal calcite: Earth and Planetary Science Letters, v. 383, p. 134-141.

Burton, E. A., 1993, Controls on marine carbonate cement mineralogy: review and reassessment: Chemical Geology, v. 105, no. 1, p. 163-179.

Burton, E. A., and Walter, L. M., 1987, Relative precipitation rates of aragonite and Mg calcite from seawater: Temperature or carbonate ion control?: Geology, v. 15, no. 2, p. 111-114.

Burton, E. A., Walter, Lynn M, 1991, The effects of PCO2 and temperature on magnesium incorporation in calcite in seawater and MgCl2-CaCl2 solutions: Geochimica et Cosmochimica Acta, v. 55, no. 3, p. 777-785.

Busenberg, E., and Niel Plummer, L., 1985, Kinetic and thermodynamic factors controlling the distribution of SO32− and Na+ in calcites and selected aragonites: Geochimica et Cosmochimica Acta, v. 49, no. 3, p. 713-725.

-, 1989, Thermodynamics of magnesian calcite solid-solutions at 25°C and 1 atm total pressure: Geochimica et Cosmochimica Acta, v. 53, no. 6, p. 1189-1208.

Busenberg, E., and Plummer, L. N., 1989, Thermodynamics of magnesian calcite solid-solutions at 25 C and 1 atm total pressure: Geochimica et Cosmochimica Acta, v. 53, no. 6, p. 1189-1208.

Caldeira, K., and Wickett, M. E., 2003, Anthropogenic carbon and ocean pH: Nature, v. 425, p. 365.

Cantaert, B., Kim, Y. Y., Ludwig, H., Nudelman, F., Sommerdijk, N. A., and Meldrum, F. C., 2012, Think positive: phase separation enables a positively charged additive to induce dramatic changes in calcium carbonate morphology: Advanced Functional Materials, v. 22, no. 5, p. 907-915.

Chang, V. T. C., Williams, R. J. P., Makishima, A., Belshawl, N. S., and O'Nions, R. K., 2004, Mg and Ca isotope fractionation during CaCO3 biomineralisation: Biochemical and Biophysical Research Communications, v. 323, no. 1, p. 79-85.

Chen, L.-S., Mai, Y.-W., and Cotterell, B., 1989, Impact fracture energy of mineral-filled polypropylene: Polymer Engineering & Science, v. 29, no. 8, p. 505-512.

Coggon, R. M., Teagle, D. A. H., Smith-Duque, C. E., Alt, J. C., and Cooper, M. J., 2010, Reconstructing Past Seawater Mg/Ca and Sr/Ca from Mid-Ocean Ridge Flank Calcium Carbonate Veins: Science, v. 327, no. 5969, p. 1114-1117.

Cohen, A. L., Owens, K. E., Layne, G. D., and Shimizu, N., 2002, The Effect of Algal Symbionts on the Accuracy of Sr/Ca Paleotemperatures from Coral: Science, v. 296, no. 5566, p. 331-333.

Crowley, T. J., and Berner, R. A., 2001, CO₂ and Climate Change: Science, v. 292, no. 5518, p. 870-872.

Cusack, M., and Freer, A., 2008, Biomineralization: Elemental and Organic Influence in Carbonate Systems: Chemical Reviews, v. 108, no. 11, p. 4433-4454.

Davis, K. J., Dove, P. M., and De Yoreo, J. J., 2000a, The role of Mg2+ as an impurity in calcite growth: Science, v. 290, no. 5494, p. 1134-1137.

Davis, K. J., Dove, P. M., and De Yoreo, J. J., 2000b, The Role of Mg²⁺ as an Impurity in Calcite Growth: Science, v. 290, no. 5494, p. 1134-1137.

Davis, K. J., Dove, P. M., Wasylenki, L. E., and De Yoreo, J. J., 2004, Morphological consequences of differential Mg2+ incorporation at structurally distinct steps on calcite: American Mineralogist, v. 89, no. 5-6, p. 714-720.

De Choudens-Sánchez, V., and González, L. A., 2009, Calcite and Aragonite Precipitation Under Controlled Instantaneous Supersaturation: Elucidating the Role of CaCO3 Saturation State and Mg/Ca Ratio on Calcium Carbonate Polymorphism: Journal of Sedimentary Research, v. 79, no. 6, p. 363-376.

de Villiers, S., Dickson, J. A. D., and Ellam, R. M., 2005, The composition of the continental river weathering flux deduced from seawater Mg isotopes: Chemical Geology, v. 216, no. 1, p. 133-142.

Demicco, R. V., Lowenstein, T. K., Hardie, L. A., and Spencer, R. J., 2005, Model of seawater composition for the Phanerozoic: Geology, v. 33, no. 11, p. 877-880.

Dickson, J. A. D., 2002, Fossil Echinoderms As Monitor of the Mg/Ca Ratio of Phanerozoic Oceans: Science, v. 298, no. 5596, p. 1222-1224.

-, 2004, Echinoderm Skeletal Preservation: Calcite-Aragonite Seas and the Mg/Ca Ratio of Phanerozoic Oceans: Journal of Sedimentary Research, v. 74, no. 3, p. 355-365.

Doner, H. E., and Pratt, P. F., 1969, Solubility of Calcium Carbonate Precipitated in Aqueous Solutions of Magnesium and Sulfate Salts1: Soil Science Society of America Journal, v. 33, no. 5, p. 690-693.

Doney, S. C., Fabry, V. J., Feely, R. A., and Kleypas, J. A., 2009, Ocean acidification: the other CO2 problem.

Dwyer, G. S., Cronin, T. M., Baker, P. A., Raymo, M. E., Buzas, J. S., Corrège. T., 1995, North atlantic deepwater temperature change during late pliocene and late quaternary climatic cycles, Science, Volume 270, p. 1347 - 1351.

Elderfield, H., Bertram, C. J., and Erez, J., 1996, A biomineralization model for the incorporation of trace elements into foraminiferal calcium carbonate: Earth and Planetary Science Letters, v. 142, no. 3, p. 409-423.

Elizabeth A. Burton, a. L. M. W., 1991, The effects of PCO2 and temperature on magnesium incorporation in calcite in seawater and MgCl2-CaCl2 solutions: Geochimica et Cosmochimica Acta, v. 55, no. 3, p. 777-785.

Elizabeth A. Burton, L. M. W., 1987, Relative precipitation rates of aragonite and Mg calcite from seawater: Temperature or carbonate ion control?: Geology, v. 15, no. 2, p. 111-114.

Falini, G., Fermani, S., Gazzano, M., and Ripamonti, A., 1998, Structure and morphology of synthetic magnesium calcite: Journal of Materials Chemistry, v. 8, no. 4, p. 1061-1065.

Falini, G., Fermani, S., Tosi, G., and Dinelli, E., 2009, Calcium carbonate morphology and structure in the presence of seawater ions and humic acids: Crystal Growth and Design, v. 9, no. 5, p. 2065-2072.

Fantle, M. S., and DePaolo, D. J., 2007, Ca isotopes in carbonate sediment and pore fluid from ODP Site 807A: The Ca2+(aq)–calcite equilibrium fractionation

factor and calcite recrystallization rates in Pleistocene sediments: Geochimica et Cosmochimica Acta, v. 71, no. 10, p. 2524-2546.

Feely, R. A., Sabine, C. L., Hernandez-Ayon, J. M., Ianson, D., and Hales, B., 2008, Evidence for Upwelling of Corrosive "Acidified" Water onto the Continental Shelf: Science, v. 320, no. 5882, p. 1490-1492.

Fernández-Díaz, L., Fernández-González, Á., and Prieto, M., 2010, The role of sulfate groups in controlling CaCO3 polymorphism: Geochimica et Cosmochimica Acta, v. 74, no. 21, p. 6064-6076.

Finch, A. A., and Allison, N., 2008, Mg structural state in coral aragonite and implications for the paleoenvironmental proxy: Geophysical Research Letters, v. 35, no. 8.

Folk, R. L., 1974, The natural history of crystalline calcium carbonate; effect of magnesium content and salinity: Journal of Sedimentary Research, v. 44, no. 1, p. 40-53.

Fred T. Mackenzie, W. D. B., Finley C. Bishop, Michele Loijens, Jane Schoonmaker and Roland Wollast, 1983, Magnesian calcites; low-temperature occurrence, solubility and solid-solution behavior: Reviews in Mineralogy and Geochemistry, v. 11, no. 1, p. 97-144.

Galy, A., Bar-Matthews, M., Halicz, L., and O'Nions, R. K., 2002, Mg isotopic composition of carbonate: insight from speleothem formation: Earth and Planetary Science Letters, v. 201, no. 1, p. 105-115.

García Carmona, J., Gómez Morales, J., and Rodríguez Clemente, R., 2003, Rhombohedral-scalenohedral calcite transition produced by adjusting the solution electrical conductivity in the system Ca (OH) 2-CO2-H2O: Journal of colloid and interface science, v. 261, p. 434-440.

Garrard, S. L., Gambi, M. C., Scipione, M. B., Patti, F. P., Lorenti, M., Zupo, V., Paterson, D. M., and Buia, M. C., 2014, Indirect effects may buffer negative responses of seagrass invertebrate communities to ocean acidification: Journal of experimental marine biology and ecology, v. 461, p. 31-38.

Gebauer, D., Gunawidjaja, P. N., Ko, J. Y. P., Bacsik, Z., Aziz, B., Liu, L., Hu, Y., Bergström, L., Tai, C.-W., Sham, T.-K., Edén, M., and Hedin, N., 2010, Proto-Calcite and Proto-Vaterite in Amorphous Calcium Carbonates: Angewandte Chemie International Edition, v. 49, no. 47, p. 8889-8891.

Gleeson, D. F., WILLIAMSON, C., GRASBY, S. E., PAPPALARDO, R. T., SPEAR, J. R., and TEMPLETON, A. S., 2011, Low temperature S0 biomineralization at a supraglacial spring system in the Canadian High Arctic: Geobiology, v. 9, no. 4, p. 360-375.

Gomes, M. L., Hurtgen, M. T., and Sageman, B. B., 2016, Biogeochemical sulfur cycling during Cretaceous oceanic anoxic events: A comparison of OAE1a and OAE2: Paleoceanography, v. 31, no. 2, p. 233-251.

Goodwin, A. L., Michel, F. M., Phillips, B. L., Keen, D. A., Dove, M. T., and Reeder, R. J., 2010, Nanoporous Structure and Medium-Range Order in Synthetic Amorphous Calcium Carbonate: Chemistry of Materials, v. 22, no. 10, p. 3197-3205.

Graf, D. L., 1961, Crystallographic tables for the rhombohedral carbonates: American Mineralogist: Journal of Earth and Planetary Materials, v. 46, no. 11-12, p. 1283-1316.

Hardie, L. A., 1990, The roles of rifting and hydrothermal CaCl 2 brines in the origin of potash evaporites; an hypothesis: American Journal of Science, v. 290, no. 1, p. 43-106.

Hardie, L. A., 1991, On the Significance of Evaporites: Annual Review of Earth and Planetary Sciences, v. 19, no. 1, p. 131-168.

Hardie, L. A., 1996, Secular variation in seawater chemistry: An explanation for the coupled secular variation in the mineralogies of marine limestones and potash evaporites over the past 600 m.y: Geology, v. 24, no. 3, p. 279-283.

Hartley, G., and Mucci, A., 1996, The influence of PCO2 on the partitioning of magnesium in calcite overgrowths precipitated from artificial seawater at 25° and 1 atm total pressure: Geochimica et Cosmochimica Acta, v. 60, no. 2, p. 315-324.

Hasiuk, F. J., and Lohmann, K. C., 2008, Mississippian Paleocean Chemistry from Biotic and Abiotic Carbonate, Muleshoe Mound, Lake Valley Formation, New Mexico, U.S.A: Journal of Sedimentary Research, v. 78, no. 2, p. 147-164.

Holland, H. D., 2005, Sea level, sediments and the composition of seawater: American Journal of Science, v. 305, no. 3, p. 220-239.

Holland, H. D., Horita, J., and Seyfried, J. W. E., 1996, On the secular variations in the composition of Phanerozoic marine potash evaporites: Geology, v. 24, no. 11, p. 993-996.

Holt, N. M., García-Veigas, J., Lowenstein, T. K., Giles, P. S., and Williams-Stroud, S., 2014, The major-ion composition of Carboniferous seawater: Geochimica et Cosmochimica Acta, v. 134, p. 317-334.

Hönisch, B., Ridgwell, A., Schmidt, D. N., Thomas, E., Gibbs, S. J., Sluijs, A., Zeebe, R., Kump, L., Martindale, R. C., Greene, S. E., Kiessling, W., Ries, J., Zachos, J. C., Royer, D. L., Barker, S., Marchitto, T. M., Moyer, R., Pelejero, C., Ziveri, P., Foster, G. L., and Williams, B., 2012, The Geological Record of Ocean Acidification: Science, v. 335, no. 6072, p. 1058-1063.

Horita, J., Zimmermann, H., and Holland, H. D., 2002, Chemical evolution of seawater during the Phanerozoic: Implications from the record of marine evaporites: Geochimica et Cosmochimica Acta, v. 66, no. 21, p. 3733-3756.

Huber, B. T., Norris, R. D., and MacLeod, K. G., 2002, Deep-sea paleotemperature record of extreme warmth during the Cretaceous: Geology, v. 30, no. 2, p. 123-126.

Immenhauser, A., Buhl, D., Richter, D., Niedermayr, A., Riechelmann, D., Dietzel, M., and Schulte, U., 2010, Magnesium-isotope fractionation during low-Mg calcite precipitation in a limestone cave–Field study and experiments: Geochimica et Cosmochimica Acta, v. 74, no. 15, p. 4346-4364.

Janie Lee, J. W. M., 2010, Influences of alkalinity and pCO2 on CaCO3 nucleation from estimated Cretaceous composition seawater representative of "calcite seas": Geology v. 38, no. 2, p. 115-118.

Jarvis, K. E., Gray, A. L., Houk, R. S., Jarvis, I., McLaren, J., and Williams, J. G., 1992, Handbook of inductively coupled plasma mass spectrometry, Blackie Glasgow.

Kamhi, S. R., 1963, On the structure of vaterite CaCO3: Acta Crystallographica, v. 16, no. 8, p. 770-772.

Katz, A., 1973, The interaction of magnesium with calcite during crystal growth at 25–90°C and one atmosphere: Geochimica et Cosmochimica Acta, v. 37, no. 6, p. 1563-1586.

Kester, D. R., Duedall, I. W., Connors, D. N., and Pytkowicz, R. M., 1967, PREPARATION OF ARTIFICIAL SEAWATER1: Limnology and Oceanography, v. 12, no. 1, p. 176-179.

Kitano, Y., Kanamori, N., and Oomori, T., 1971, Measurements of distribution coefficients and barium between carbonate precipitate —Abnormally high values of distribution measured at early stages of carbonate of strontium and solution coefficients formation: GEOCHEMICAL JOURNAL, v. 4, no. 4, p. 183-206.

Kontrec, J., Kralj, D., Brečević, L., Falini, G., Fermani, S., Noethig-Laslo, V., and Mirosavljević, K., 2004a, Incorporation of Inorganic Anions in Calcite: European Journal of Inorganic Chemistry, v. 2004, no. 23, p. 4579-4585.

Kontrec, J., Kralj, D., Brečević, L., Falini, G., Fermani, S., Noethig-Laslo, V., and Mirosavljević, K., 2004b, Incorporation of inorganic anions in calcite: European Journal of Inorganic Chemistry, v. 2004, no. 23, p. 4579-4585.

Küther, J., Seshadri, R., Knoll, W., and Tremel, W., 1998, Templated growth of calcite, vaterite and aragonite crystals onself-assembled monolayers of substituted alkylthiols on gold: Journal of Materials Chemistry, v. 8, no. 3, p. 641-650.

Lacroix, O., and Larachi, F., 2008, Scrubber Designs for Enzyme-Mediated Capture of CO2: Recent Patents on Chemical Engineering, v. 1, no. 2, p. 93-105.

Lam, R. S. K., Charnock, J. M., Lennie, A., and Meldrum, F. C., 2007, Synthesis-dependant structural variations in amorphous calcium carbonate: CrystEngComm, v. 9, no. 12, p. 1226-1236.

Land, L. S., and Hoops, G. K., 1973, Sodium in carbonate sediments and rocks; a possible index to the salinity of diagenetic solutions: Journal of Sedimentary Research, v. 43, no. 3, p. 614-617.

Le Bail, A., Ouhenia, S., and Chateigner, D., 2011, Microtwinning hypothesis for a more ordered vaterite model: Powder Diffraction, v. 26, no. 1, p. 16-21.

Lear, C. H., Elderfield, H., and Wilson, P. A., 2000, Cenozoic Deep-Sea Temperatures and Global Ice Volumes from Mg/Ca in Benthic Foraminiferal Calcite: Science, v. 287, no. 5451, p. 269-272.

Lear, C. H., Rosenthal, Y., and Slowey, N., 2002, Benthic foraminiferal Mg/Ca-paleothermometry: a revised core-top calibration: Geochimica et Cosmochimica Acta, v. 66, no. 19, p. 3375-3387.

Lee, I., Han, S. W., Choi, H. J., and Kim, K., 2001, Nanoparticle-Directed Crystallization of Calcium Carbonate: Advanced Materials, v. 13, no. 21, p. 1617-1620.

Lee, J., and Morse, J. W., 2010, Influences of alkalinity and pCO2 on CaCO3 nucleation from estimated Cretaceous composition seawater representative of “calcite seas”: Geology, v. 38, no. 2, p. 115-118.

Li, W., Chakraborty, S., Beard, B. L., Romanek, C. S., and Johnson, C. M., 2012, Magnesium isotope fractionation during precipitation of inorganic calcite under laboratory conditions: Earth and Planetary Science Letters, v. 333-334, p. 304-316.

Lippmann, F., 1973, Sedimentary Carbonate Minerals: Springer.

-, 2012, Sedimentary Carbonate Minerals: Science & Business Media.

Lopez, O., Zuddas, P., and Faivre, D., 2009, The influence of temperature and seawater composition on calcite crystal growth mechanisms and kinetics: Implications for Mg incorporation in calcite lattice: Geochimica et Cosmochimica Acta, v. 73, no. 2, p. 337-347.

Lorens, R. B., and Bender, M. L., 1980, The impact of solution chemistry on Mytilus edulis calcite and aragonite: Geochimica et Cosmochimica Acta, v. 44, no. 9, p. 1265-1278.

Loste, E., Park, R. J., Warren, J., and Meldrum, F. C., 2004, Precipitation of calcium carbonate in confinement: Advanced Functional Materials, v. 14, no. 12, p. 1211-1220.

Loste, E., Wilson, R. M., Seshadri, R., and Meldrum, F. C., 2003a, The role of magnesium in stabilising amorphous calcium carbonate and controlling calcite morphologies: Journal of Crystal Growth, v. 254, no. 1-2, p. 206-218.

Loste, E., Wilson, R. M., Seshadri, R., and Meldrum, F. C., 2003b, The role of magnesium in stabilising amorphous calcium carbonate and controlling calcite morphologies: Journal of Crystal Growth, v. 254, no. 1, p. 206-218.

Lowenstein, T. K., Hardie, L. A., Timofeeff, M. N., and Demicco, R. V., 2003, Secular variation in seawater chemistry and the origin of calcium chloride basinal brines: Geology, v. 31, no. 10, p. 857-860.

Lowenstein, T. K., Timofeeff, M. N., Brennan, S. T., Hardie, L. A., and Demicco, R. V., 2001, Oscillations in Phanerozoic Seawater Chemistry: Evidence from Fluid Inclusions: Science, v. 294, no. 5544, p. 1086-1088.

M. C. Nash, S. U., A. P. Negri and N. E. Cantin, 2015, Ocean acidification does not affect magnesium composition or dolomite formation in living crustose coralline algae, Porolithon onkodes in an experimental system: Biogeosciences Discussions, v. 12, p. 1373-1404.

Mackenzie, F. T., and Morse, J. W., 1992, Sedimentary carbonates through Phanerozoic time: Geochimica et Cosmochimica Acta, v. 56, no. 8, p. 3281-3295.

Mackenzie, F. T., and Pigott, J. D., 1981, Tectonic controls of Phanerozoic sedimentary rock cycling: Journal of the Geological Society, v. 138, no. 2, p. 183-196.

Mahamid, J., Aichmayer, B., Shimoni, E., Ziblat, R., Li, C., Siegel, S., Paris, O., Fratzl, P., Weiner, S., and Addadi, L., 2010, Mapping amorphous calcium phosphate transformation into crystalline mineral from the cell to the bone in

zebrafish fin rays: Proceedings of the National Academy of Sciences, v. 107, no. 14, p. 6316-6321.

Manoli, F., and Dalas, E., 2000, Spontaneous precipitation of calcium carbonate in the presence of ethanol, isopropanol and diethylene glycol: Journal of Crystal Growth, v. 218, no. 2-4, p. 359-364.

Martin, R. E., 1995, Cyclic and secular variation in microfossil biomineralization: clues to the biogeochemical evolution of Phanerozoic oceans: Global and Planetary Change, v. 11, no. 1, p. 1-23.

Mavromatis, V., Gautier, Q., Bosc, O., and Schott, J., 2013, Kinetics of Mg partition and Mg stable isotope fractionation during its incorporation in calcite: Geochimica et Cosmochimica Acta, v. 114, p. 188-203.

Medeiros, S., Albuquerque, E., Maia Jr, F., Caetano, E., and Freire, V., 2007, First-principles calculations of structural, electronic, and optical absorption properties of CaCO3 Vaterite: Chemical Physics Letters, v. 435, no. 1-3, p. 59-64.

Meldrum, F. C., and Cölfen, H., 2008, Controlling Mineral Morphologies and Structures in Biological and Synthetic Systems: Chemical Reviews, v. 108, no. 11, p. 4332-4432.

Meyer, H., 1969, Struktur und fehlordnung des vaterits: Zeitschrift für Kristallographie-Crystalline Materials, v. 128, no. 1-6, p. 183-212.

Michel, F. M., MacDonald, J., Feng, J., Phillips, B. L., Ehm, L., Tarabrella, C., Parise, J. B., and Reeder, R. J., 2008, Structural Characteristics of Synthetic Amorphous Calcium Carbonate: Chemistry of Materials, v. 20, no. 14, p. 4720-4728.

MmxcRAF, S., and Rrnnrn, R., 1985, High-temperature structure refinements of calcite and magnesite: American Mineralogist, v. 70, p. 590400.

Morse, J. W., & Mackenzie, F. T., 1990, Geochemistry of sedimentary carbonates: Elsevier, v. 48.

Morse, J. W., Arvidson, R. S., and Lüttge, A., 2007, Calcium Carbonate Formation and Dissolution: Chemical Reviews, v. 107, no. 2, p. 342-381.

Morse, J. W., and Bender, M. L., 1990, Partition coefficients in calcite: Examination of factors influencing the validity of experimental results and their application to natural systems: Chemical Geology, v. 82, p. 265-277.

Morse, J. W., and Casey, W. H., 1988, Ostwald processes and mineral paragenesis in sediments: American Journal of Science, v. 288, no. 6, p. 537-560.

Morse, J. W., and Mackenzie, F. T., 1990, Geochemistry of sedimentary carbonates, Elsevier.

Morse, J. W., Wang, Q., and Tsio, M. Y., 1997a, Influences of temperature and Mg: Ca ratio on CaCO3 precipitates from seawater: Geology, v. 25, no. 1, p. 85-87.

Morse, J. W., Wang, Q., and Tsio, M. Y., 1997b, Influences of temperature and Mg:Ca ratio on CaCO3 precipitates from seawater: Geology, v. 25, no. 1, p. 85-87.

Mucci, A., 1987, Influence of temperature on the composition of magnesian calcite overgrowths precipitated from seawater: Geochimica et Cosmochimica Acta, v. 51, no. 7, p. 1977-1984.

Mucci, A., and Morse, J. W., 1983, The incorporation of Mg2+ and Sr2+ into calcite overgrowths: influences of growth rate and solution composition: Geochimica et Cosmochimica Acta, v. 47, no. 2, p. 217-233.

Mucci, A., Morse, J. W., and Kaminsky, M. S., 1985, Auger spectroscopy analysis of magnesian calcite overgrowths precipitated from seawater and solutions of similar composition: Am. J. Sci.; (United States), p. Medium: X; Size: Pages: 289-305.

Newton, R. J., Reeves, E. P., Kafousia, N., Wignall, P. B., Bottrell, S. H., and Sha, J.-G., 2011, Low marine sulfate concentrations and the isolation of the European epicontinental sea during the Early Jurassic: Geology, v. 39, no. 1, p. 7-10.

Nürnberg, D., Bijma, J., and Hemleben, C., 1996, Assessing the reliability of magnesium in foraminiferal calcite as a proxy for water mass temperatures: Geochimica et Cosmochimica Acta, v. 60, no. 5, p. 803-814.

O'Neil, J. R., Clayton, R. N., and Mayeda, T. K., 1969, Oxygen isotope fractionation in divalent metal carbonates: The Journal of Chemical Physics, v. 51, no. 12, p. 5547-5558.

Ota, Y., Inui, S., Iwashita, T., Kasuga, T., and Abe, Y., 1995, Preparation of aragonite whiskers: Journal of the American Ceramic Society, v. 78, no. 7, p. 1983-1984.

Paris, G., Fehrenbacher, J. S., Sessions, A. L., Spero, H. J., and Adkins, J. F., 2014, Experimental determination of carbonate-associated sulfate δ34S in planktonic foraminifera shells: Geochemistry, Geophysics, Geosystems, v. 15, no. 4, p. 1452-1461.

Pascual-Cebrian, E., Götz, S., Bover-Arnal, T., Skelton, P. W., Gili, E., Salas, R., and Stinnesbeck, W., 2016, Calcite/aragonite ratio fluctuations in Aptian rudist bivalves: Correlation with changing temperatures: Geology, v. 44, no. 2, p. 135-138.

Pearce, C. R., Saldi, G. D., Schott, J., and Oelkers, E. H., 2012, Isotopic fractionation during congruent dissolution, precipitation and at equilibrium: Evidence from Mg isotopes: Geochimica et Cosmochimica Acta, v. 92, p. 170-183.

Pingitore, N. E., Meitzner, G., and Love, K. M., 1995, Identification of sulfate in natural carbonates by x-ray absorption spectroscopy: Geochimica et Cosmochimica Acta, v. 59, no. 12, p. 2477-2483.

Plummer, L. N., 1979, Critical review of the kinetics of calcite dissolution and precipitation: Chemical Modeling in Aqueous Systems., p. 539-573.

Plummer, L. N., and Busenberg, E., 1982, The solubilities of calcite, aragonite and vaterite in CO2-H2O solutions between 0 and 90 C, and an evaluation of the aqueous model for the system CaCO3-CO2-H2O: Geochimica et Cosmochimica Acta, v. 46, no. 6, p. 1011-1040.

Pogge von Strandmann, P. A., Forshaw, J., and Schmidt, D., 2014, Modern and Cenozoic records of seawater magnesium from foraminiferal Mg isotopes: Biogeosciences, v. 11, no. 18, p. 5155-5168.

Poulton, S. W., Henkel, S., März, C., Urquhart, H., Flögel, S., Kasten, S., Damsté, J. S. S., and Wagner, T., 2015, A continental-weathering control on orbitally driven redox-nutrient cycling during Cretaceous Oceanic Anoxic Event 2: Geology, v. 43, no. 11, p. 963-966.

Qi, L., Li, J., and Ma, J., 2002, Biomimetic morphogenesis of calcium carbonate in mixed solutions of surfactants and double-hydrophilic block copolymers: Advanced Materials, v. 14, no. 4, p. 300-303.

Quigley, D., and Rodger, P. M., 2008, Free energy and structure of calcium carbonate nanoparticles during early stages of crystallization: The Journal of Chemical Physics, v. 128, no. 22, p. 221101.

Railsback, L. B., and Anderson, T. F., 1987, Control of Triassic seawater chemistry and temperature on the evolution of post-Paleozoic aragonite-secreting faunas: Geology, v. 15, no. 11, p. 1002-1005.

Raiteri, P., and Gale, J. D., 2010, Water is the key to nonclassical nucleation of amorphous calcium carbonate: Journal of the American Chemical Society, v. 132, no. 49, p. 17623-17634.

Raven, J., Caldeira, K., Elderfield, H., Hoegh-Guldberg, O., Liss, P., Riebesell, U., Shepherd, J., Turley, C., and Watson, A., 2005, Ocean acidification due to increasing atmospheric carbon dioxide, The Royal Society.

Reynaud, S., Ferrier-Pagès, C., Meibom, A., Mostefaoui, S., Mortlock, R., Fairbanks, R., and Allemand, D., 2007, Light and temperature effects on Sr/Ca and Mg/Ca ratios in the scleractinian coral Acropora sp: Geochimica et Cosmochimica Acta, v. 71, no. 2, p. 354-362.

Ridgwell, A., and Zeebe, R. E., 2005, The role of the global carbonate cycle in the regulation and evolution of the Earth system: Earth and Planetary Science Letters, v. 234, no. 3, p. 299-315.

Ries, J. B., Cohen, A. L., and McCorkle, D. C., 2009, Marine calcifiers exhibit mixed responses to CO2-induced ocean acidification: Geology, v. 37, no. 12, p. 1131-1134.

Robert V. Demicco, T. K. L., Lawrence A. Hardie, and Ronald J. Spencer, 2005, Model of seawater composition for the Phanerozoic: Geology, v. 33, no. 11, p. 877-880.

Rodriguez-Blanco, J., Shaw, S., and Benning, L., 2008, How to make 'stable'ACC: protocol and preliminary structural characterization: Mineralogical Magazine, v. 72, no. 1, p. 283-286.

Rodriguez-Blanco, J. D., Shaw, S., and Benning, L. G., 2011, The kinetics and mechanisms of amorphous calcium carbonate (ACC) crystallization to calcite, via vaterite: Nanoscale, v. 3, no. 1, p. 265-271.

Rodriguez-Blanco, J. D., Shaw, S., Bots, P., Roncal-Herrero, T., and Benning, L. G., 2012, The role of pH and Mg on the stability and crystallization of amorphous calcium carbonate: Journal of Alloys and Compounds, v. 536, p. S477-S479.

Rosenthal, Y., Boyle, E. A., and Slowey, N., 1997, Temperature control on the incorporation of magnesium, strontium, fluorine, and cadmium into benthic foraminiferal shells from Little Bahama Bank: Prospects for thermocline paleoceanography: Geochimica et Cosmochimica Acta, v. 61, no. 17, p. 3633-3643.

Saenger, C., and Wang, Z., 2014, Magnesium isotope fractionation in biogenic and abiogenic carbonates: implications for paleoenvironmental proxies: Quaternary Science Reviews, v. 90, p. 1-21.

Sandberg, P. A., 1983a, An oscillating trend in Phanerozoic non-skeletal carbonate mineralogy: Nature, v. 305, no. 5929, p. 19-22.

-, 1983b, An oscillating trend in Phanerozoic non-skeletal carbonate mineralogy: Nature, v. 305, p. 19.

Sandberg, P. A., 1985, Nonskeletal Aragonite and pCO2 in the Phanerozoic and Proterozoic, The Carbon Cycle and Atmospheric CO2: Natural Variations Archean to Present, p. 585-594.

Sha, F., Zhu, N., Bai, Y., Li, Q., Guo, B., Zhao, T., Zhang, F., and Zhang, J., 2016, Controllable synthesis of various CaCO3 morphologies based on a CCUS idea: ACS Sustainable Chemistry & Engineering, v. 4, no. 6, p. 3032-3044.

Smeets, P. J., Cho, K. R., Kempen, R. G., Sommerdijk, N. A., and De Yoreo, J. J., 2015, Calcium carbonate nucleation driven by ion binding in a biomimetic matrix revealed by in situ electron microscopy: Nature materials, v. 14, no. 4, p. 394.

Spencer, R., and Hardie, L., 1990, Control of seawater composition by mixing of river waters and mid-ocean ridge hydrothermal brines: Fluid-mineral interactions: A tribute to HP Eugster: Geochemical Society Special Publication, v. 19, p. 409-419.

Stack, A. G., and Grantham, M. C., 2010, Growth Rate of Calcite Steps As a Function of Aqueous Calcium-to-Carbonate Ratio: Independent Attachment and Detachment of Calcium and Carbonate Ions: Crystal Growth & Design, v. 10, no. 3, p. 1409-1413.

Stanley, S. M., 2006, Influence of seawater chemistry on biomineralization throughout phanerozoic time: Paleontological and experimental evidence: Palaeogeography, Palaeoclimatology, Palaeoecology, v. 232, no. 2, p. 214-236.

Stanley, S. M., and Hardie, L. A., 1998, Secular oscillations in the carbonate mineralogy of reef-building and sediment-producing organisms driven by tectonically forced shifts in seawater chemistry: Palaeogeography, Palaeoclimatology, Palaeoecology, v. 144, no. 1, p. 3-19.

Stephens, C. J., Ladden, S. F., Meldrum, F. C., and Christenson, H. K., 2010, Amorphous calcium carbonate is stabilized in confinement: Advanced Functional Materials, v. 20, no. 13, p. 2108-2115.

Tai, C. Y., and Chen, F. B., 1998, Polymorphism of CaCO3, precipitated in a constant-composition environment: AIChE Journal, v. 44, no. 8, p. 1790-1798.

Takano, B., 1985, Geochemical implications of sulfate in sedimentary carbonates: Chemical Geology, v. 49, no. 4, p. 393-403.

Tester, C. C., Brock, R. E., Wu, C.-H., Krejci, M. R., Weigand, S., and Joester, D., 2011, In vitro synthesis and stabilization of amorphous calcium carbonate (ACC) nanoparticles within liposomes: CrystEngComm, v. 13, no. 12, p. 3975-3978.

Tester, C. C., and Joester, D., 2013, Precipitation in liposomes as a model for intracellular biomineralization, Methods in enzymology, Volume 532, Elsevier, p. 257-276.

Tester, C. C., Whittaker, M. L., and Joester, D., 2014, Controlling nucleation in giant liposomes: Chemical Communications, v. 50, no. 42, p. 5619-5622.

Tester, C. C., Wu, C.-H., Weigand, S., and Joester, D., 2012, Precipitation of ACC in liposomes—a model for biomineralization in confined volumes: Faraday Discussions, v. 159, p. 345-356.

Tribello, G. A., Bruneval, F., Liew, C., and Parrinello, M., 2009, A Molecular Dynamics Study of the Early Stages of Calcium Carbonate Growth: The Journal of Physical Chemistry B, v. 113, no. 34, p. 11680-11687.

Videtich, P. E., 1985, Electron Microprobe Study of Mg Distribution in Recent Mg Calcites and Recrystallized Equivalents from the Pleistocene and Tertiary: Journal of Sedimentary Research, v. 55, no. 3, p. 421-429.

Volodymyr M. Kovalevich, Tadeusz Marek Peryt, and Oleg I. Petrichenko, 1998, Secular Variation in Seawater Chemistry during the Phanerozoic as Indicated by Brine Inclusions in Halite: The Journal of Geology, v. 106, no. 6, p. 695-712.

Wada, N., Yamashita, K., and Umegaki, T., 1995, Effects of divalent cations upon nucleation, growth and transformation of calcium carbonate polymorphs under conditions of double diffusion: Journal of Crystal Growth, v. 148, no. 3, p. 297-304.

Wallmann, K., 2001, Controls on the cretaceous and cenozoic evolution of seawater composition, atmospheric CO2 and climate: Geochimica et Cosmochimica Acta, v. 65, no. 18, p. 3005-3025.

Walsh, D., Lebeau, B., and Mann, S., 1999, Morphosynthesis of calcium carbonate (vaterite) microsponges: Advanced Materials, v. 11, no. 4, p. 324-328.

Walter, L. M., 1983, An oscillating trend in Phanerozoic non-skeletal carbonate mineralogy: Nature, v. 305, p. 19.

-, 1986, Relative efficiency of carbonate dissolution and precipitation during diagenesis: a progress report on the role of solution chemistry.

Wang, J., and Becker, U., 2009, Structure and carbonate orientation of vaterite (CaCO3): American Mineralogist, v. 94, no. 2-3, p. 380-386.

Wang, Z., Hu, P., Gaetani, G., Liu, C., Saenger, C., Cohen, A., and Hart, S., 2013, Experimental calibration of Mg isotope fractionation between aragonite and seawater: Geochimica et Cosmochimica Acta, v. 102, p. 113-123.

Wei, G., Sun, M., Li, X., and Nie, B., 2000, Mg/Ca, Sr/Ca and U/Ca ratios of a porites coral from Sanya Bay, Hainan Island, South China Sea and their

relationships to sea surface temperature: Palaeogeography, Palaeoclimatology, Palaeoecology, v. 162, no. 1–2, p. 59-74.

Weiner, S., and Dove, P. M., 2003, An Overview of Biomineralization Processes and the Problem of the Vital Effect: Reviews in Mineralogy and Geochemistry, v. 54, no. 1, p. 1-29.

Wilkinson, B. H., and Algeo, T. J., 1989, Sedimentary carbonate record of calcium-magnesium cycling: American Journal of Science, v. 289, no. 10, p. 1158-1194.

Wilkinson, B. H., Buczynski, C., and Owen, R. M., 1984, Chemical control of carbonate phases; implications from Upper Pennsylvanian calcite-aragonite ooids of southeastern Kansas: Journal of Sedimentary Research, v. 54, no. 3, p. 932-947.

Wilkinson, B. H., and Given, R. K., 1986, Secular Variation in Abiotic Marine Carbonates: Constraints on Phanerozoic Atmospheric Carbon Dioxide Contents and Oceanic Mg/Ca Ratios: The Journal of Geology, v. 94, no. 3, p. 321-333.

Wilkinson, B. H., Owen, R. M., and Carroll, A. R., 1985, Submarine hydrothermal weathering, global eustasy, and carbonate polymorphism in Phanerozoic marine oolites: Journal of Sedimentary Research, v. 55, no. 2, p. 171-183.

Wortmann, U. G., and Chernyavsky, B. M., 2007, Effect of evaporite deposition on Early Cretaceous carbon and sulphur cycling: Nature, v. 446, no. 7136, p. 654-656.

Yasushi, K., 1962, The Behavior of Various Inorganic Ions in the Separation of Calcium Carbonate from a Bicarbonate Solution: Bulletin of the Chemical Society of Japan, v. 35, no. 12, p. 1973-1980.

Young, E. D., and Galy, A., 2004, The Isotope Geochemistry and Cosmochemistry of Magnesium: Reviews in Mineralogy and Geochemistry, v. 55, no. 1, p. 197-230.

Yu, J., Lei, M., Cheng, B., and Zhao, X., 2004, Effects of PAA additive and temperature on morphology of calcium carbonate particles: Journal of Solid State Chemistry, v. 177, no. 3, p. 681-689.

Yu, K.-F., Zhao, J.-X., Wei, G.-J., Cheng, X.-R., Chen, T.-G., Felis, T., Wang, P.-X., and Liu, T.-S., 2005, δ18O, Sr/Ca and Mg/Ca records of Porites lutea corals from Leizhou Peninsula, northern South China Sea, and their applicability as paleoclimatic indicators: Palaeogeography, Palaeoclimatology, Palaeoecology, v. 218, no. 1–2, p. 57-73.

Zhao, X., Guo, C., Han, Y., Che, Z., Wang, Y., Wang, X., Chai, X., Wu, H., and Liu, G., 2017, Ocean acidification decreases mussel byssal attachment strength and induces molecular byssal responses: Marine Ecology Progress Series, v. 565, p. 67-77.

Zhuravlev, A. Y., and Wood, R. A., 2009, Controls on carbonate skeletal mineralogy: Global CO2 evolution and mass extinctions: Geology, v. 37, no. 12, p. 1123-1126.

Zimmermann, H., 2000, Tertiary seawater chemistry; implications from primary fluid inclusions in marine halite: American Journal of Science, v. 300, no. 10, p. 723-767.

Appendix A
Supplementary Information for Chapter 4

A.1. Summary of mineralogical and chemical composition of the various $CaCO_3$ polymorphs obtained from all constant addition experiments.

Powder X-ray diffraction (XRD) analyses of the solids were performed using a Bruker D8 X-Ray Diffractometer (Cu kα_1) with a silicon internal standard. The detection limit of the X-ray diffraction technique is ≈ 3% of the mass of the analysed sample.

Table A. 1: *Results from XRD and Rietveld refinement analyses of the solid reaction products from all constant addition experiments (Medeiros et al.) carried out at various initial solution compositions.*

T (°C)	Solution chemistry		Polymorph distribution		
	Mg:Ca (molar)	SO_4 (mM)	Calcite (%)	Aragonite (%)	Vaterite (%)
5	0.00	5	54	0	46
5	0.00	15	18	0	82
5	0.00	36	0	27	73
5	0.00	44	0	48	52
5	0.00	60	0	67	33
5	0.00	110	0	80	20
5	0.22	0	89	0	11
5	0.22	5	61	0	39
5	0.22	10	11	20	69
5	0.22	15	6	32	62
5	0.22	36	0	67	33

T (°C)	Solution chemistry		Polymorph distribution		
	Mg:Ca (molar)	SO_4 (mM)	Calcite (%)	Aragonite (%)	Vaterite (%)
5	0.35	0	79	0	21
5	0.35	5	56	3	41
5	0.45	0	81	19	0
5	0.55	0	67	20	13
5	0.55	5	6	50	44
5	0.55	10	6	54	40
5	0.55	15	11	52	37
5	0.55	28	2	69	29
5	0.55	44	0	61	39
5	0.55	60	0	54	46
5	0.55	80	0	55	45
5	0.65	0	57	33	10
5	0.65	5	5	72	23
5	0.65	10	6	55	39
5	0.65	15	8	58	34
5	0.65	28	6	59	35
5	0.65	60	0	67	33
5	0.75	0	48	52	0
5	1.00	0	11	89	0
5	1.00	28	0	82	18
5	5.20	0	0	100	0
5	5.20	110	0	100	0

T (°C)	Solution chemistry		Polymorph distribution		
	Mg:Ca (molar)	SO_4 (mM)		Mg:Ca (molar)	SO_4 (mM)
21	0.00	5	65	0	35
21	0.00	10	90	0	10
21	0.00	15	18	0	82
21	0.00	36	6	20	74
21	0.00	44	0	42	58
21	0.00	60	0	70	30
21	0.00	110	0	85	15
21	0.10	15	54	46	0
21	0.10	36	0	83	17
21	0.10	44	0	87	13
21	0.10	60	0	88	12
21	0.10	80	0	100	0
21	0.22	0	93	7	0
21	0.22	5	55	45	0
21	0.22	10	35	65	0
21	0.22	15	4	96	0
21	0.22	28	0	100	0
21	0.22	36	0	100	0
21	0.35	0	83	17	0
21	0.35	5	27	73	0
21	0.35	15	0	100	0
21	0.45	0	66	34	0

T (°C)	Solution chemistry		Polymorph distribution		
	Mg:Ca (molar)	SO_4 (mM)		Mg:Ca (molar)	SO_4 (mM)
21	0.55	0	63	37	0
21	0.55	5	28	72	0
21	0.55	10	19	81	0
21	0.55	15	0	100	0
21	0.55	28	0	100	0
21	0.55	60	0	100	0
21	0.55	80	0	100	0
21	0.65	0	44	56	0
21	0.65	5	21	79	0
21	0.65	10	0	100	0
21	0.65	15	0	100	0
21	0.65	28	0	100	0
21	0.65	60	0	100	0
21	0.75	0	7	93	0
21	0.85	5	0	100	0
21	1.00	0	0	100	0
21	1.00	28	0	100	0
21	5.20	0	0	100	0
21	5.20	110	0	100	0
35	0.00	5	100	0	0
35	0.00	10	78	0	12
35	0.00	15	43	0	57

T (°C)	Solution chemistry		Polymorph distribution		
	Mg:Ca (molar)	SO_4 (mM)		Mg:Ca (molar)	SO_4 (mM)
35	0.00	36	16	34	50
35	0.00	44	4	66	30
35	0.00	60	0	85	15
35	0.00	110	0	94	6
35	0.10	36	0	100	0
35	0.10	44	0	100	0
35	0.10	60	0	100	0
35	0.10	80	0	100	0
35	0.22	0	87	13	0
35	0.22	5	84	16	0
35	0.22	10	13	87	0
35	0.22	15	4	96	0
35	0.22	28	0	100	0
35	0.22	36	0	100	0
35	0.35	0	70	30	0
35	0.35	15	0	100	0
35	0.45	0	63	37	0
35	0.55	0	8	92	0
35	0.55	5	3	97	0
35	0.55	10	0	100	0
35	0.55	15	0	100	0
35	0.55	28	0	100	0

T (°C)	Solution chemistry		Polymorph distribution		
	Mg:Ca (molar)	SO_4 (mM)		Mg:Ca (molar)	SO_4 (mM)
35	0.55	60	0	100	0
35	0.55	80	0	100	0
35	0.65	0	7	93	0
35	0.65	5	0	100	0
35	0.65	10	0	100	0
35	0.65	15	0	100	0
35	0.65	28	0	100	0
35	0.65	60	0	100	0
35	0.75	0	0	100	0
35	0.85	5	0	100	0
35	1.00	0	0	100	0
35	1.00	28	0	100	0
35	5.20	0	0	100	0
35	5.20	110	0	100	0

Table A. 2:*Results of polymorph distributions from XRD and composition from EPMA measurements of the solid reaction products from CAE carried out at various initial solution compositions and temperatures.*

T (°C)	Solution chemistry		Polymorph distribution			Solid composition					
						Calcite		Aragonite		Vaterite	
	Mg:Ca (molar)	SO_4 (mM)	Calcite (%)	Aragonite (%)	Vaterite (%)	$Mg/CaCO_3$ (%)	$S/CaCO_3$ (%)	$Mg/CaCO_3$ (%)	$S/CaCO_3$ (%)	$Mg/CaCO_3$ (%)	$S/CaCO_3$ (%)
5	0.22	0	89	0	11	0.17	0.00	---	---	0.00	0.00
5	0.22	5	61	0	39	0.19	0.59	---	---	0.00	0.20
5	0.22	10	11	20	69	0.15	0.98	0.00	0.14*	0.00	0.14*
5	0.22	15	6	32	62	0.15	1.11	0.00	0.27*	0.00	0.27*
5	0.55	0	67	20	13	0.40	0.00	0.00	0.00	0.00	0.00
5	0.55	5	6	50	44	0.38	0.59	0.00	0.15*	0.00	0.15*
5	0.55	10	6	54	40	0.51	0.79	0.00	0.23*	0.00	0.23*
5	0.55	15	11	52	37	0.56	0.83	0.00	0.27*	0.00	0.27*
5	0.65	0	57	33	10	0.56	0.00	0.00	0.00	0.00	0.00
21	0.00	5	65	0	35	0.00	0.59	---	---	0.00	0.23
21	0.00	10	90	0	10	0.00	0.93	---	---	0.00	0.32

T (°C)	Solution chemistry		Polymorph distribution			Solid composition					
						Calcite		Aragonite		Vaterite	
	Mg:Ca (molar)	SO_4 (mM)	Calcite (%)	Aragonite (%)	Vaterite (%)	$Mg/CaCO_3$ (%)	$S/CaCO_3$ (%)	$Mg/CaCO_3$ (%)	$S/CaCO_3$ (%)	$Mg/CaCO_3$ (%)	$S/CaCO_3$ (%)
21	0.00	15	18	0	82	0.00	1.17	---	---	0.00	0.39
21	0.10	15	54	46	0	0.20	0.91	0.00	0.33	---	---
21	0.22	0	93	7	0	0.39	0.00	0.00	0.00	---	---
21	0.22	5	55	45	0	0.39	0.52	0.00	0.30	---	---
21	0.22	10	35	65	0	0.41	0.96	0.00	0.18	---	---
21	0.22	15	4	96	0	0.47	0.82	0.00	0.23	---	---
21	0.55	0	63	37	0	0.95	0.00	0.00	0.00	---	---
21	0.55	5	28	72	0	0.96	0.42	0.00	0.12	---	---
21	0.55	10	19	81	0	0.80	0.77	0.00	0.21	---	---
21	0.55	15	16	84	0	0.76	0.85	0.00	0.25	---	---
21	0.65	0	44	56	0	1.46	0.00	0.00	0.00	---	---
35	0.22	0	87	13	0	0.65	0.00	0.00	0.00	---	---

T (°C)	Solution chemistry		Polymorph distribution			Solid composition					
						Calcite		Aragonite		Vaterite	
	Mg:Ca (molar)	SO_4 (mM)	Calcite (%)	Aragonite (%)	Vaterite (%)	$Mg/CaCO_3$ (%)	$S/CaCO_3$ (%)	$Mg/CaCO_3$ (%)	$S/CaCO_3$ (%)	$Mg/CaCO_3$ (%)	$S/CaCO_3$ (%)
35	0.22	5	84	16	0	0.17	0.50	0.00	0.20	---	---
35	0.22	10	13	87	0	0.57	0.67	0.00	0.14	---	---
35	0.22	15	4	96	0	0.38	0.75	0.00	0.22	---	---
35	0.55	0	8	92	0	1.83	0.00	0.00	0.00	---	---
35	0.65	0	7	93	0	2.10	0.00	0.00	0.00	---	---

*Data from analysis of aragonite-vaterite mixtures. Due to the small particle size of aragonite and vaterite and because both polymorphs always occurred as a mixture of phases, it was not possible to accurately determine the sulfate contents in small individual grains.

A.2. Ageing experiments

Three ageing experiments were performed in order to test whether the small differences in the predominant polymorph distribution observed with temperature (see Figure 4.3 and Table A.1 and A.2) were due to differences in temperature itself or due to kinetic effects. For selected experimental conditions, the precipitates were allowed to age in the original solution for up to 21 days, while continuing to shake the reactors at 270 rpm and keeping the solutions at the same temperature at which the precipitations were carried out. The experiments at 21 and 35°C described in the main document where run for 96 hours (see Figure 4.3) and the solid reaction products were either, pure phases (calcite or aragonite) or a mixture of two phases (calcite + aragonite, calcite + vaterite or aragonite + vaterite). When we evaluated the polymorph distribution by XRD at the end of the ageing experiments, the results indicated that the polymorphic composition of the samples grown at 21 and 35°C did not change even after 21 days of ageing (Table A.3). This suggests that these polymorph distributions and compositions are representative of the solubility controlling phase for each experimental condition. However, in experiments at 5°C, which also contained high proportions of vaterite, the aging lead to part of the vaterite present after 96 hours to be transformed into a more stable phase (calcite or aragonite) during ageing. This implied that at 5°C, longer reaction periods are needed to reach an equilibrium polymorph distribution, yet the predominant polymorph produced at 21 and 35°C remain the same. Thus, considering a geological time scale, we predict that for a specific solution chemistry (Mg:Ca ratio and SO_4 concentration), the predominant polymorph distribution would not vary with changes in temperature.

Table A. 3: *Polymorph distribution in the solid reaction products obtained 96 hours after injection and after 21 days of ageing post injection.*

T (°C)	Solution chemistry		Polymorph distribution Constant addition experiments			Polymorph distribution Ageing experiments (21 days)		
	Mg:Ca (molar)	**SO_4 (mM)**	**Calcite (%)**	**Aragonite (%)**	**Vaterite (%)**	**Calcite (%)**	**Aragonite (%)**	**Vaterite (%)**
5	0.22	10.60	11	20	69	28	32	40
21	0.65	5.00	2	98	0	3	97	0
35	0.22	10.60	13	87	0	12	88	0

A.3. ICP-OES analysis. Validation of the constant addition method.

Throughout each experiment, 5 sample aliquots (5 ml) were extracted from the reacting solution at various time steps. Each sample was immediately filtered through a 0.2 μm syringe filter, and the resulting fluids were diluted and acidified with HCl 1%. ICP-OES analysis of these sample aliquots clearly documented that as intended the main solution chemistry remained constant (± 5%) throughout the constant addition experiments (Table A.4). In Table A.4, only one set of time resolved experiment is shown as an example because the same behaviour was observed in all the cases. The detection limits of our ICP-OES analysis were approximately 0.007 ppm for Mg, 0.04 for Ca ppm and 0.005 ppm for S. The analytical uncertainty was ≤ 3%.

Table A. 4: *Example of ICP-OES data of the sample aliquots extracted during an experiment with an initial calculated solution of: [Ca] = 400.78 ppm (10 mM), [Mg] = 53.47 ppm (Mg:Ca= 0.22 molar) and [S]= 480.98 ppm (SO_4= 15 mM).*

Reaction time (hours)	Solution chemistry		
	Ca (ppm)	Mg (ppm)	S (ppm)
0	405.10	53.08	479.54
5	410.02	53.35	470.68
15	412.50	52.76	468.47
30	416.40	52.43	461.83
48	415.25	52.55	459.25

A.4. Electron probe microanalyses (EPMA)

During our electron probe microanalysis (EPMA) we faced some difficulties such as having the three $CaCO_3$ polymorphs (calcite, aragonite and vaterite) present in the sample and some of the crystals being very small, sometimes of a size closed to the defocused spot at which the electron probe instrument was operated at (Figure A.1).

The detection limits of our EPMA were approximately 312 ppm for Ca, 164 ppm for Mg, 272 ppm for S and 345 ppm for Si. To have a reliable statistical study at least 10 different crystals of each polymorph present in each sample were analysed. Those analyses with anomalously high concentrations of Si were assumed to have been contaminated by matrix silicates and so were removed from the datasets.

Electron probe micro-analysis data from samples formed at high temperature (35°C) and especially those from the experiments at high temperature and high Mg:Ca ratios (Mg:Ca≥ 0.55) or/and seawater SO_4 concentrations (SO_4≥ 10.6 mM), show higher errors than the ones from samples grown at lower temperatures, or lower Mg:Ca ratios and SO_4 concentrations (Figure 4.2b, 4.2c in main text & Figure A.2).

This is due to a combination of two main factors: (a) a low proportion of calcite in the sample as Mg:Ca ratio and SO_4 concentration in solution increases and (b) smaller $CaCO_3$ crystal sizes as temperature increased (Figure A.1). In an experiment

carried out at Mg:Ca= 0.22, SO4= 15 mM and 35°C, calcite particle sizes were about 1 μm or smaller which is close to the 1 μm defocused spot at which the electron probe instrument was operated at. Thus, it is quite likely that a mixture of calcite and aragonite particles were present in the interaction volume and thus analyses volume, leading to the lower values of the Mg or S partition coefficients and to higher errors (Figure A.2).

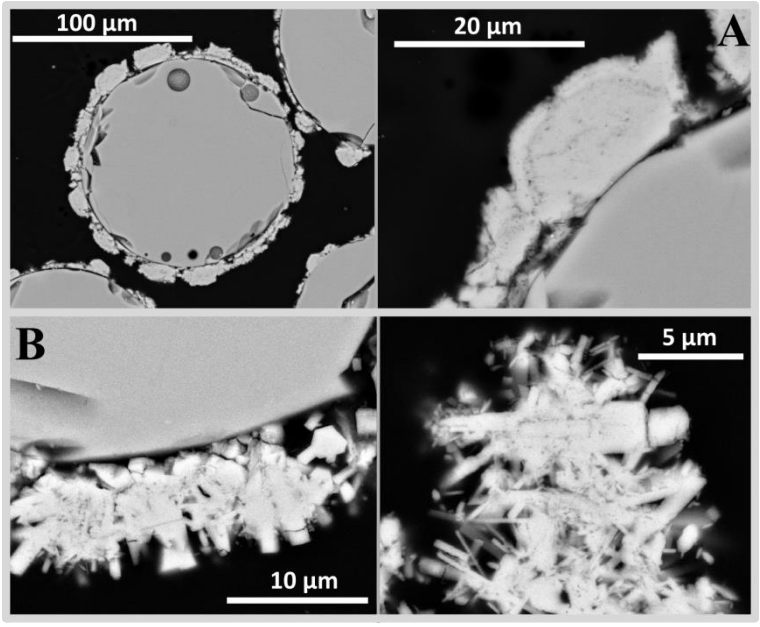

Figure A. 1: *SEM images of the polished sample grown at: a) Mg:Ca= 0.22, SO_4= 5 mM and 21°C; b) Mg:Ca= 0.22, SO_4= 15 mM and 35°C. Note the marked calcite crystal size differences as a function of SO_4 concentration in solution and temperature.*

Our EPMA and ICP-OES data also confirmed that the influence of temperature on SO_4 incorporation into calcite is insignificant when seawater SO_4 concentration is ≤5 mM. Nevertheless, when SO_4 concentration in seawater is ≥10 mM, the influence of temperature on SO_4 incorporation into calcite is quite denoting, decreasing the SO_4 content in calcite about 65% when temperature increases from 5 to 35°C (Figure 4.2 D and Figure A.2 A).

The incorporation of SO_4 into aragonite was almost negligible (Figure A.2 B & C). In Figures A.2 B and C is possible to observe how SO_4 incorporation into aragonite slightly decreases as temperature increases but because this decrease is almost within the analytical error, it cannot be considered. Overall, SO_4 incorporation into calcite and aragonite increases as seawater SO_4 concentration increases and decreases as seawater Mg:Ca ratio increases (Figure A.2).

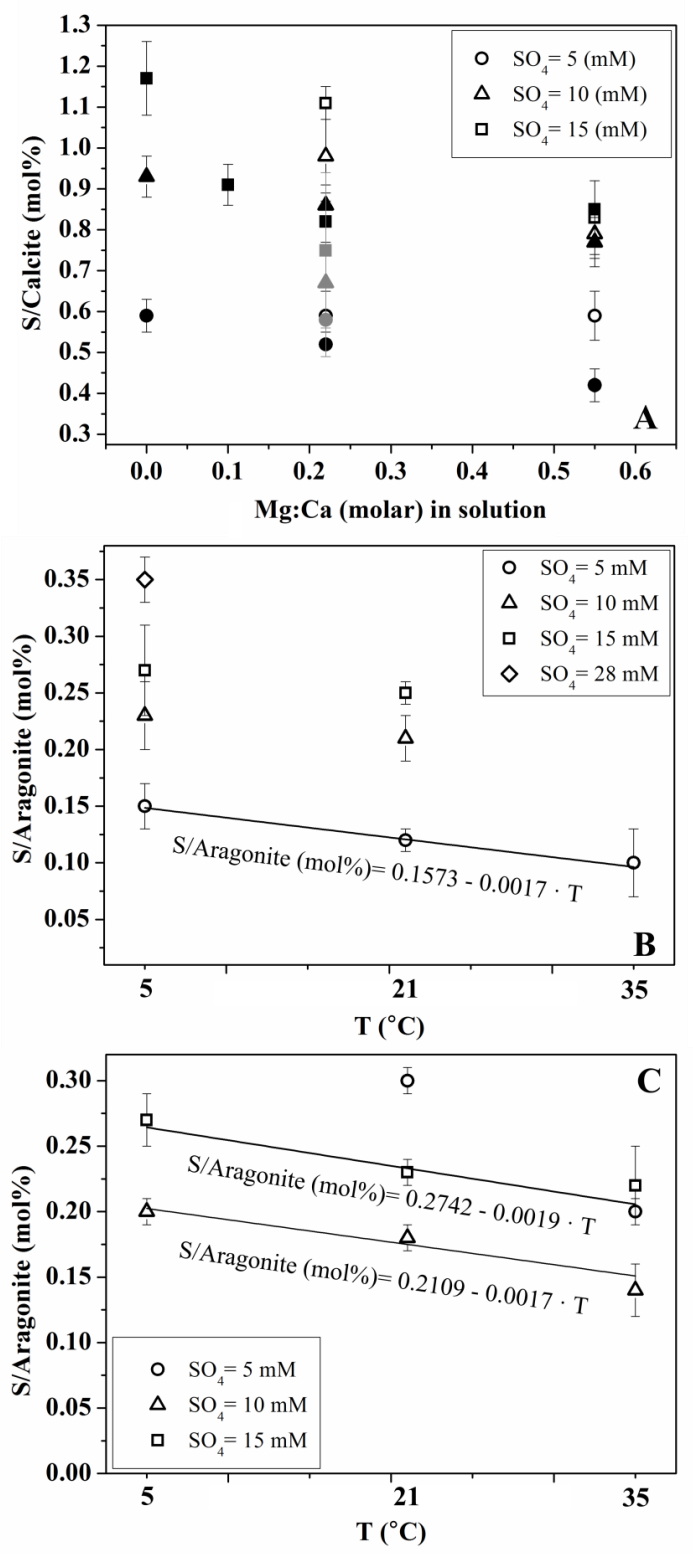

Figure A. 2: *S incorporation into calcite and aragonite; A) S in calcite for seawater Mg:Ca= 0.22 and as a function of temperature and SO_4 concentration; B) S in calcite as a function of temperature, seawater Mg:Ca ratio and seawater SO_4 concentration; open black symbols represent data at 5ºC, closed black symbols represent data at 21ºC and closed grey symbols represent data from experiments at 35ºC; C & D) S in aragonite as a function of temperature and seawater SO_4 concentration and for seawater Mg:Ca= 0.22 and Mg:Ca= 0.55 respectively.*

A.5. Aragonite-calcite co-existence field

A quantitative evaluation of the dependence of the aragonite proportion in our solid reaction products as a function of solution Mg:Ca ratio, SO_4 concentration and temperature, showed that the aragonite precipitation field becomes wider with increasing SO_4 concentration; in contrary, the calcite and aragonite-calcite co-precipitation fields become narrower (Figure A.3). The data in Figure A.3 reveal a clear inter-dependence between aragonite proportion and temperature. This inter-dependence is at high SO_4 concentrations and particularly at 5°C and 21°C. However, our data from the ageing experiments (Table A.3) revealed that at 5°C vaterite transforms into either calcite or aragonite over longer time periods. Thus, considering a geological time scale, it is clear that the effect of temperature on the $CaCO_3$ polymorph distribution is almost negligible and that the predicted boundary between the calcite-aragonite co-existence and the aragonite fields only vary by ~ ± 0.1 units in Mg:Ca ratio when temperature changes from 5 to 35°C. However, the plots below clearly show that sulfate has indeed a bigger effect on the calcite, calcite-aragonite coexistence and aragonite field sizes.

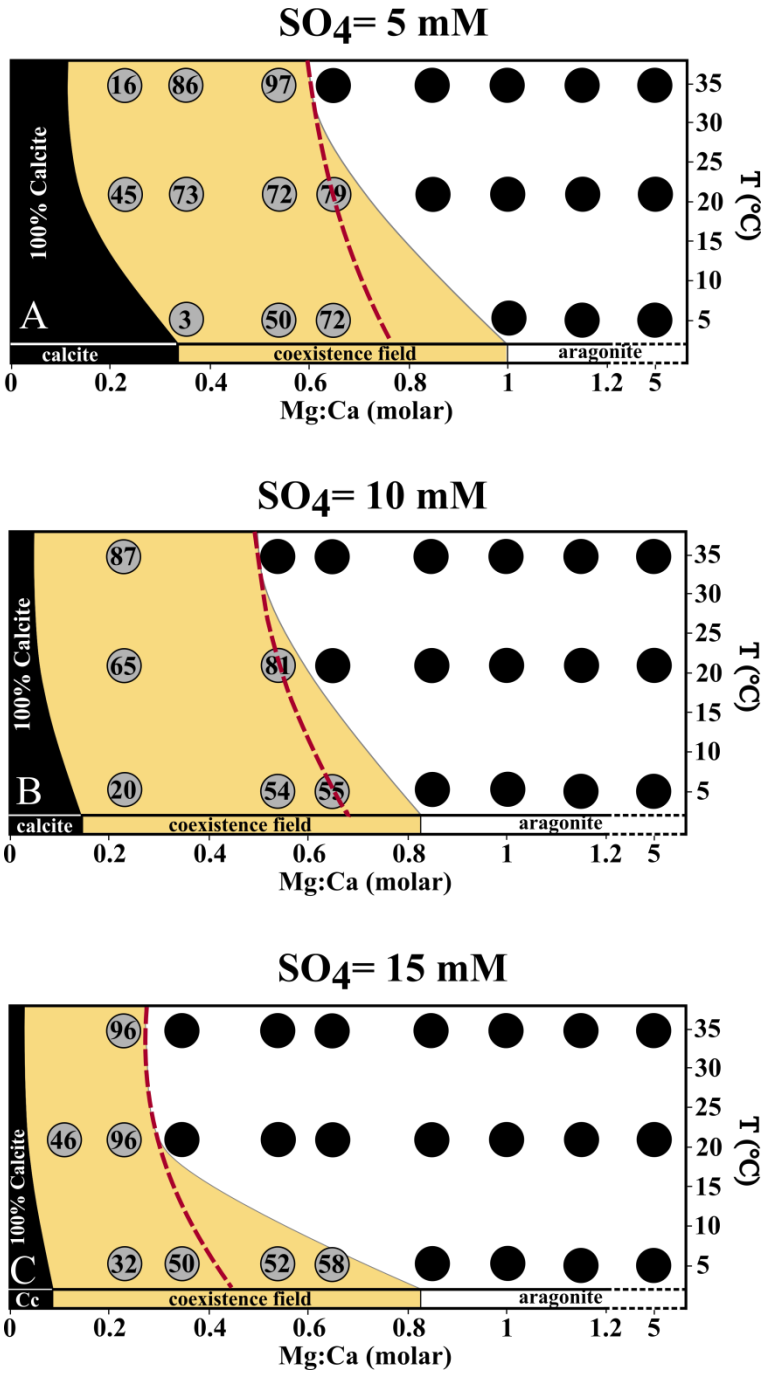

Figure A. 3: *Average proportion of aragonite in the solid reaction products as a function of Mg:Ca ratio, temperature and SO_4 concentration and with; a) SO_4= 5 mM; b) SO_4= 10 mM; c) SO_4= 15 mM. Numbers in circles represent the proportion of aragonite present in each sample; black circles represent 100 % aragonite; black areas represent the calcite field, yellow areas represent the aragonite-calcite coexistence field of the current study; dashed lines indicate position of the predicted boundary between aragonite and calcite precipitation after ageing experiments.*

A.6. Flow rate and timescale of constant addition experiments

To test which injection flow rate and timescale lead to obtain the stable $CaCO_3$ phase/s for our experimental conditions, several constant addition experiments were performed at either, 0.5 ml/h for 48 and 96 hours and 1.0 ml/h for 48.

A comparison of the mineral composition of the solid samples obtained from experiments carried out at an injection flow rate of 0.5 ml/h and for 48 and 96 hours showed:

- Most of the solid samples from experiments performed for 48 hours contained high proportions of vaterite, which is a metastable phase. However, solid samples from experiments carried out for 96 hours did not present vaterite at all or had a very low proportion depending on the experimental condition. This decrease of vaterite proportion turned into an increase of either calcite and aragonite according to the experimental condition. These results indicated that the mineral composition of the samples from the experiments performed at 0.5 ml/h flow rate and for 48 hours was not the stable one.

- In order to decrease the experiment timescale, we also carried out experiments at 1.0 ml/h injection flow rate and for 48 hours. In this way, the total injection volume is the same than injecting at a flow rate of 0.5 ml/h for 96 hours. The results from these test experiments showed that for the same experimental condition, the mineral composition was similar when the injection flow rate was doubled and the timescale was made half.

To test whether the obtained mineral composition of the solid samples was the stable one or not, we carried out ageing experiments (see A.2). The precipitates were allowed to age in the original solution for up to 21 days, while continuing to shake the reactors at 270 rpm and keeping the solutions at the same temperature at which the precipitations were carried out. XRD analysis of the solid samples revealed that the mineral composition of our samples kept almost constant after ageing (± 5-7%).

Appendix B

Supplementary Information for Chapter 5.

B.1. Summary of mineralogical and chemical composition of the various $CaCO_3$ polymorphs obtained from all constant addition experiments.

Powder X-ray diffraction (XRD) analyses of the solids were performed using a Bruker D8 X-Ray Diffractometer (Cu $k\alpha_1$) with a silicon internal standard. The detection limit of the X-ray diffraction technique is ≈ 3% of the mass of the analysed sample.

Table B. 1: *Results from XRD and Rietveld refinement analyses of the solid reaction products from all constant addition experiments (Medeiros et al.) carried out at various initial solution compositions and at a partial pressure of carbon dioxide (pCO_2) of 300, 1500 and 3000 ppm.*

pCO_2 (ppm)	Solution chemistry		Polymorph distribution		
	Mg:Ca (M)	SO_4 (mM)	Calcite (%)	Aragonite (%)	Vaterite (%)
400	0.00	5.0	65	0	35
400	0.00	10.0	90	0	10
400	0.00	15.0	18	0	82
400	0.00	36.0	6	20	74
400	0.00	44.0	0	42	58
400	0.00	60.0	0	70	30
400	0.00	110.0	0	85	15
400	0.10	15.0	54	46	0
400	0.10	36.0	0	83	17

pCO_2 (ppm)	Solution chemistry		Polymorph distribution		
	Mg:Ca (M)	SO_4 (mM)	Calcite (%)	Aragonite (%)	Vaterite (%)
400	010	44.0	0	87	13
400	0.10	60.0	0	88	12
400	0.10	80.0	0	100	0
400	0.22	0.0	93	7	0
400	0.22	5.0	55	45	0
400	0.22	10.0	35	65	0
400	0.22	15.0	4	96	0
400	0.22	28.0	0	100	0
400	0.22	36.0	0	100	0
400	0.22	44.0	0	100	0
400	0.22	60.0	0	100	0
400	0.35	0.0	83	17	0
400	0.35	5.0	27	73	0
400	0.35	15.0	0	100	0
400	0.45	0.0	66	34	0
400	0.55	0.0	63	37	0
400	0.55	5.0	28	72	0
400	0.55	10.0	19	81	0
400	0.55	15.0	0	100	0
400	0.55	28.0	0	100	0
400	0.65	0.0	44	56	0
400	0.65	5.0	21	79	0

pCO_2 (ppm)	Solution chemistry		Polymorph distribution		
	Mg:Ca (M)	SO_4 (mM)	Calcite (%)	Aragonite (%)	Vaterite (%)
400	0.65	10.0	0	100	0
400	0.65	15.0	0	100	0
400	0.75	0.0	7	93	0
400	0.85	5.0	0	100	0
400	1.00	0.0	0	100	0
1500	0.00	5.0	100	0	0
1500	0.00	10.0	79	0	21
1500	0.00	15.0	23	21	56
1500	0.00	28.0	0	36	64
1500	0.00	36.0	0	87	13
1500	0.10	2.5	95	5	0
1500	0.10	15.0	22	78	0
1500	0.10	28.0	0	100	0
1500	0.22	0.0	100	0	0
1500	0.22	5.0	59	41	0
1500	0.22	10.0	10	90	0
1500	0.35	0.0	96	4	0
1500	0.35	10.0	16	84	0
1500	0.35	15.0	0	100	0
1500	0.45	5.0	34	66	0
1500	0.45	10.0	0	100	0
1500	0.55	2.5	4	96	0

pCO_2 (ppm)	Solution chemistry		Polymorph distribution		
	Mg:Ca (M)	SO_4 (mM)	Calcite (%)	Aragonite (%)	Vaterite (%)
1500	0.65	0.0	68	32	0
1500	0.65	5.0	0	100	0
1500	0.85	0.0	7	93	0
1500	1.00	0.0	0	100	0
3000	0.00	5.0	100	0	0
3000	0.00	10.0	80	20	0
3000	0.00	15.0	7	93	0
3000	0.22	5.0	100	0	0
3000	0.22	10.0	3	97	0
3000	0.35	2.5	100	0	0
3000	0.35	5.0	41	59	0
3000	0.35	10.0	0	100	0
3000	0.45	2.5	100	0	0
3000	0.55	0.0	100	0	0
3000	0.55	2.5	37	63	0
3000	0.55	5.0	3	97	0
3000	0.55	28.8	0	100	0
3000	0.65	2.5	1	99	0
3000	0.65	5.0	0	100	0
3000	0.75	0.0	56	44	0
3000	0.85	0.0	6	94	0
3000	1.0	0.0	0	100	0

pCO_2 (ppm)	Solution chemistry		Polymorph distribution		
	Mg:Ca (M)	SO_4 (mM)		Mg:Ca (M)	SO_4 (mM)
3000	1.0	5.0	0	100	0
3000	1.5	0.0	0	100	0

Table B. 2:*Results of polymorph distributions from XRD and composition from EPMA measurements of the solid reaction products from CAE carried out at various initial solution compositions and pCO_2.*

	Solution chemistry		**Polymorph distribution**			**Solid composition**					
						Calcite		**Aragonite**		**Vaterite**	
pCO_2 (ppm)	**Mg:Ca (molar)**	**SO_4 (mM)**	**Calcite (%)**	**Aragonite (%)**	**Vaterite (%)**	**$Mg/CaCO_3$ (%)**	**$S/CaCO_3$ (%)**	**$Mg/CaCO_3$ (%)**	**$S/CaCO_3$ (%)**	**$Mg/CaCO_3$ (%)**	**$S/CaCO_3$ (%)**
400	0.00	5	65	0	35	0.00	0.59	---	---	0.00	0.23
400	0.00	10	90	0	10	0.00	0.93	---	---	0.00	0.32
400	0.00	15	18	0	82	0.00	1.17	---	---	0.00	0.39
400	0.10	15	54	46	0	0.20	0.91	0.00	0.33	---	---
400	0.22	0	93	7	0	0.39	0.00	0.00	0.00	---	---
400	0.22	5	55	45	0	0.39	0.52	0.00	0.15	---	---
400	0.22	10	35	65	0	0.41	0.96	0.00	0.18	---	---
400	0.22	15	4	96	0	0.47	0.82	0.00	0.23	---	---
400	0.22	36	0	100	0	---	---	0.00	0.38	---	---
400	0.35	0	83	17	0	0.47	0.00	0.00	0.00	---	---

pCO_2 (ppm)	Solution chemistry		Polymorph distribution			Solid composition					
						Calcite		Aragonite		Vaterite	
	Mg:Ca (molar)	SO_4 (mM)	Calcite (%)	Aragonite (%)	Vaterite (%)	$Mg/CaCO_3$ (%)	$S/CaCO_3$ (%)	$Mg/CaCO_3$ (%)	$S/CaCO_3$ (%)	$Mg/CaCO_3$ (%)	$S/CaCO_3$ (%)
400	0.35	15	0	100	0	---	---	0.00	0.21	---	---
400	0.55	0	63	37	0	0.95	0.00	0.00	0.00	---	---
400	0.55	5	28	72	0	0.96	0.42	0.00	0.12	---	---
400	0.55	10	19	81	0	0.80	0.77	0.00	0.21	---	---
400	0.55	15	16	84	0	0.76	0.85	0.00	0.25	---	---
400	0.55	28	0	100	0	---	---	0.00	0.40	---	---
400	0.65	0	44	56	0	1.46	0.00	0.00	0.00	---	---
1500	0.00	5	100	0	0	0.00	0.40	---	---	---	---
1500	0.00	10	79	0	21	0.00	0.72	---	---	0.00	0.34
1500	0.00	15	23	21	56	0.00	0.65	0.00	0.18*	0.00	0.18*
1500	0.22	0	100	0	0	0.32	0.00	---	---	---	---
1500	0.22	5	59	41	0	0.40	0.46	0.00	0.11	---	---

pCO_2 (ppm)	Solution chemistry		Polymorph distribution			Solid composition					
						Calcite		Aragonite		Vaterite	
	Mg:Ca (molar)	SO_4 (mM)	Calcite (%)	Aragonite (%)	Vaterite (%)	$Mg/CaCO_3$ (%)	$S/CaCO_3$ (%)	$Mg/CaCO_3$ (%)	$S/CaCO_3$ (%)	$Mg/CaCO_3$ (%)	$S/CaCO_3$ (%)
1500	0.22	10	10	90	0	0.40	0.56	0.00	0.11	---	---
1500	0.35	0	96	4	0	0.52	0.00	0.00	0.20	---	---
1500	0.35	10	16	84	0	---	---	0.00	0.16	---	---
1500	0.35	15	0	100	0	---	---	0.00	0.20	---	---
1500	0.45	5	34	66	0	0.64	0.40	0.00	0.08	---	---
1500	0.65	0	68	32	0	0.89	0.00	0.00	0.00	---	---
1500	0.85	0	7	93	0	1.33	0.00	0.00	0.00	---	---
3000	0.00	5	100	0	0	0.00	0.55	---	---	---	---
3000	0.00	10	80	20	0	0.00	0.53	---	---	---	---
3000	0.22	5	100	0	0	0.34	0.56	---	---	---	---
3000	0.35	2.5	100	0	0	0.62	0.35	---	---	---	---
3000	0.35	5	41	59	0	0.50	0.50	0.00	0.11	---	---

pCO_2 (ppm)	Solution chemistry		Polymorph distribution			Solid composition					
						Calcite		Aragonite		Vaterite	
	Mg:Ca (molar)	SO_4 (mM)	Calcite (%)	Aragonite (%)	Vaterite (%)	$Mg/CaCO_3$ (%)	$S/CaCO_3$ (%)	$Mg/CaCO_3$ (%)	$S/CaCO_3$ (%)	$Mg/CaCO_3$ (%)	$S/CaCO_3$ (%)
3000	0.35	10	0	100	0	---	---	0.00	0.18	---	---
3000	0.55	0	100	0	0	0.64	0.00	---	---	---	---
3000	0.55	2.5	37	63	0	0.59	0.74	0.00	0.15	---	---
3000	0.55	5	3	97	0	1.06	0.27	0.00	---	---	---
3000	0.55	28	0	100	0	---	---	0.00	0.25	---	---
3000	0.65	5	1	99	0	---	---	0.00	0.34	---	---
3000	0.75	0	56	44	0	0.98	0.00	0.00	0.00	---	---
3000	0.85	0	6	94	0	1.32	0.00	0.00	0.00	---	---
3000	1.00	5	0	100	0	---	---	0.00	0.14	---	---

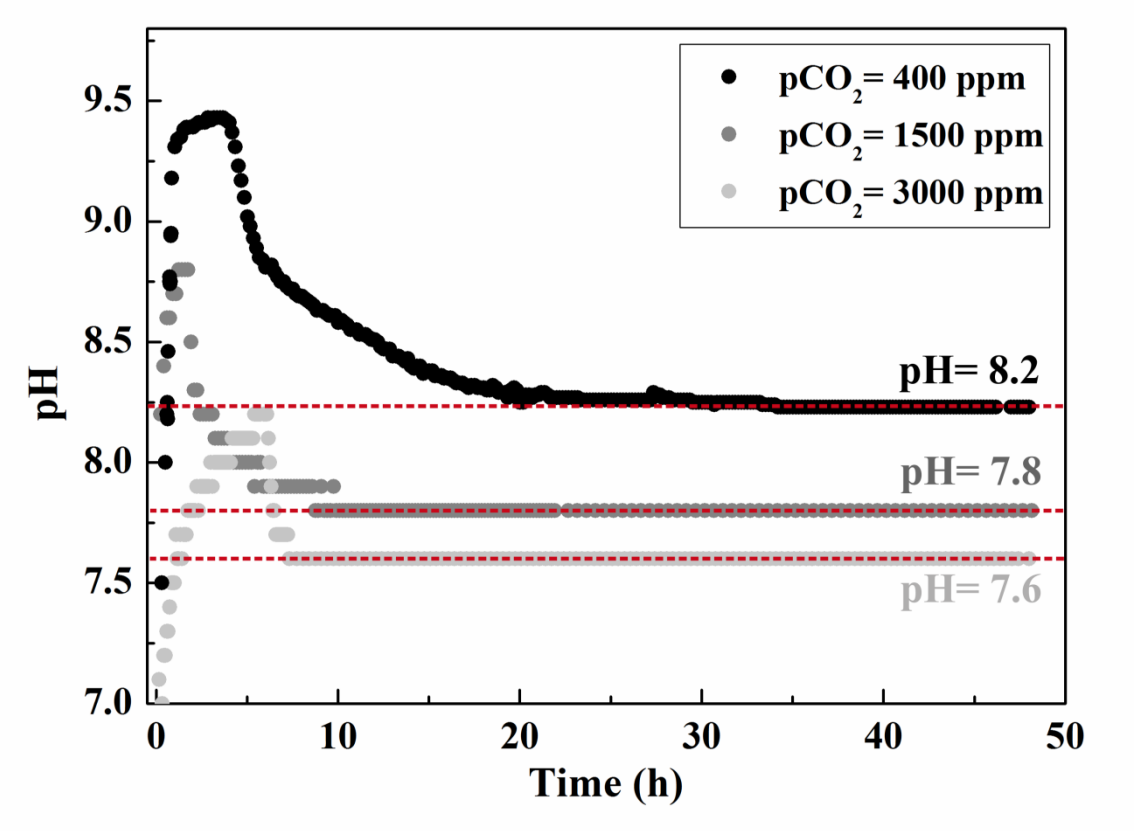

Figure B. 1: *pH profile of experiments carried out at current seawater conditions (Mg:Ca= 5.2 and SO_4= 28 mM) and at 400, 1500 and 3000 ppm of pCO_2.*

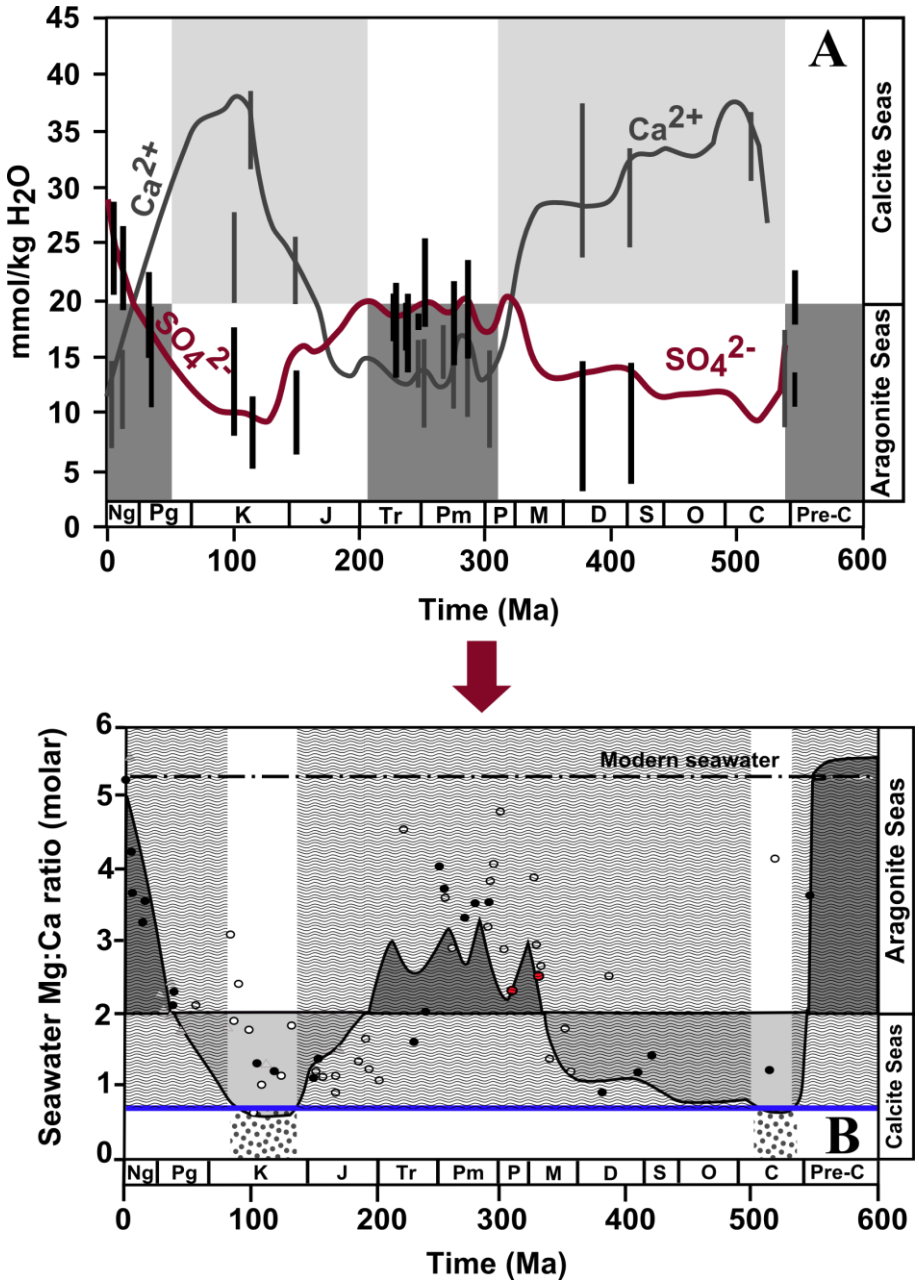

Figure B. 2: *A) Secular variation in concentration of Ca^{2+} and SO_4^{2-} in seawater during the Phanerozoic from primary fluid inclusions in marine halite (grey and black bars). Ca^{2+} and SO_4^{2-} curves are from model of Phanerozoic seawater composition (Robert V. Demicco, 2005). Figure modified after Holt et al., 2014. Red line represents the proposed curve for $SO4^{2-}$ Phanerozoic seawater concentrations in literature (Holt et al., 2014). B) Secular variation in the Mg:Ca ratio of seawater during Phanerozoic. Horizontal black line at Mg:Ca= 2 represents the approximate divide between aragonite and calcite nucleation fields in seawater at 25ºC; .Figure modified after Holt et al., 2014. Horizontal dashed black line represent the current seawater Mg:Ca. Horizontal blue line represents the seawater Mg:Ca ratio (Mg:Ca≈ 0.65±0.1) proposed from this study and M.P. Ramírez-García et al., 2018. Wavy grey shaded areas and dotted grey shaded areas represent our proposed periods of time for aragonite and calcite seas respectively.*